

# Multigrid Hirsch-Fye quantum Monte Carlo method for dynamical mean-field theory

Nils Blümer, Univ. Mainz

## Outline

Introduction: Hubbard model, DMFT, HF-QMC

Efficiency of QMC DMFT solvers

Unbiased Green functions and spectra from HF-QMC

Multigrid Hirsch-Fye quantum Monte Carlo algorithm

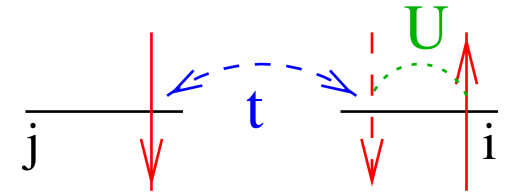
Applications: Mott transitions at large degeneracy / in 3-spin system

Summary and outlook

# Introduction

## Hubbard model

(i) Single band: 
$$\hat{H} = \sum_{(i,j),\sigma} t_{ij} (\hat{c}_{i\sigma}^\dagger \hat{c}_{j\sigma} + \text{h.c.}) + U \sum_i \hat{n}_{i\uparrow} \hat{n}_{i\downarrow}$$



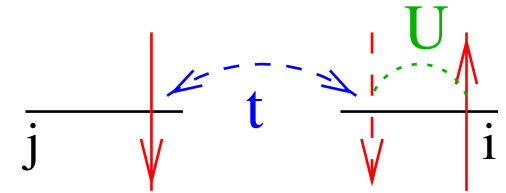
Captures important **strong-correlation phenomena**: Mott metal-insulator transition, (anti-) ferromagnetism, heavy fermions, high- $T_c$  superconductivity (?), . . .

**Few parameters**: interaction  $U/W$ , temperature  $T/W$ , filling  $n$ , dispersion  $\epsilon_{\mathbf{k}}$

# Introduction

## Hubbard model

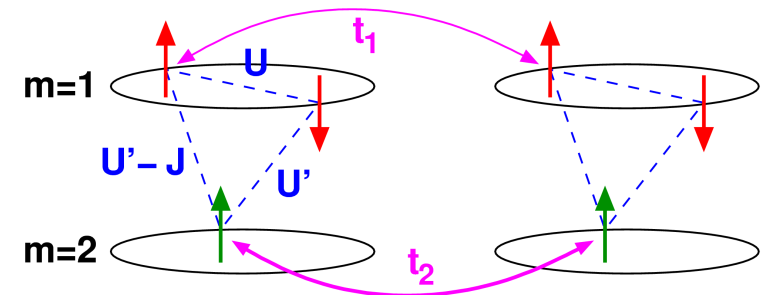
(i) Single band: 
$$\hat{H} = \sum_{(i,j),\sigma} t_{ij} (\hat{c}_{i\sigma}^\dagger \hat{c}_{j\sigma} + \text{h.c.}) + U \sum_i \hat{n}_{i\uparrow} \hat{n}_{i\downarrow}$$



Captures important **strong-correlation phenomena**: Mott metal-insulator transition, (anti-) ferromagnetism, heavy fermions, high- $T_c$  superconductivity (?), . . .

**Few parameters**: interaction  $U/W$ , temperature  $T/W$ , filling  $n$ , dispersion  $\epsilon_{\mathbf{k}}$

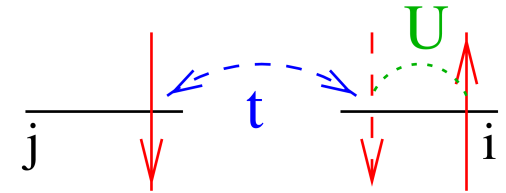
(ii) Multi-band model, e.g., 2-band model with inequivalent bands:



# Introduction

## Hubbard model

(i) Single band: 
$$\hat{H} = \sum_{(i,j),\sigma} t_{ij} (\hat{c}_{i\sigma}^\dagger \hat{c}_{j\sigma} + \text{h.c.}) + U \sum_i \hat{n}_{i\uparrow} \hat{n}_{i\downarrow}$$

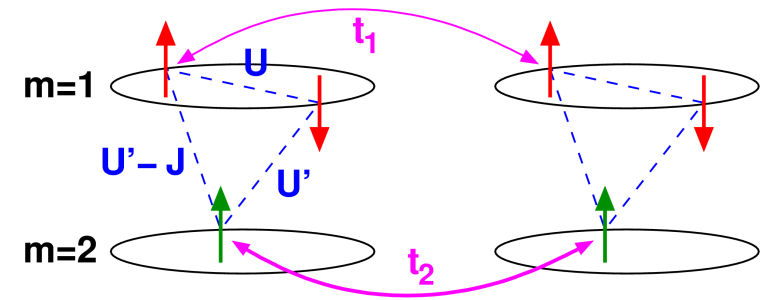


Captures important **strong-correlation phenomena**: Mott metal-insulator transition, (anti-) ferromagnetism, heavy fermions, high- $T_c$  superconductivity (?), ...

**Few parameters**: interaction  $U/W$ , temperature  $T/W$ , filling  $n$ , dispersion  $\epsilon_{\mathbf{k}}$

(ii) Multi-band model, e.g., 2-band model with inequivalent bands:

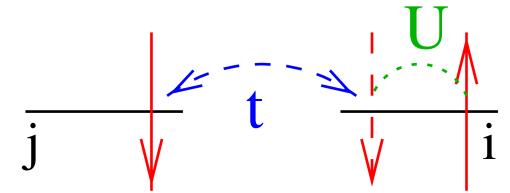
$$H = \sum_{m=1}^2 \left[ - \sum_{\langle ij \rangle \sigma} t_m c_{im\sigma}^\dagger c_{jm\sigma} + U \sum_i n_{im\uparrow} n_{im\downarrow} \right] + \sum_{i\sigma\sigma'} (U' - \delta_{\sigma\sigma'} J_z) n_{i1\sigma} n_{i2\sigma'} + \frac{1}{2} J_\perp \sum_{i\sigma} \left[ c_{i1\sigma}^\dagger \left( c_{i2\bar{\sigma}}^\dagger c_{i1\bar{\sigma}} + c_{i1\bar{\sigma}}^\dagger c_{i2\bar{\sigma}} \right) c_{i2\sigma} + \text{h.c.} \right]$$



# Introduction

## Hubbard model

(i) Single band: 
$$\hat{H} = \sum_{(i,j),\sigma} t_{ij} (\hat{c}_{i\sigma}^\dagger \hat{c}_{j\sigma} + \text{h.c.}) + U \sum_i \hat{n}_{i\uparrow} \hat{n}_{i\downarrow}$$

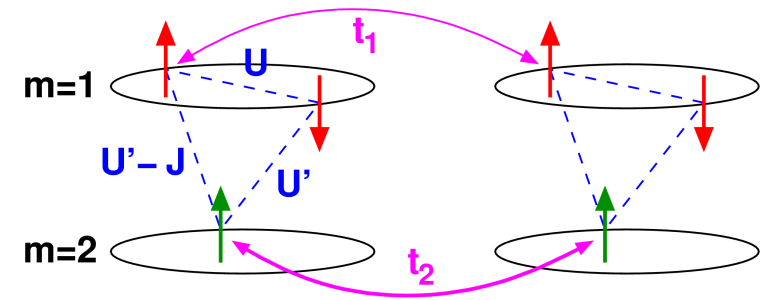


Captures important **strong-correlation phenomena**: Mott metal-insulator transition, (anti-) ferromagnetism, heavy fermions, high- $T_c$  superconductivity (?), . . .

**Few parameters**: interaction  $U/W$ , temperature  $T/W$ , filling  $n$ , dispersion  $\epsilon_{\mathbf{k}}$

(ii) Multi-band model, e.g., 2-band model with inequivalent bands:

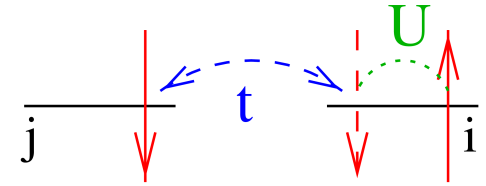
$$H = \sum_{m=1}^2 \left[ - \sum_{\langle ij \rangle \sigma} t_m c_{im\sigma}^\dagger c_{jm\sigma} + U \sum_i n_{im\uparrow} n_{im\downarrow} \right] + \sum_{i\sigma\sigma'} (U' - \delta_{\sigma\sigma'} J_z) n_{i1\sigma} n_{i2\sigma'} + \frac{1}{2} J_\perp \sum_{i\sigma} \left[ c_{i1\sigma}^\dagger \left( c_{i2\bar{\sigma}}^\dagger c_{i1\bar{\sigma}} + c_{i1\bar{\sigma}}^\dagger c_{i2\bar{\sigma}} \right) c_{i2\sigma} + \text{h.c.} \right]$$



**More complexity, more realistic**: OSMT, spin+orbital order, LDA+DMFT, . . .

# Approaches for Hubbard-type models

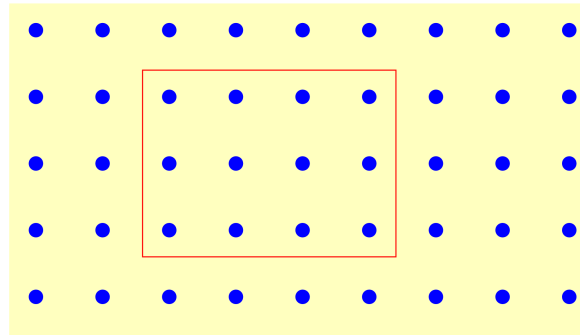
$$\hat{H} = \sum_{(i,j),\sigma} t_{ij} (\hat{c}_{i\sigma}^\dagger \hat{c}_{j\sigma} + \text{h.c.}) + U \sum_i \hat{n}_{i\uparrow} \hat{n}_{i\downarrow}$$



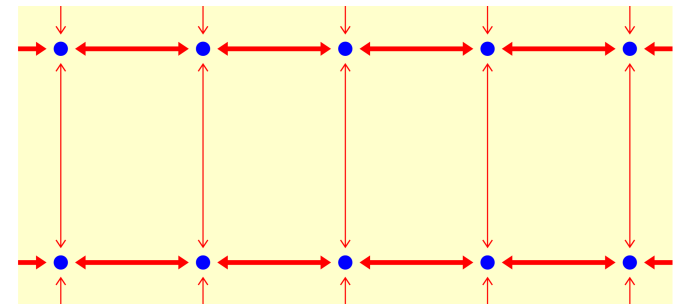
## Perturbation theory

- $U \rightarrow 0$ : Hartree-Fock  
2<sup>nd</sup> order PT, . . . .
- $t/U \rightarrow 0$  (for  $n = 1$ )  
 $\rightsquigarrow$  Heisenberg model

finite clusters: ED, QMC

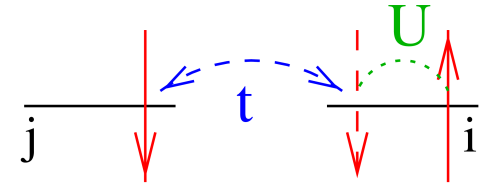


$d \rightarrow 1$ : Bethe ansatz, DMRG



# Approaches for Hubbard-type models

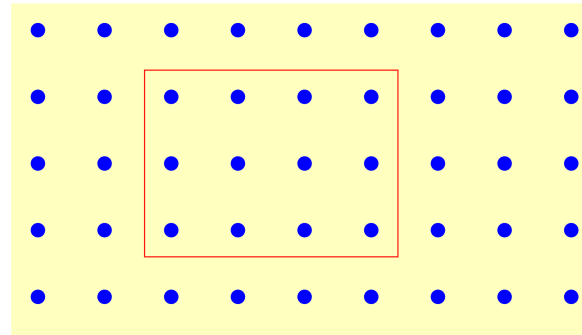
$$\hat{H} = \sum_{(i,j),\sigma} t_{ij} (\hat{c}_{i\sigma}^\dagger \hat{c}_{j\sigma} + \text{h.c.}) + U \sum_i \hat{n}_{i\uparrow} \hat{n}_{i\downarrow}$$



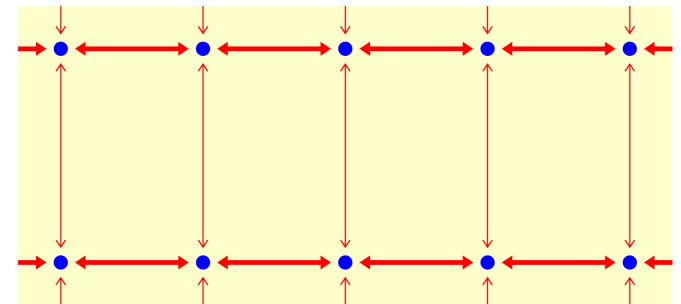
## Perturbation theory

- $U \rightarrow 0$ : Hartree-Fock  
2<sup>nd</sup> order PT, . . .
- $t/U \rightarrow 0$  (for  $n = 1$ )  
 $\rightsquigarrow$  Heisenberg model

## finite clusters: ED, QMC



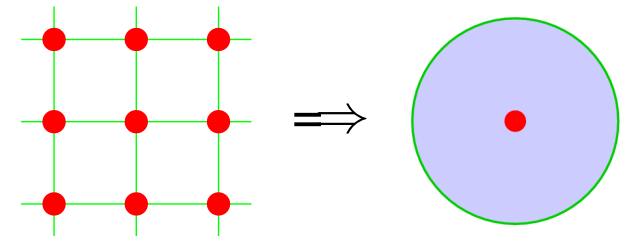
## $d \rightarrow 1$ : Bethe ansatz, DMRG



## Dynamical mean-field theory (DMFT): local self-energy $\Sigma(\mathbf{k}, \omega) \equiv \Sigma(\omega)$

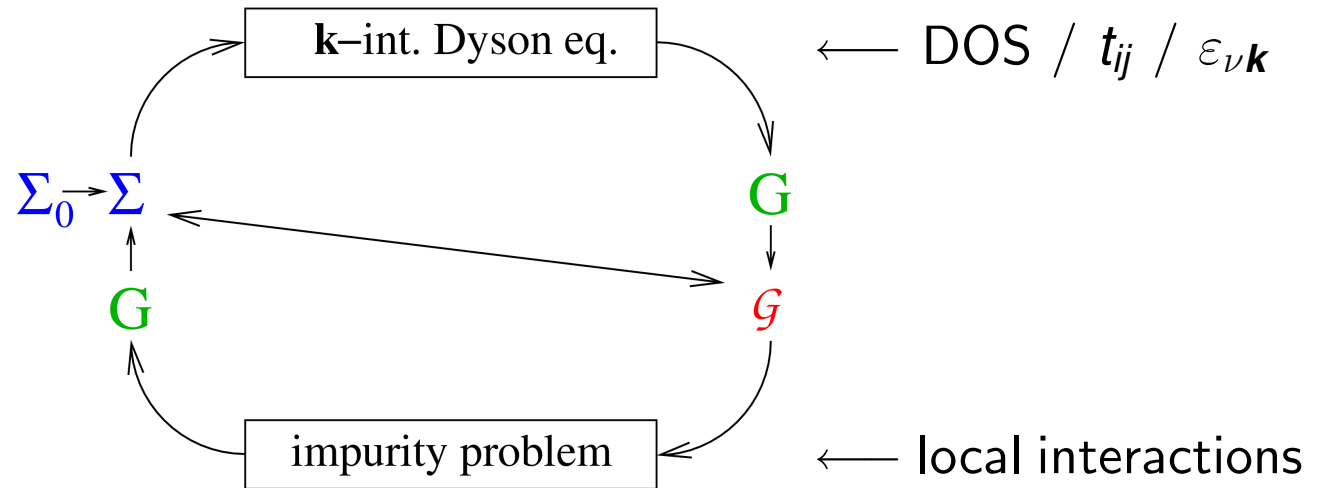
[Metzner, Vollhardt, PRL (1989), Georges, Kotliar, PRL (1992), Jarrell, PRL (1992)]

- + non-perturbative  $\rightsquigarrow$  valid at MIT
- + dynamical on-site correlations preserved
- + in thermodynamic limit
- +/- exact for coordination  $Z \rightarrow \infty$



# Iterative solution of DMFT equations

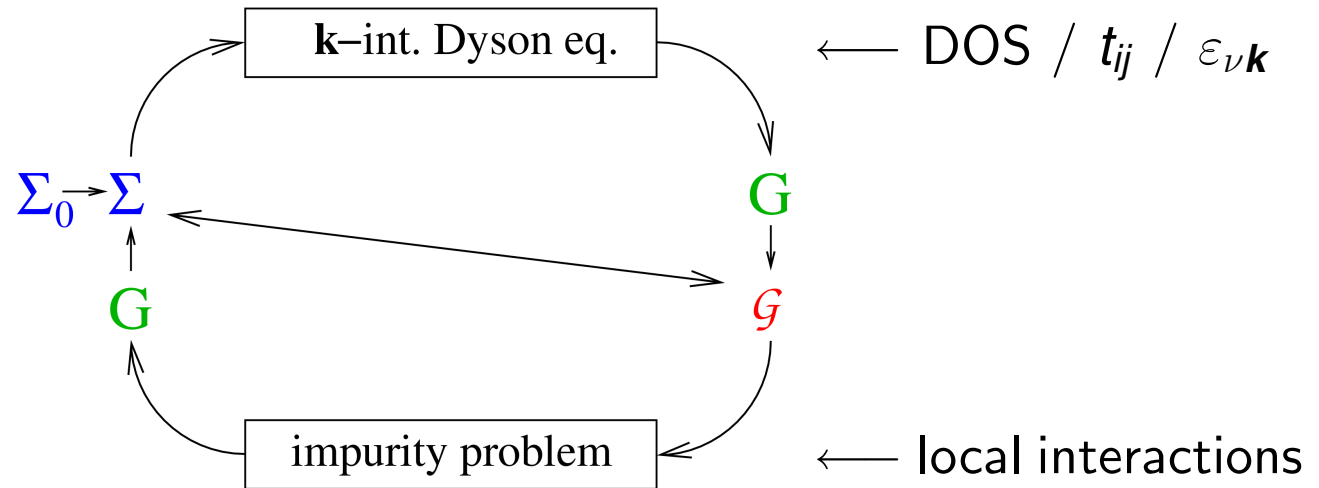
0. Initialize self-energy
1. Solve Dyson equation
2. Solve **single impurity Anderson model (SIAM)**





# Iterative solution of DMFT equations

0. Initialize self-energy
1. Solve Dyson equation
2. Solve **single impurity Anderson model (SIAM)**

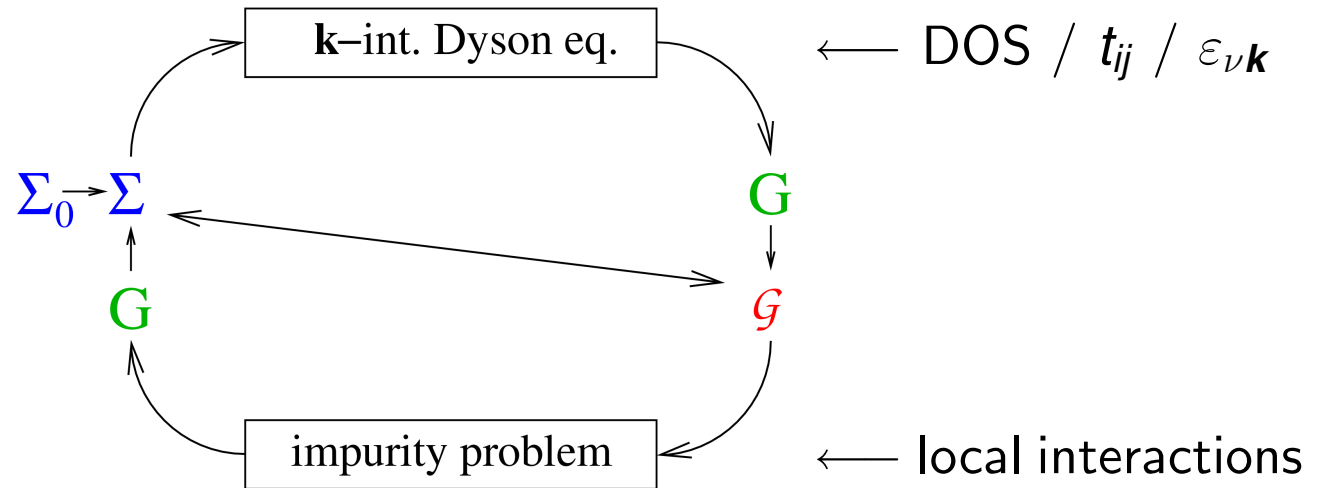


## Impurity solver:

- Iterative perturbation theory (IPT; not controlled)
- Quantum Monte Carlo (QMC)

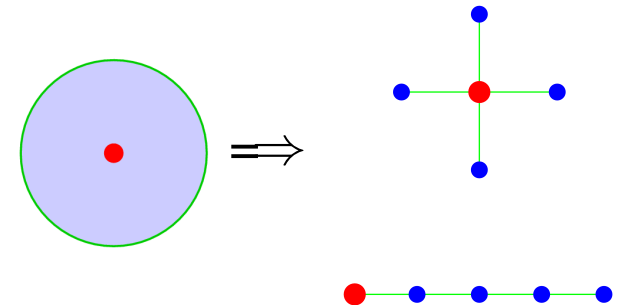
# Iterative solution of DMFT equations

0. Initialize self-energy
1. Solve Dyson equation
2. Solve **single impurity Anderson model (SIAM)**



## Impurity solver:

- Iterative perturbation theory (IPT; not controlled)
- **Quantum Monte Carlo (QMC)**
- Exact diagonalization (ED; large finite-size errors)
- Numerical renormalization group (NRG; 1-2 bands)
- Density matrix renormalization group (DMRG)
- Self-energy functional theory (SFT) + ED



# Auxiliary-field QMC algorithm [Hirsch, Fye (1986)]

Green function  $G$  in imaginary time (fermionic Grassmann variables  $\psi, \psi^*$ ):

$$G_{\sigma}(\tau_2 - \tau_1) = \frac{1}{Z} \int \mathcal{D}[\psi] \mathcal{D}[\psi^*] \psi_{\sigma}(\tau_1) \psi_{\sigma}^*(\tau_2) \exp \left[ \mathcal{A}_0 - U \sum_{\sigma\sigma'} \int_0^{\beta} d\tau \psi_{\sigma}^* \psi_{\sigma} \psi_{\sigma'}^* \psi_{\sigma'} \right]$$

# Auxiliary-field QMC algorithm [Hirsch, Fye (1986)]

Green function  $G$  in imaginary time (fermionic Grassmann variables  $\psi, \psi^*$ ):

$$G_{\sigma}(\tau_2 - \tau_1) = \frac{1}{Z} \int \mathcal{D}[\psi] \mathcal{D}[\psi^*] \psi_{\sigma}(\tau_1) \psi_{\sigma}^*(\tau_2) \exp \left[ \mathcal{A}_0 - U \sum_{\sigma\sigma'} \int_0^{\beta} d\tau \psi_{\sigma}^* \psi_{\sigma} \psi_{\sigma'}^* \psi_{\sigma'} \right]$$

- Discretization  $\beta = \Lambda \Delta\tau$ ,
- Trotter decoupling  $e^{-\beta(\hat{T}+\hat{V})} = \lim_{\Lambda \rightarrow \infty} \left[ e^{-\Delta\tau \hat{T}} e^{-\Delta\tau \hat{V}} \right]^{\Lambda}$

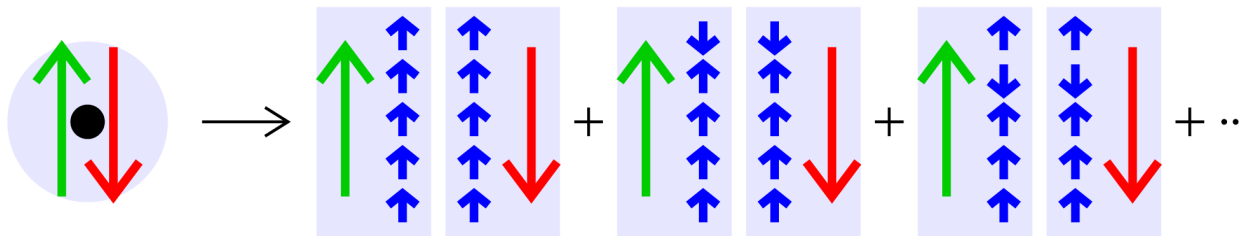
# Auxiliary-field QMC algorithm [Hirsch, Fye (1986)]

Green function  $G$  in imaginary time (fermionic Grassmann variables  $\psi, \psi^*$ ):

$$G_{\sigma}(\tau_2 - \tau_1) = \frac{1}{Z} \int \mathcal{D}[\psi] \mathcal{D}[\psi^*] \psi_{\sigma}(\tau_1) \psi_{\sigma}^*(\tau_2) \exp \left[ \mathcal{A}_0 - U \sum_{\sigma\sigma'} \int_0^{\beta} d\tau \psi_{\sigma}^* \psi_{\sigma} \psi_{\sigma'}^* \psi_{\sigma'} \right]$$

• Discretization  $\beta = \Lambda \Delta\tau$ , • Trotter decoupling  $e^{-\beta(\hat{T}+\hat{V})} = \lim_{\Lambda \rightarrow \infty} [e^{-\Delta\tau \hat{T}} e^{-\Delta\tau \hat{V}}]^{\Lambda}$

• Discrete Hubbard-Stratonovich transformation  $e^{\Delta\tau U(\hat{n}_{\uparrow} - \hat{n}_{\downarrow})^2/2} = \frac{1}{2} \sum_{s=\pm 1} e^{\lambda s (\hat{n}_{\uparrow} - \hat{n}_{\downarrow})}$



Wick theorem:

$$G = \frac{\sum M \det\{M\}}{\sum \det\{M\}}$$

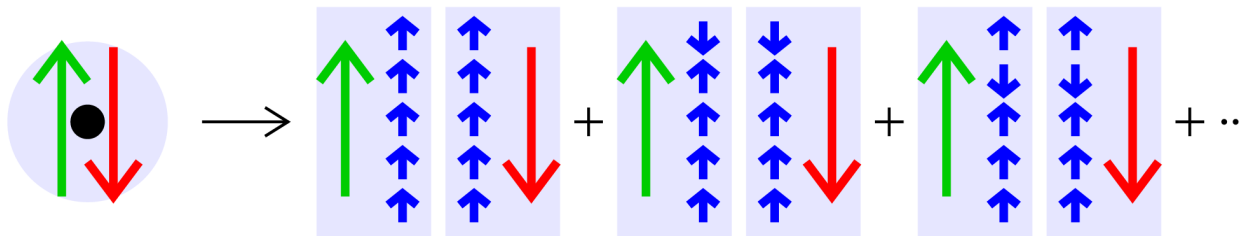
# Auxiliary-field QMC algorithm [Hirsch, Fye (1986)]

Green function  $G$  in imaginary time (fermionic Grassmann variables  $\psi, \psi^*$ ):

$$G_{\sigma}(\tau_2 - \tau_1) = \frac{1}{Z} \int \mathcal{D}[\psi] \mathcal{D}[\psi^*] \psi_{\sigma}(\tau_1) \psi_{\sigma}^*(\tau_2) \exp \left[ \mathcal{A}_0 - U \sum_{\sigma\sigma'} \int_0^{\beta} d\tau \psi_{\sigma}^* \psi_{\sigma} \psi_{\sigma'}^* \psi_{\sigma'} \right]$$

• Discretization  $\beta = \Lambda \Delta\tau$ , • Trotter decoupling  $e^{-\beta(\hat{T}+\hat{V})} = \lim_{\Lambda \rightarrow \infty} \left[ e^{-\Delta\tau \hat{T}} e^{-\Delta\tau \hat{V}} \right]^{\Lambda}$

• Discrete Hubbard-Stratonovich transformation  $e^{\Delta\tau U(\hat{n}_{\uparrow} - \hat{n}_{\downarrow})^2/2} = \frac{1}{2} \sum_{s=\pm 1} e^{\lambda s (\hat{n}_{\uparrow} - \hat{n}_{\downarrow})}$



Wick theorem:

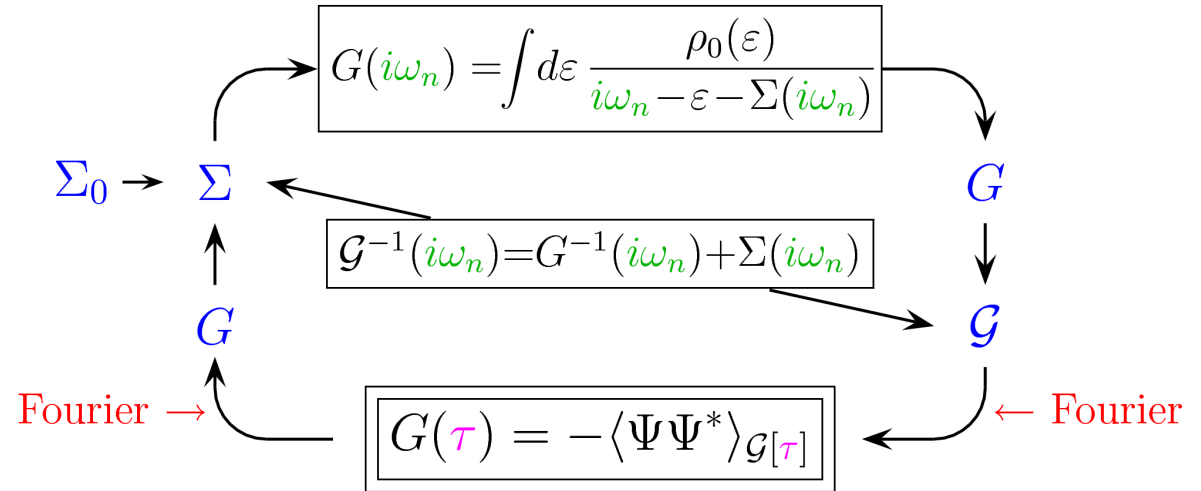
$$G = \frac{\sum M \det\{M\}}{\sum \det\{M\}}$$

Metropolis MC importance sampling over auxiliary Ising field  $\{s\}$ :  $2^{\Lambda}$  configurations

+ numerically exact, + no sign problem (density-type int.), – effort scales as  $T^{-3}$

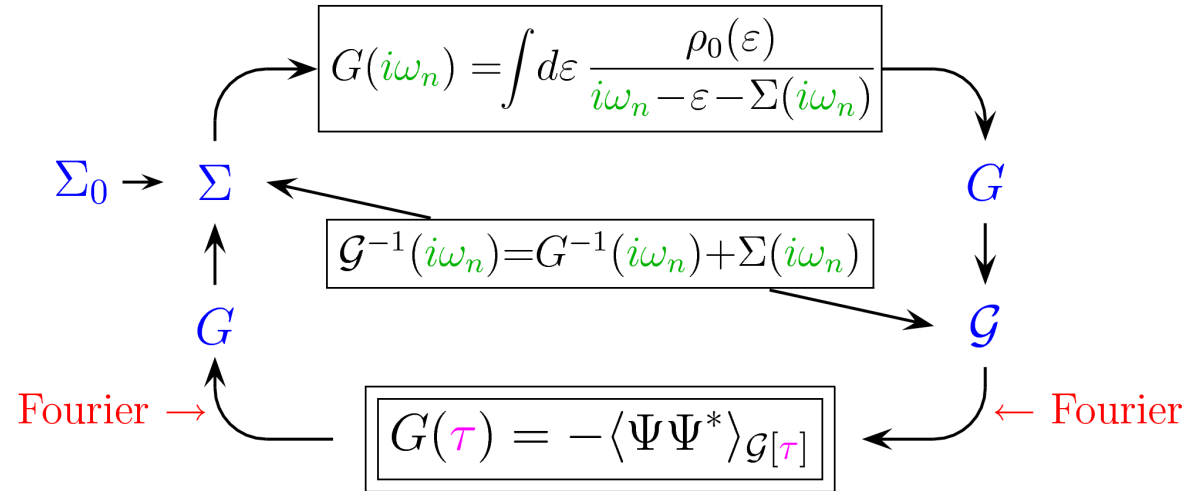
# Special issue: Fourier transformations in DMFT-QMC cycle

Iterative solution of DMFT equations (for imaginary-time impurity solver)

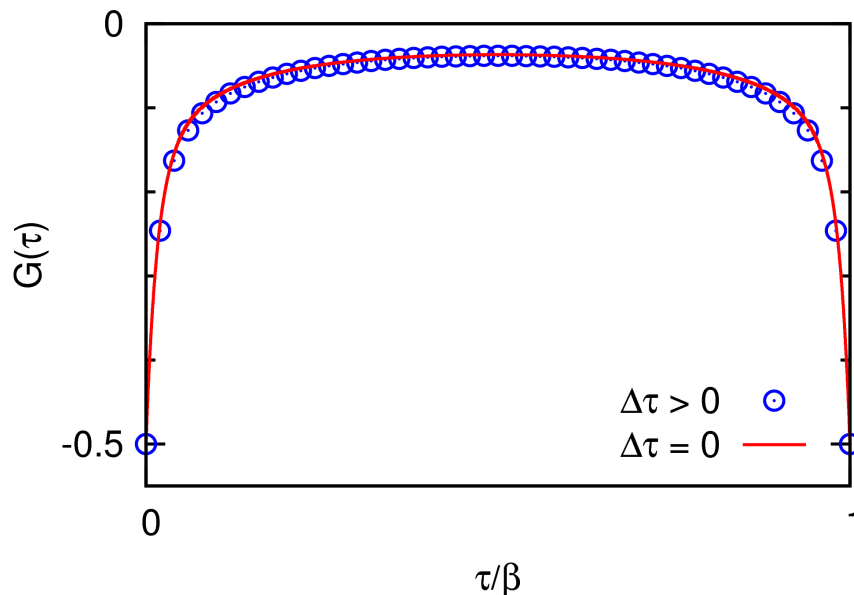


# Special issue: Fourier transformations in DMFT-QMC cycle

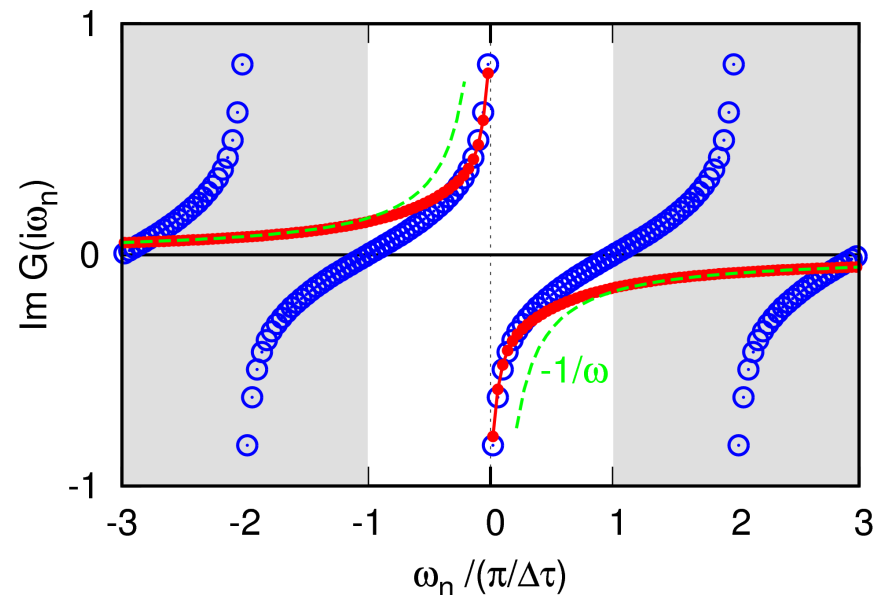
Iterative solution of DMFT equations (for imaginary-time impurity solver)



Naive discrete Fourier transformation  $\rightsquigarrow$  oscillations (instead of  $G(\omega) \xrightarrow{\omega \rightarrow \infty} 1/\omega$ )



naive FT  $\rightarrow$





Possible solution: interpolate  $G_{\text{QMC}}(\tau)$ , e.g., by cubic splines [Jarrell, Krauth, Gull, . . .]

But:  $\frac{d^2 G(\tau)}{d\tau^2}$  maximal for  $\tau \rightarrow 0, \beta \rightsquigarrow$  natural boundary conditions inappropriate

Possible solution: interpolate  $G_{\text{QMC}}(\tau)$ , e.g., by cubic splines [Jarrell, Krauth, Gull, . . .]

But:  $\frac{d^2 G(\tau)}{d\tau^2}$  maximal for  $\tau \rightarrow 0, \beta \rightsquigarrow$  natural boundary conditions inappropriate

- adjust boundary cond.

[Oudovenko]

- spline-fit only  
difference w.r.t.  
reference problem:

– IPT [Jarrell]

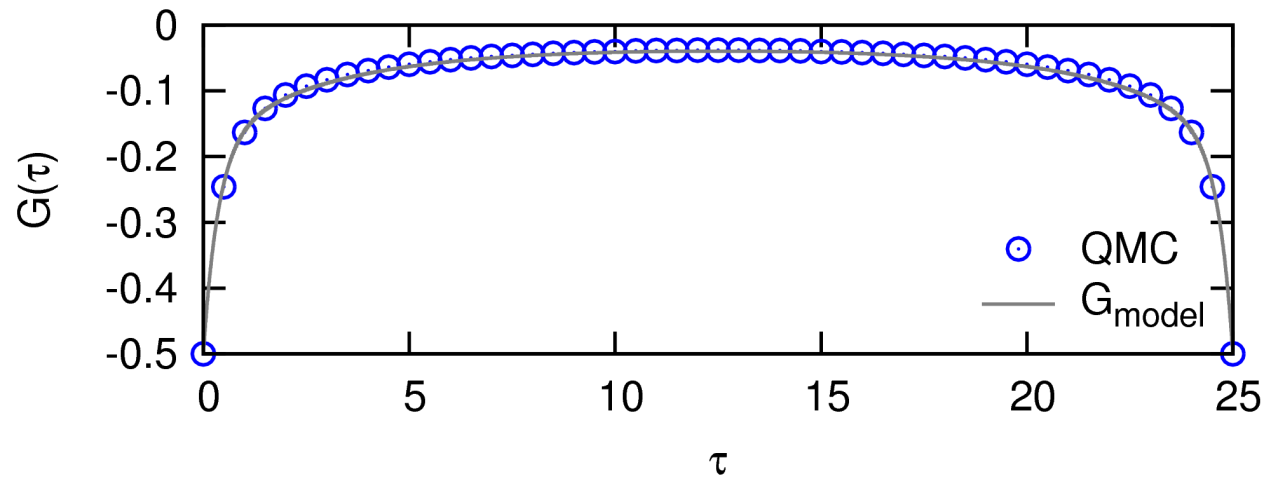
Possible solution: interpolate  $G_{\text{QMC}}(\tau)$ , e.g., by cubic splines [Jarrell, Krauth, Gull, . . .]

But:  $\frac{d^2 G(\tau)}{d\tau^2}$  maximal for  $\tau \rightarrow 0, \beta \rightsquigarrow$  natural boundary conditions inappropriate

- adjust boundary cond.  
[Oudovenko]

- spline-fit only  
difference w.r.t.  
reference problem:

- IPT [Jarrell]
- high-frequency expansion for  $\Sigma(\omega)$  + param. [Knecht, NB]



$$\Sigma_{\sigma}(\omega) = U\left(\langle \hat{n}_{-\sigma} \rangle - \frac{1}{2}\right) \omega^0 + U^2 \langle \hat{n}_{-\sigma} \rangle (1 - \langle \hat{n}_{-\sigma} \rangle) \omega^{-1} + \mathcal{O}(\omega^{-2})$$

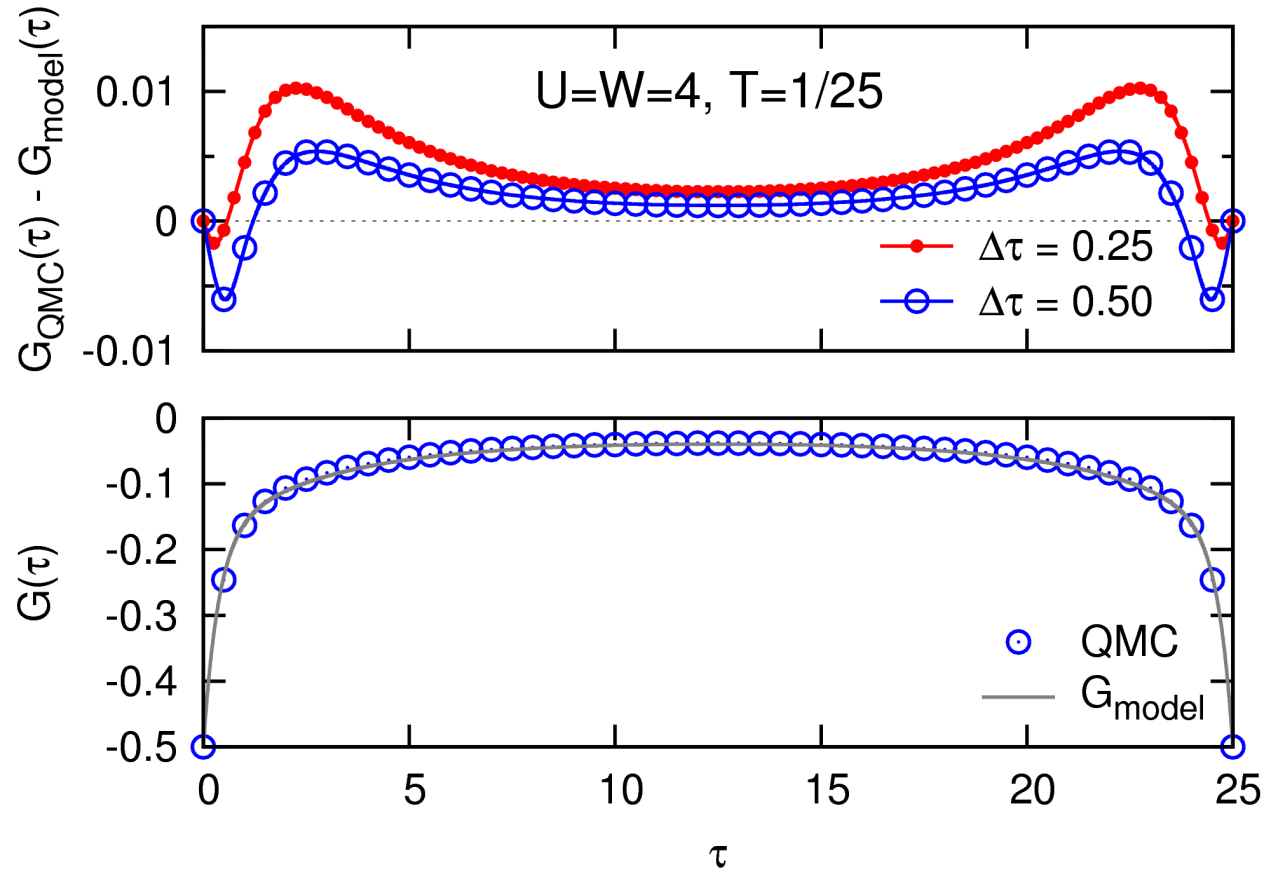
Possible solution: interpolate  $G_{\text{QMC}}(\tau)$ , e.g., by cubic splines [Jarrell, Krauth, Gull, . . .]

But:  $\frac{d^2 G(\tau)}{d\tau^2}$  maximal for  $\tau \rightarrow 0, \beta \rightsquigarrow$  natural boundary conditions inappropriate

- adjust boundary cond. [Oudovenko]

- spline-fit only difference w.r.t. reference problem:

- IPT [Jarrell]
- high-frequency expansion for  $\Sigma(\omega)$  + param. [Knecht, NB]



$$\Sigma_{\sigma}(\omega) = U \left( \langle \hat{n}_{-\sigma} \rangle - \frac{1}{2} \right) \omega^0 + U^2 \langle \hat{n}_{-\sigma} \rangle (1 - \langle \hat{n}_{-\sigma} \rangle) \omega^{-1} + \mathcal{O}(\omega^{-2})$$

multi-band case:  
additional terms

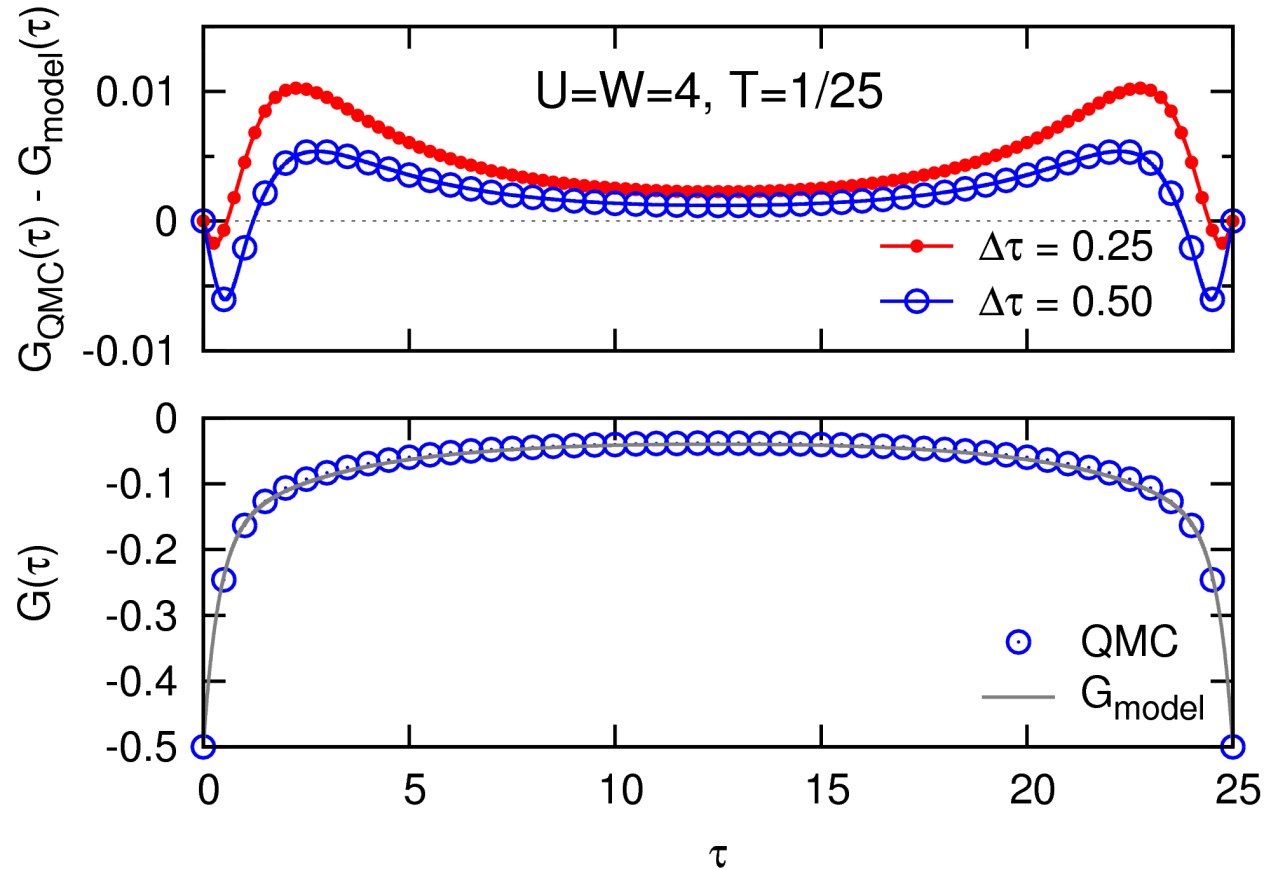
Possible solution: interpolate  $G_{\text{QMC}}(\tau)$ , e.g., by cubic splines [Jarrell, Krauth, Gull, . . .]

But:  $\frac{d^2 G(\tau)}{d\tau^2}$  maximal for  $\tau \rightarrow 0, \beta \rightsquigarrow$  natural boundary conditions inappropriate

- adjust boundary cond. [Oudovenko]

- spline-fit only difference w.r.t. reference problem:

- IPT [Jarrell]
- high-frequency expansion for  $\Sigma(\omega)$  + param. [Knecht, NB]



$$\Sigma_{\sigma}(\omega) = U(\langle \hat{n}_{-\sigma} \rangle - \frac{1}{2}) \omega^0 + U^2 \langle \hat{n}_{-\sigma} \rangle (1 - \langle \hat{n}_{-\sigma} \rangle) \omega^{-1} + \mathcal{O}(\omega^{-2})$$

multi-band case:  
additional terms

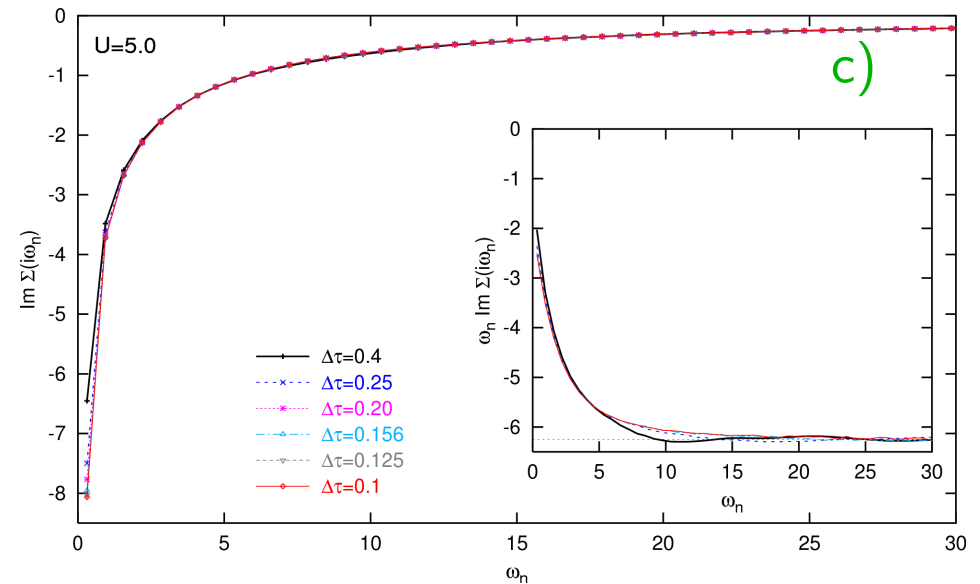
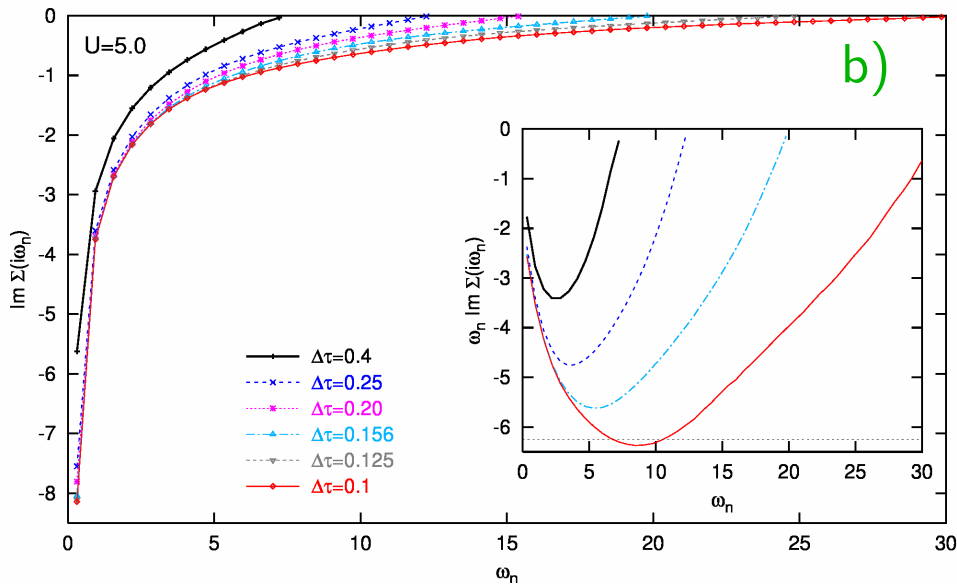
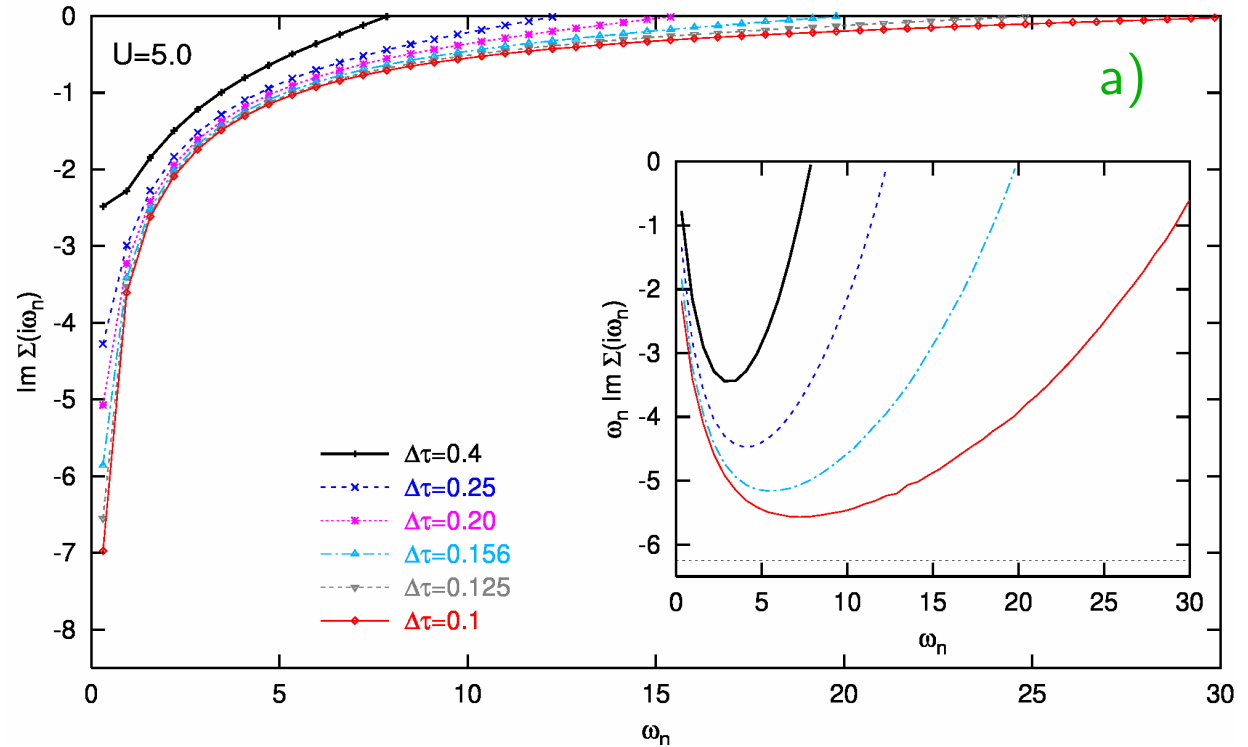
Current project: replace spline interpolation by smooth fit!

Fourier trafo schemes: self-energy  $\Sigma$  ( $T = 0.1, U = 5$ )

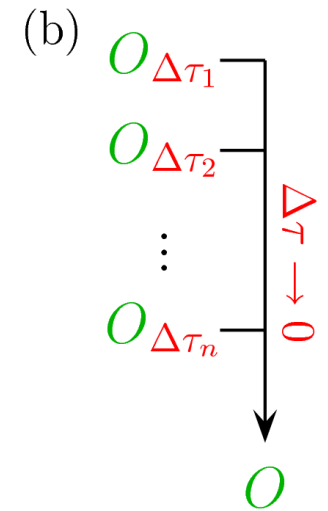
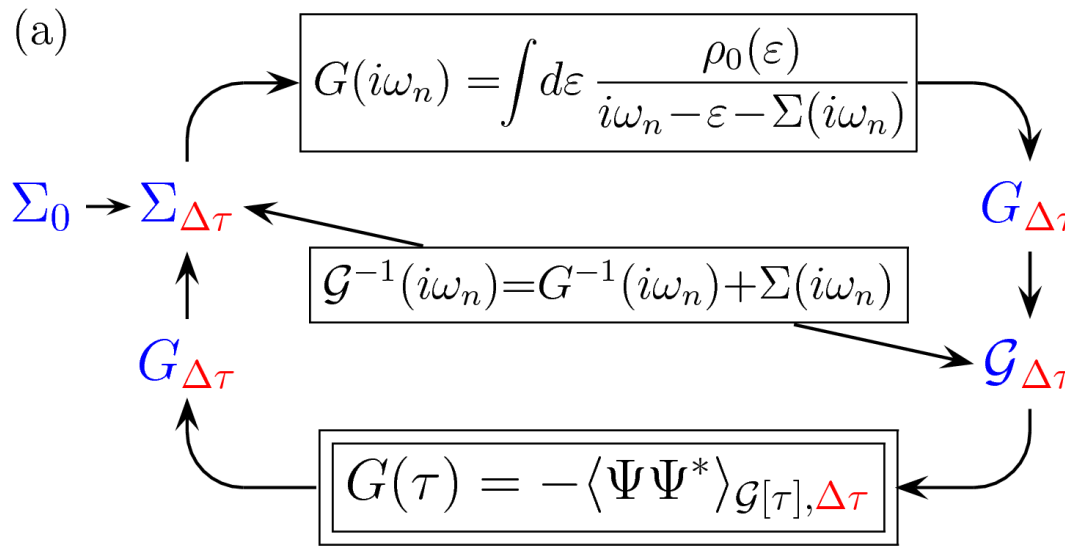
- a) “Ulmke smoothing”,
- b) improved “smoothing”,
- c) cubic spline + analytic high-frequency corrections

low-frequency errors of  $\Sigma(\omega)$ :

- large in a)
- small in b) and c)

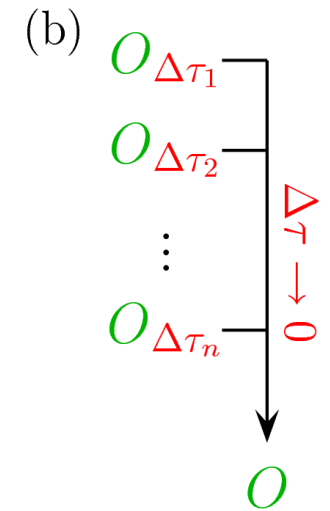
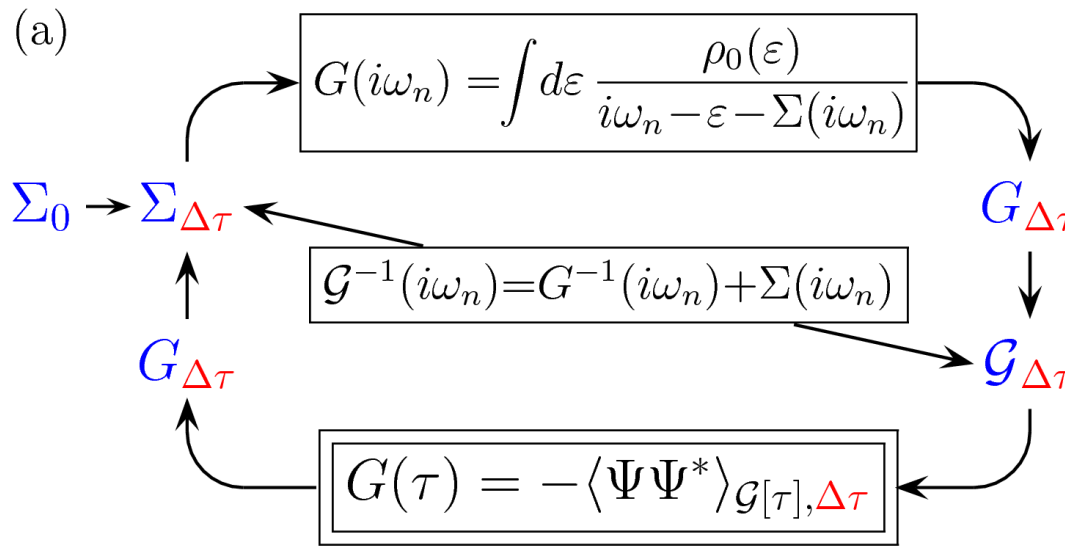


Self-consistency cycle using conventional HF-QMC



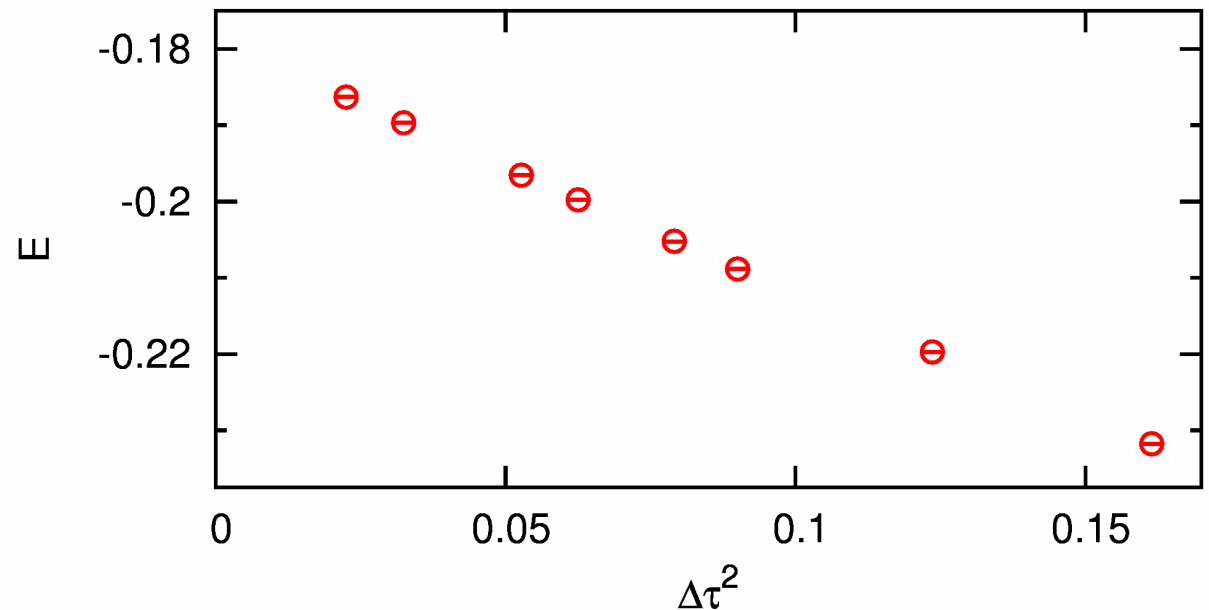
Extrapolation  $\Delta\tau \rightarrow 0$  can improve accuracy of observable estimates by several orders of magnitude ( $\sim$  same cost)

Self-consistency cycle using conventional HF-QMC



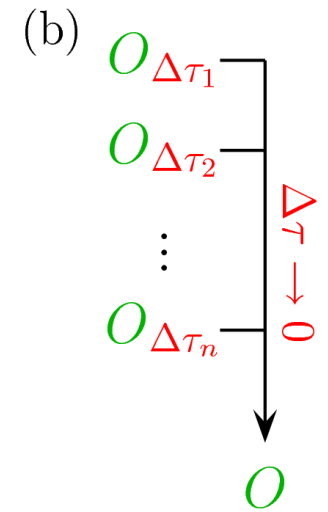
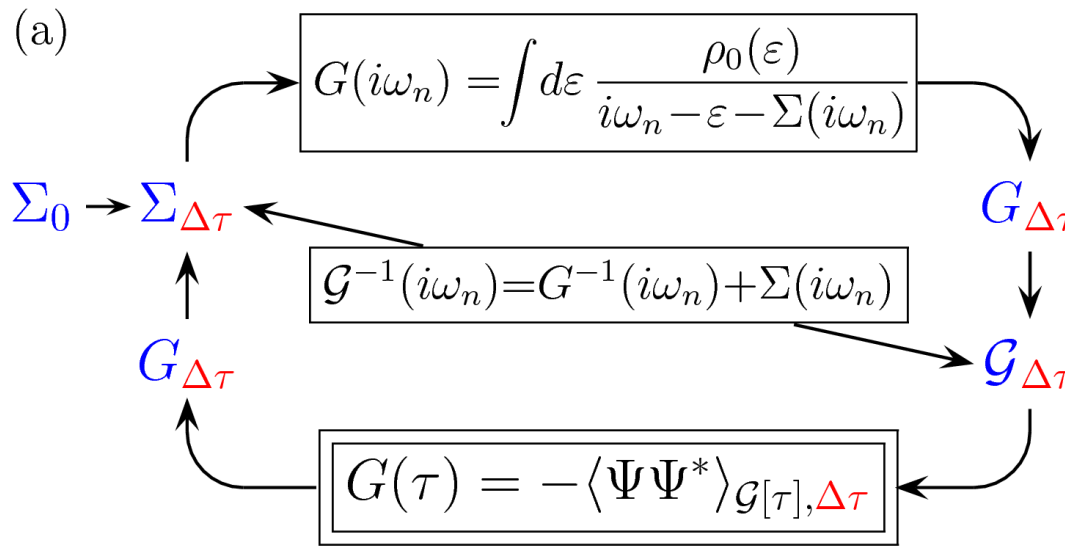
Extrapolation  $\Delta\tau \rightarrow 0$  can improve accuracy of observable estimates by several orders of magnitude ( $\sim$  same cost)

Example: energy  $E$  for  $U = W = 4$  (Bethe DOS),  $T = 1/45$   
 [NB, PRB (2007)]



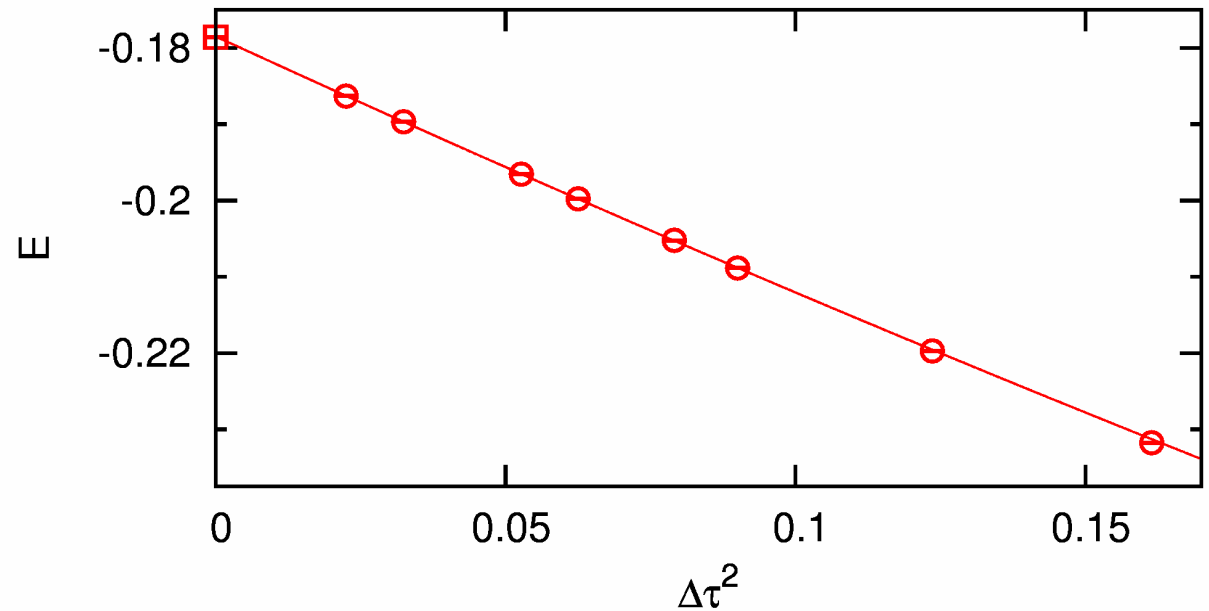


Self-consistency cycle using conventional HF-QMC



Extrapolation  $\Delta\tau \rightarrow 0$  can improve accuracy of observable estimates by several orders of magnitude ( $\sim$  same cost)

Example: energy  $E$  for  $U = W = 4$  (Bethe DOS),  $T = 1/45$   
 [NB, PRB (2007)]

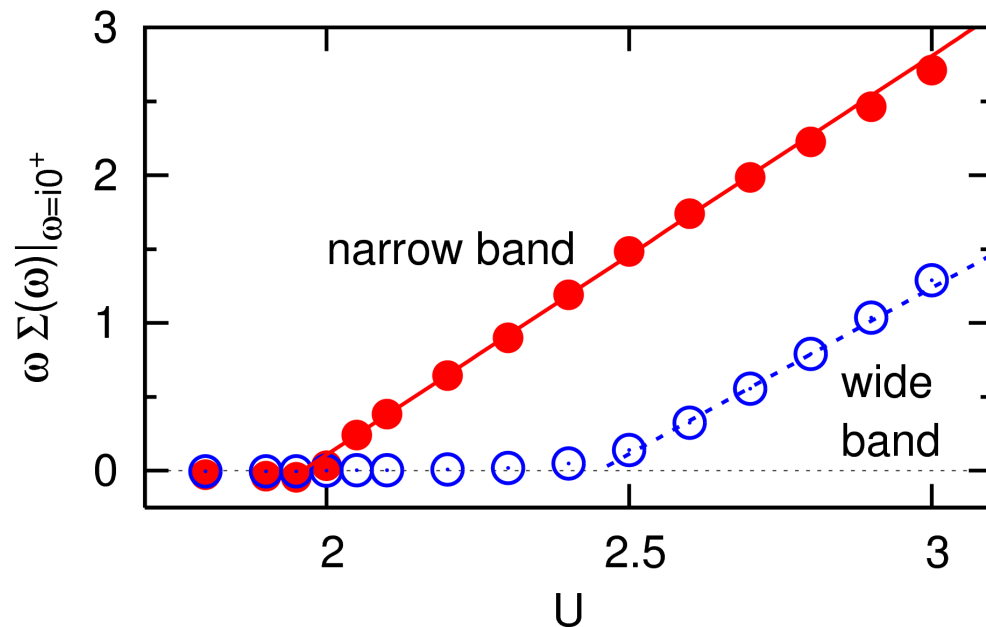


# Selected applications

High-precision calculations for 1-band model, extrapolation  $T \rightarrow 0$ :

benchmark results ( $E$ ,  $D$ ,  $Z$ ) unmatched by ED, DMRG, PQMC, NRG  
revealed errors in weak-coupling expansions

Orbital-selective Mott transitions in 2-band model



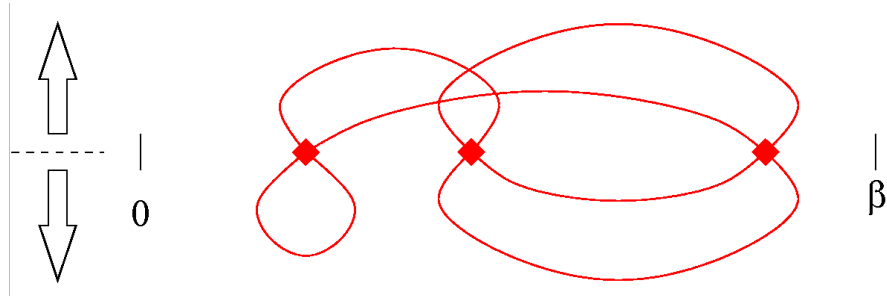
[C. Knecht, NB, and P.G.J. van Dongen, *PRB* 72, 081103(R) (2005)]

# Efficiency of QMC DMFT solvers

## New development: continuous-time QMC algorithms

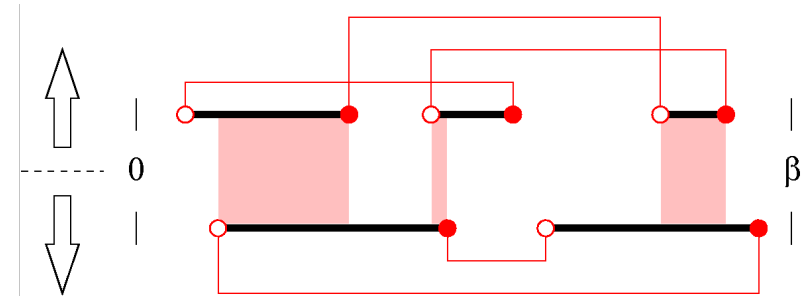
### 1. weak-coupling expansion

[Rubtsov, Savkin, Lichtenstein, PRB (2005)]



### 2. hybridization expansion

[Werner et al., PRL (2006)]

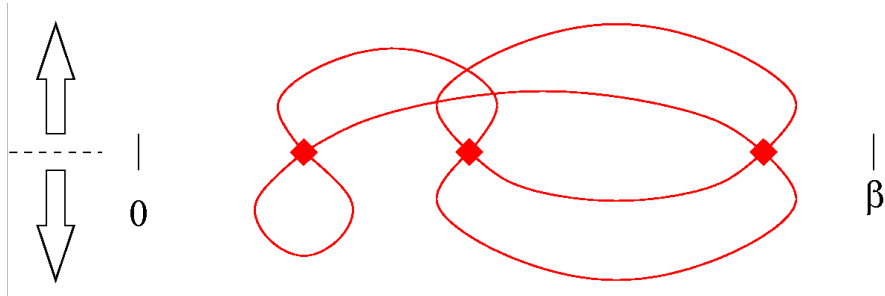


# Efficiency of QMC DMFT solvers

New development: continuous-time QMC algorithms

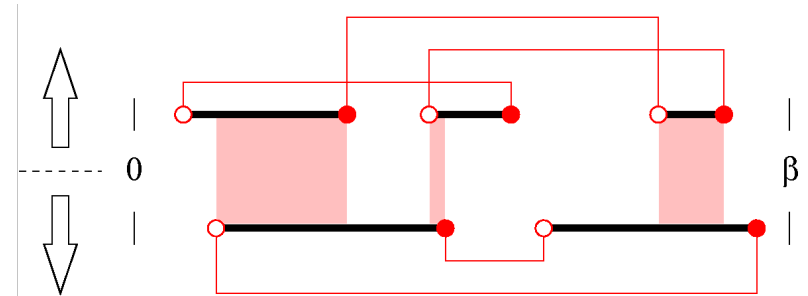
1. weak-coupling expansion

[Rubtsov, Savkin, Lichtenstein, PRB (2005)]



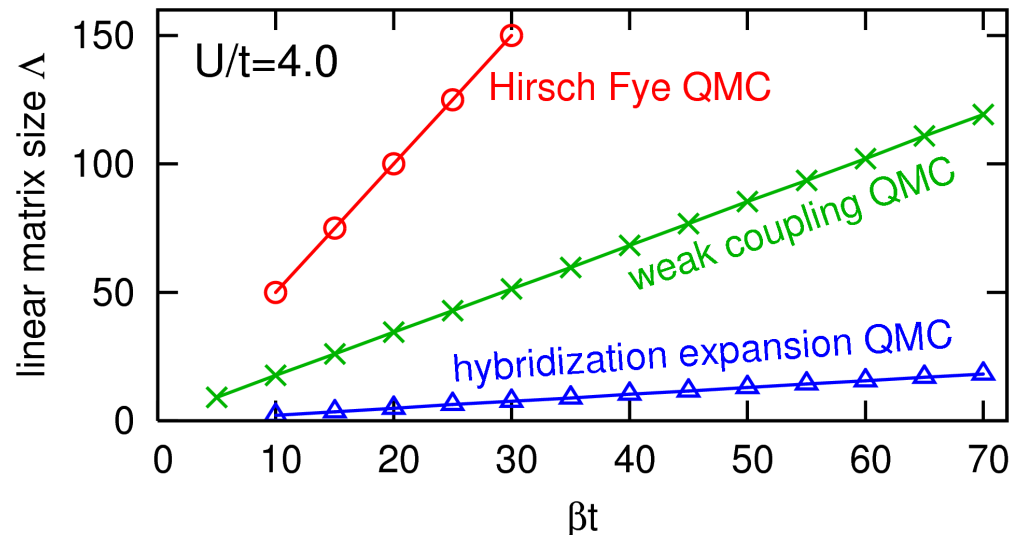
2. hybridization expansion

[Werner et al., PRL (2006)]



CT-QMC methods: smaller matrices

All QMC methods: effort  $\propto \Lambda^3$

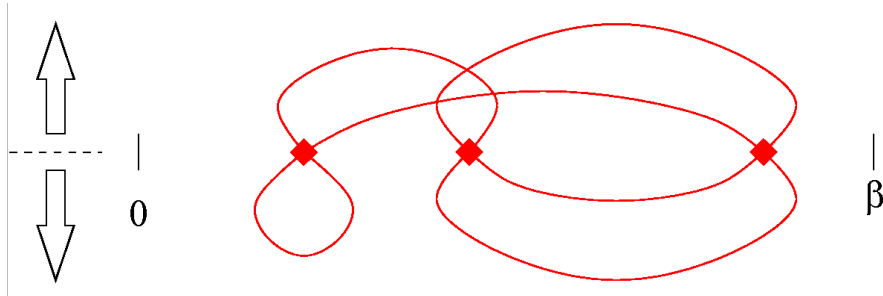


# Efficiency of QMC DMFT solvers

New development: continuous-time QMC algorithms

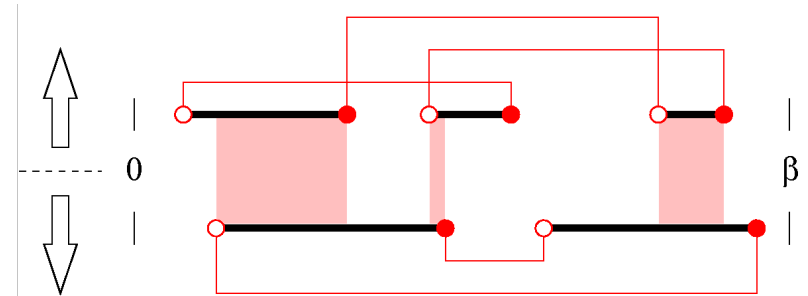
1. weak-coupling expansion

[Rubtsov, Savkin, Lichtenstein, PRB (2005)]



2. hybridization expansion

[Werner et al., PRL (2006)]

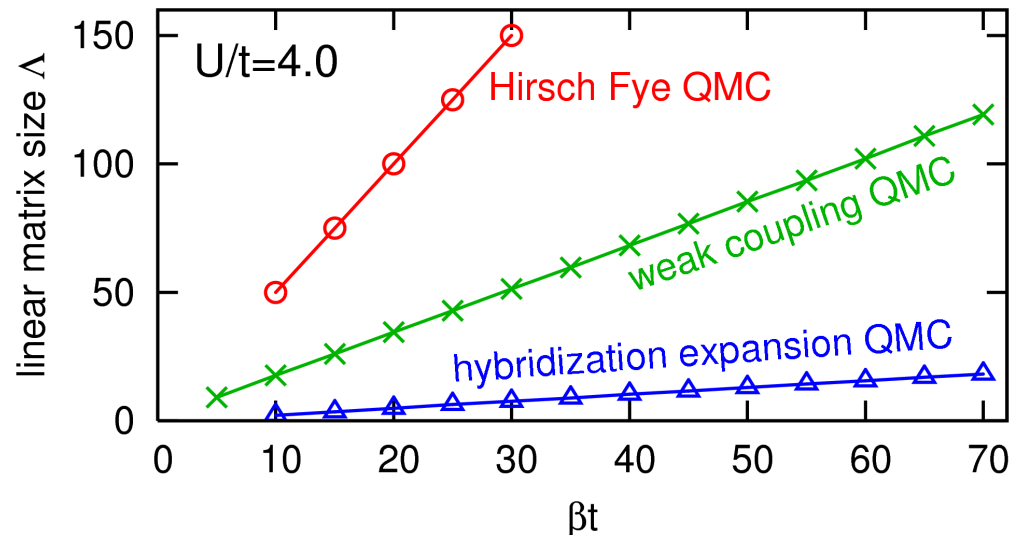


CT-QMC methods: smaller matrices

All QMC methods: effort  $\propto \Lambda^3$

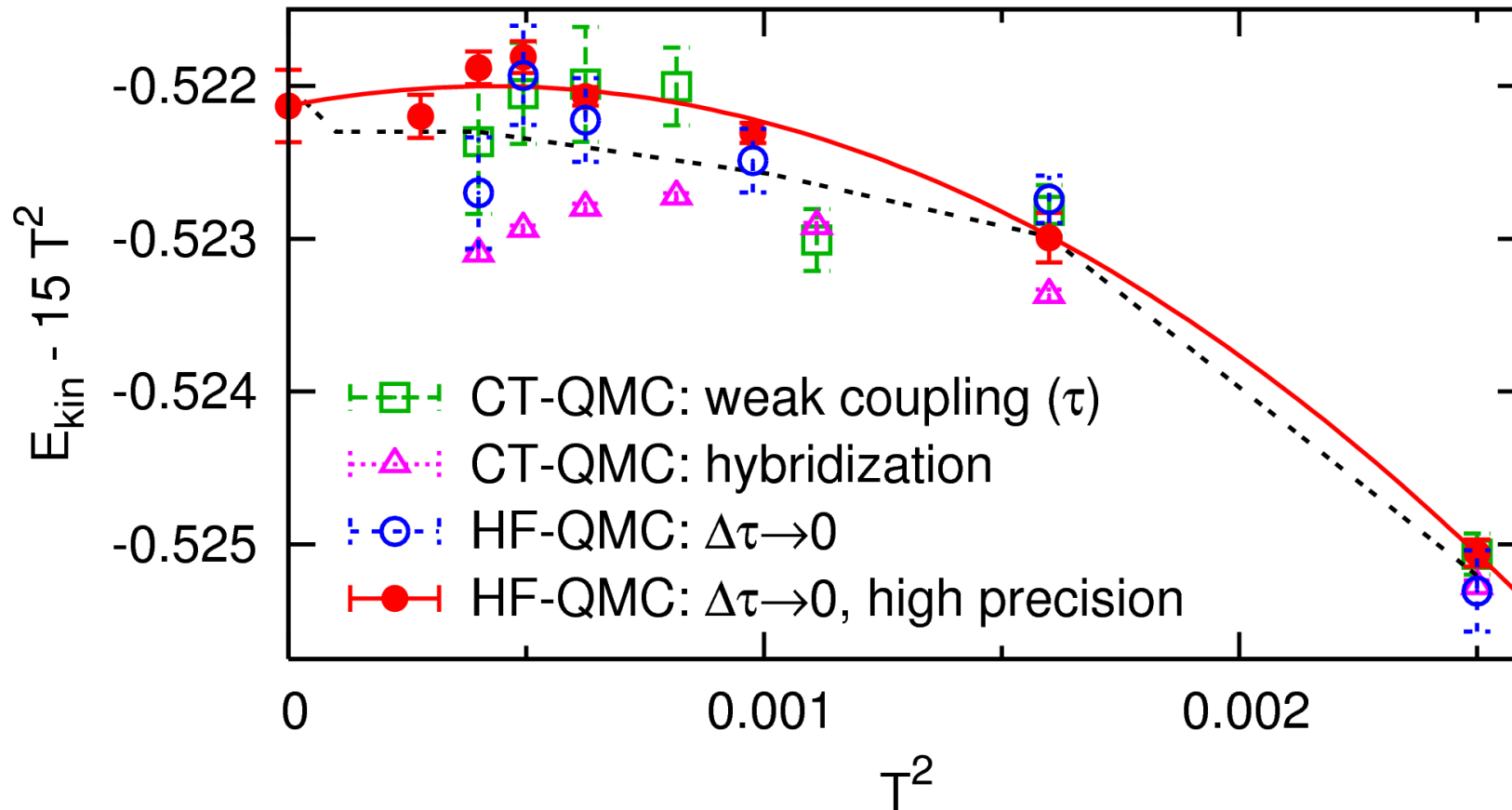
Claim [Troyer (2006)]:

“CT-QMC more efficient than HF-QMC by orders of magnitude”



# Comparisons at constant CPU time: kinetic energy (at $U = W = 4$ )

140 CPU hours on AMD Opteron 244 (serial) / mix of Opterons (parallel)

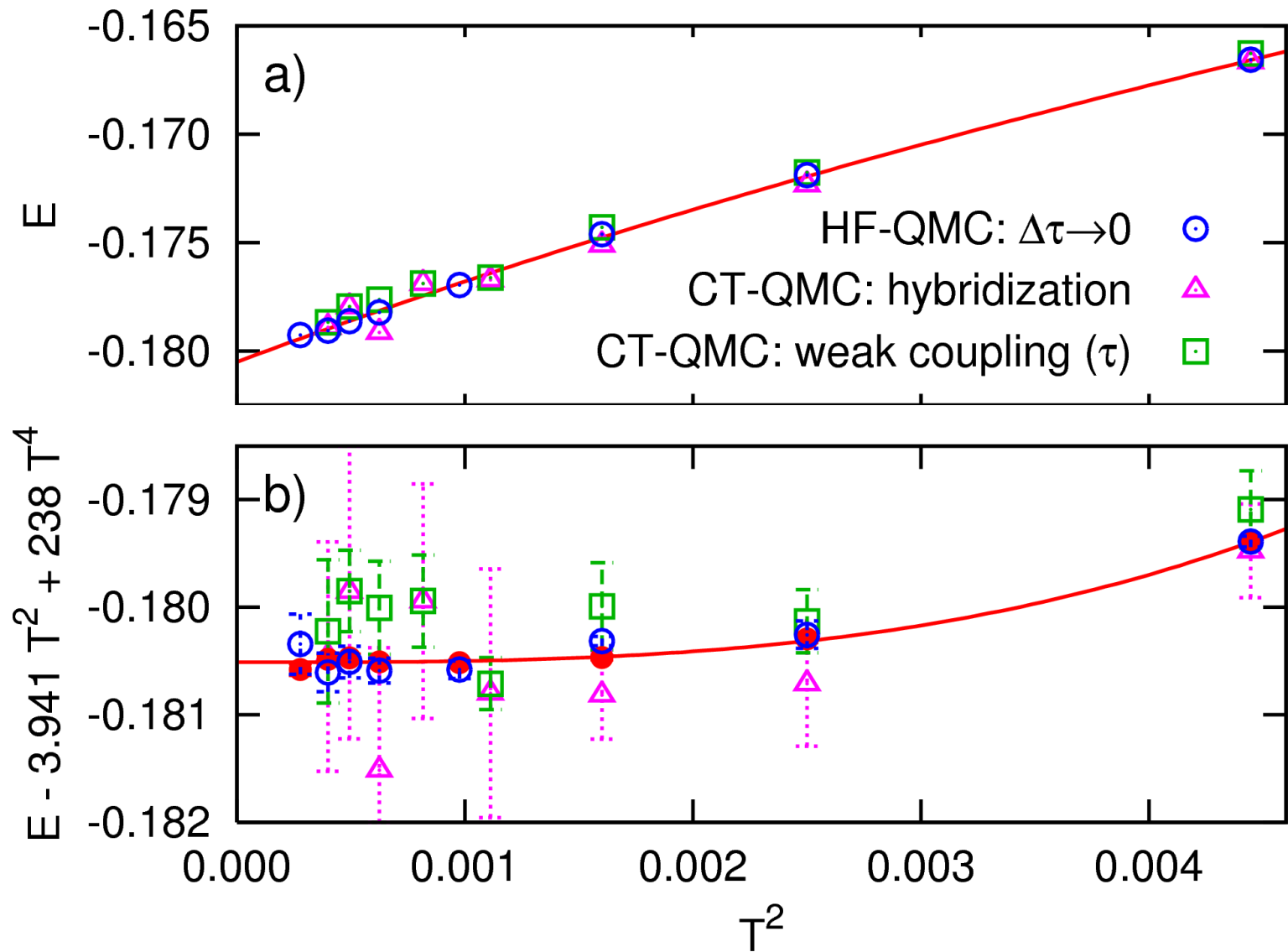


Similar precision for HF-QMC and weak-coupling CT-QMC

Systematic errors in hybridization CT-QMC data!

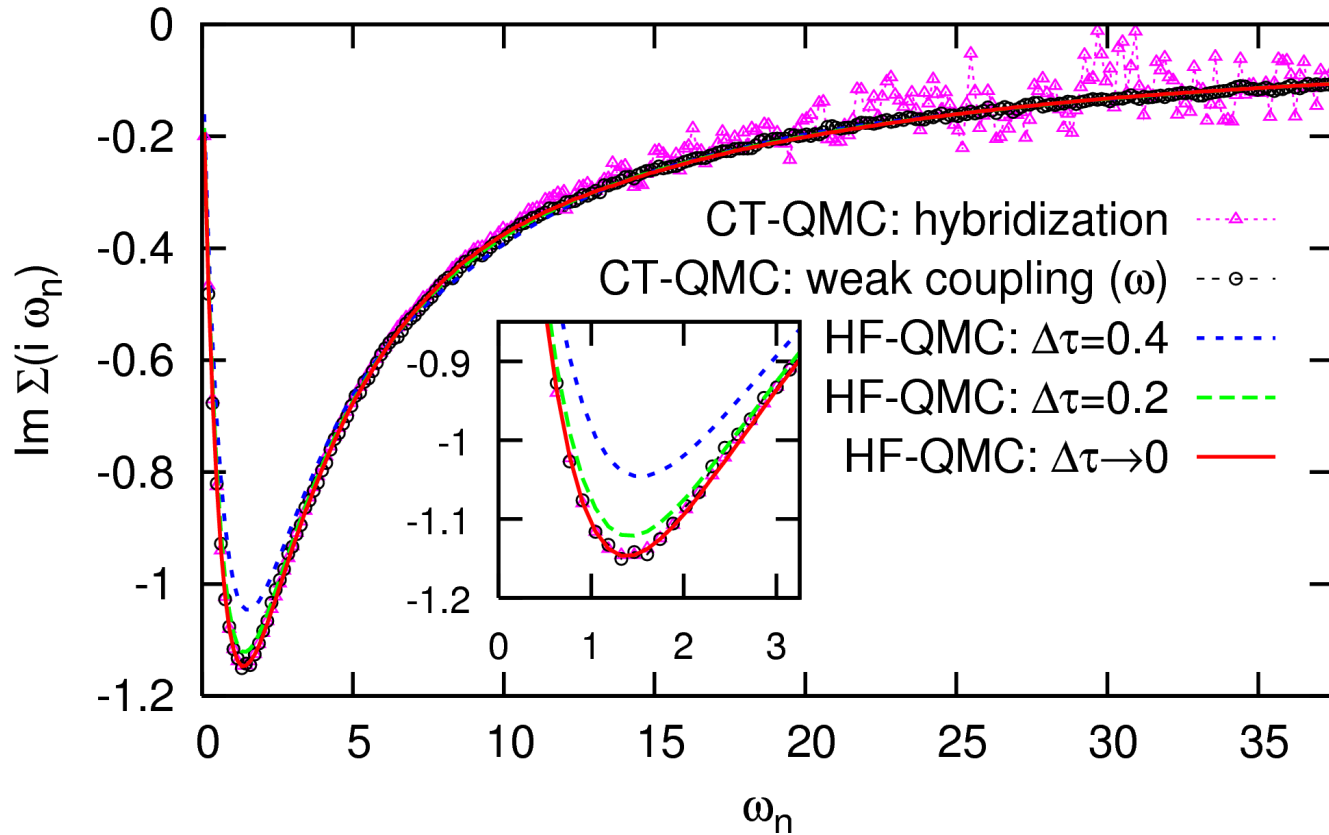
[NB, PRB 76, 205120 (2007)]

# Comparison for total energy (at $U = W = 4$ )



HF-QMC more efficient (higher precision at same cost) [NB, PRB 76, 205120 (2007)]

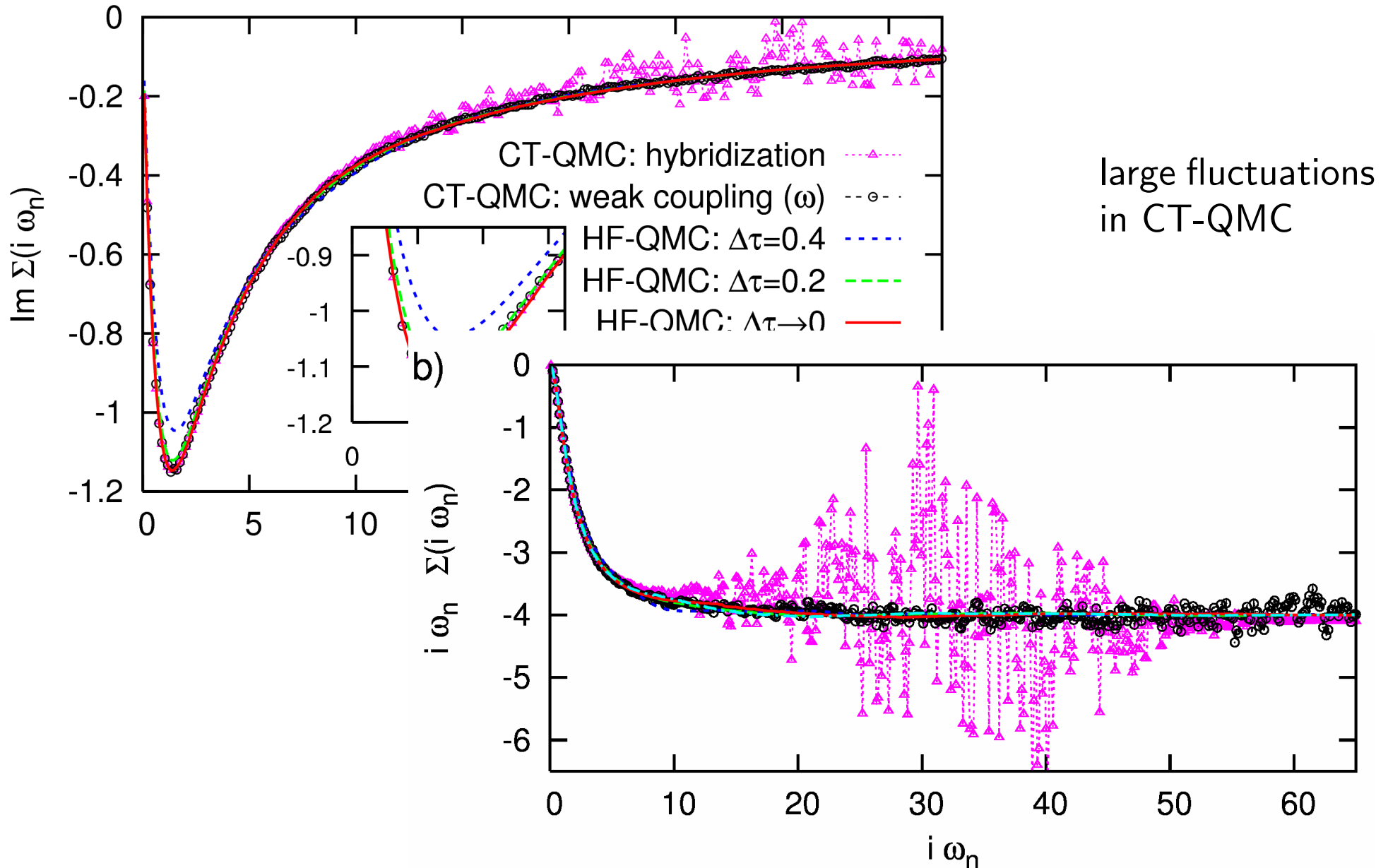
# Comparison of self energies (at $U = W = 4$ )



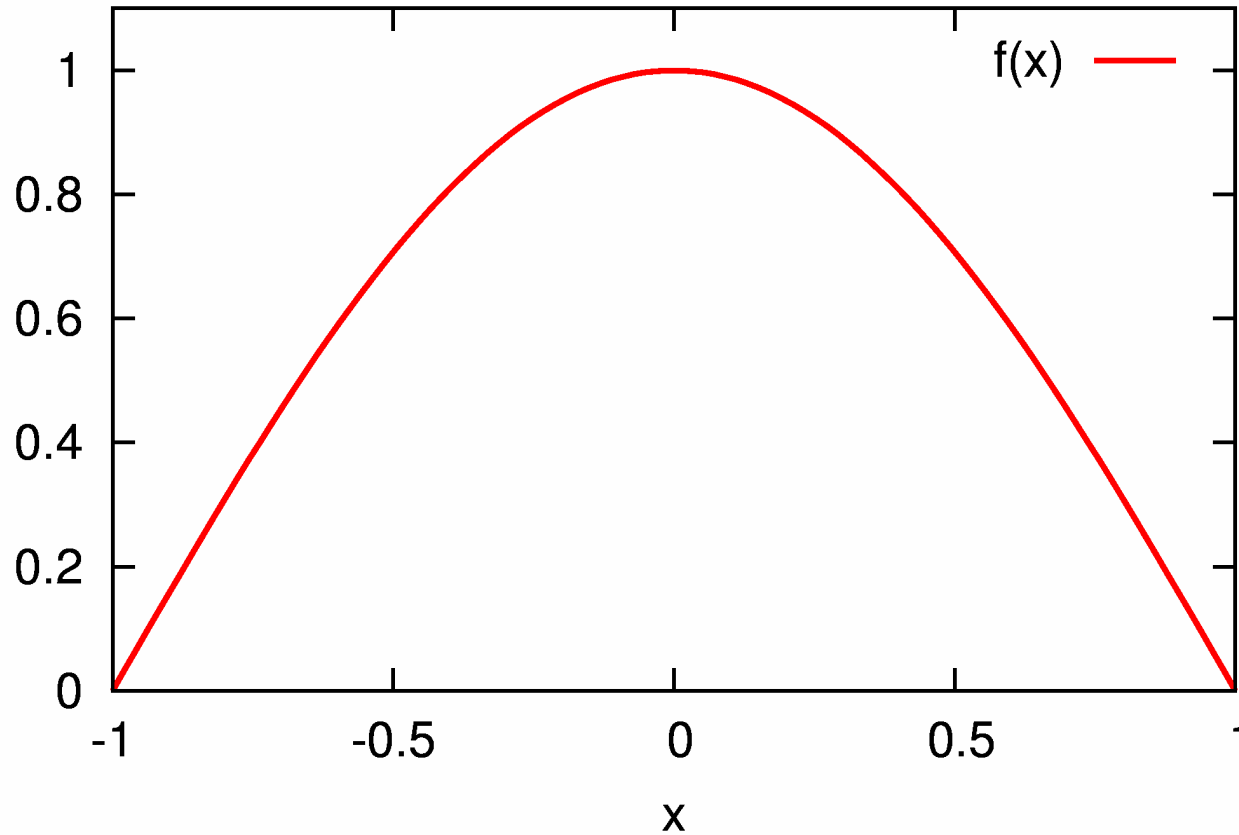
large fluctuations  
in CT-QMC



# Comparison of self energies (at $U = W = 4$ )

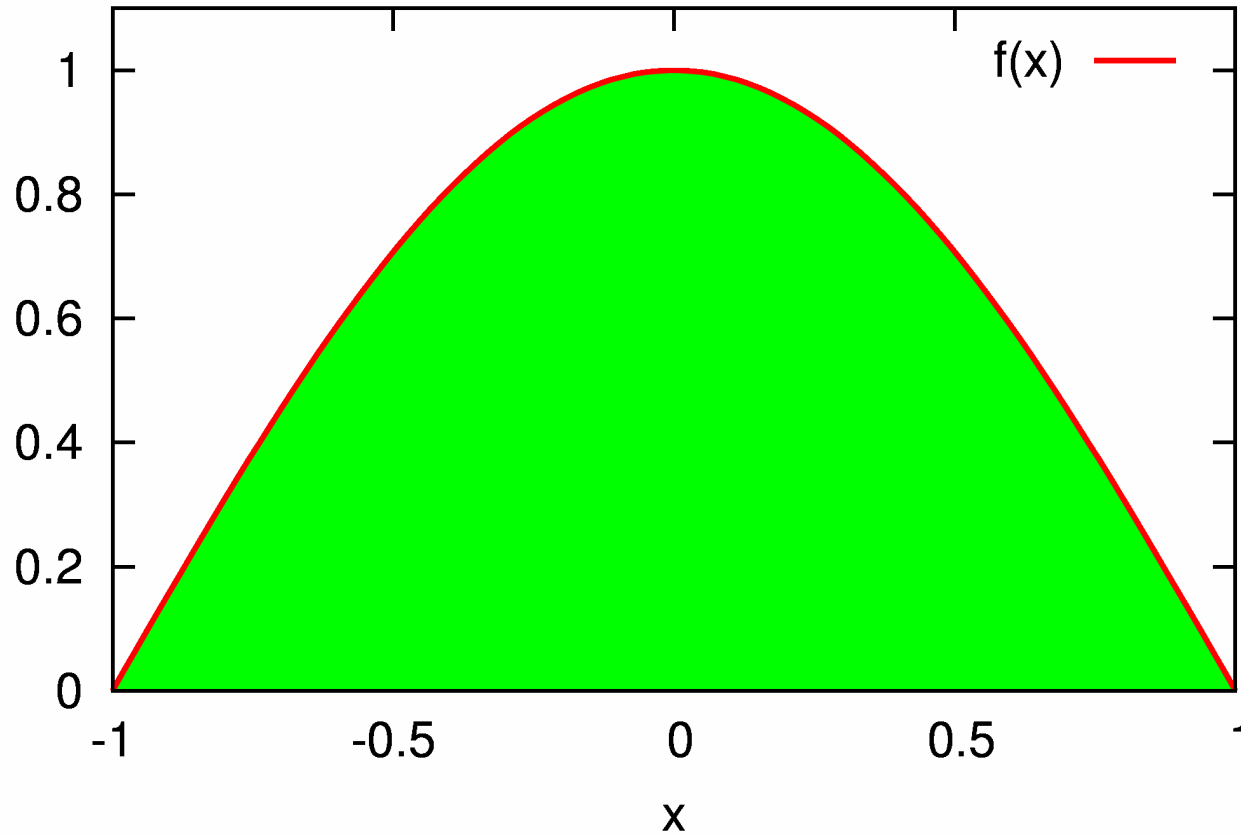


# Excursion: numerical quadrature of a convex function (in $d = 1$ )



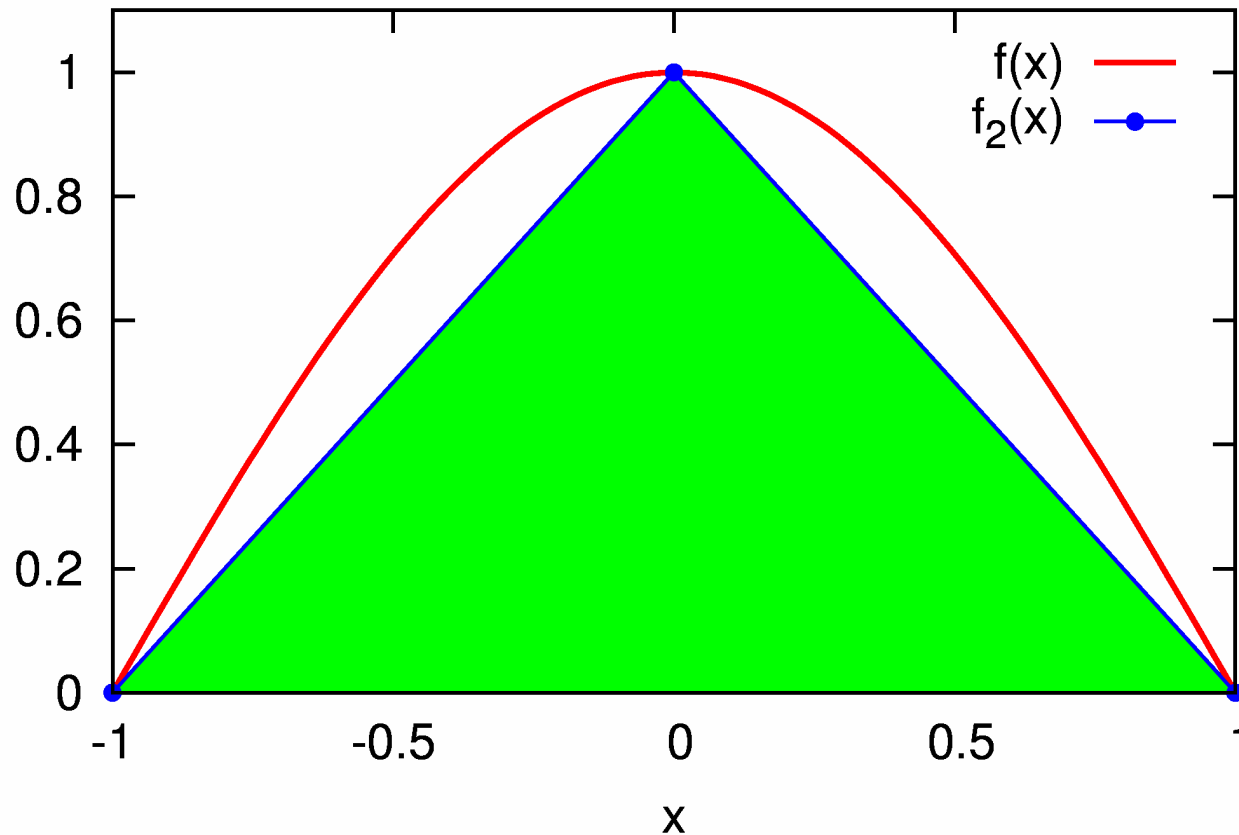
$$I = \int_a^b f(x) dx = ?$$

# Excursion: numerical quadrature of a convex function (in $d = 1$ )



$$I = \int_a^b f(x) dx = ?$$

# Excursion: numerical quadrature of a convex function (in $d = 1$ )

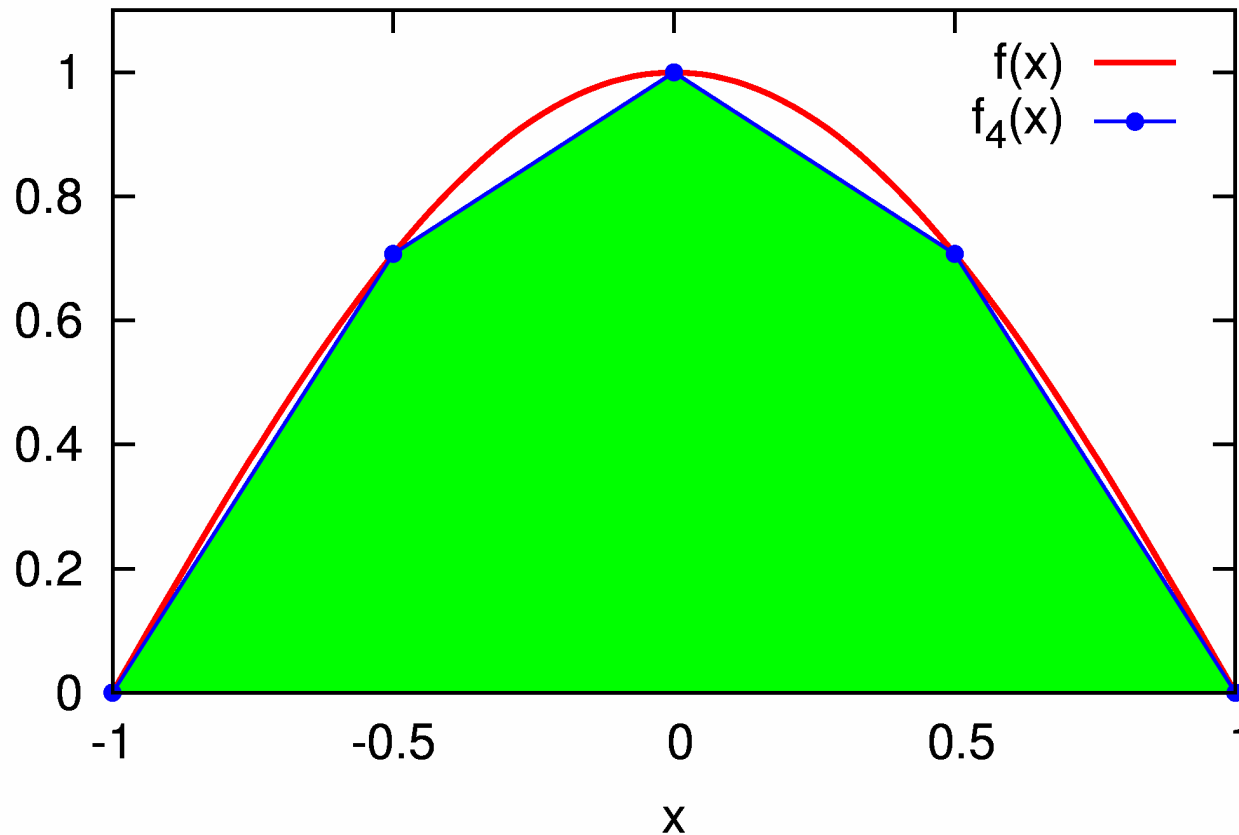


$$I = \int_a^b f(x) dx = ?$$

Numerical methods:

- discretization

# Excursion: numerical quadrature of a convex function (in $d = 1$ )

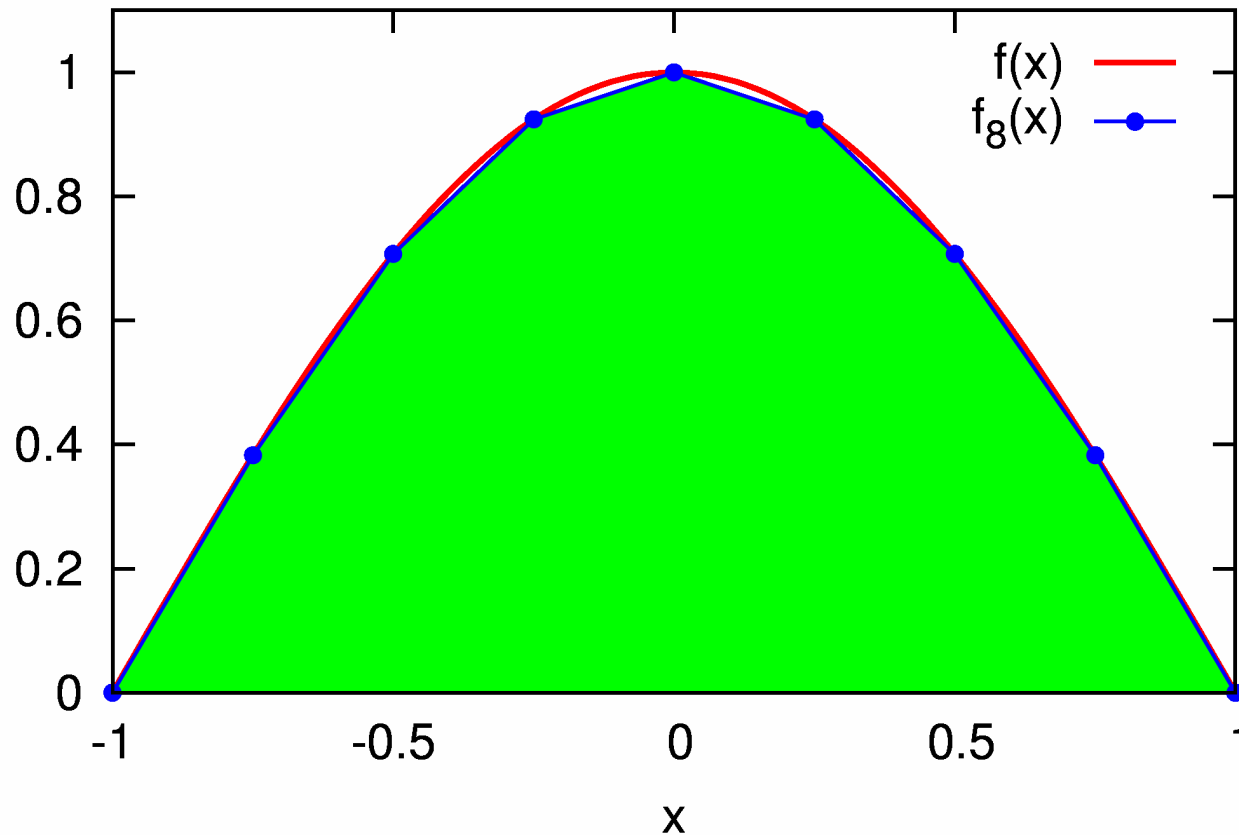


$$I = \int_a^b f(x) dx = ?$$

Numerical methods:

- discretization

# Excursion: numerical quadrature of a convex function (in $d = 1$ )

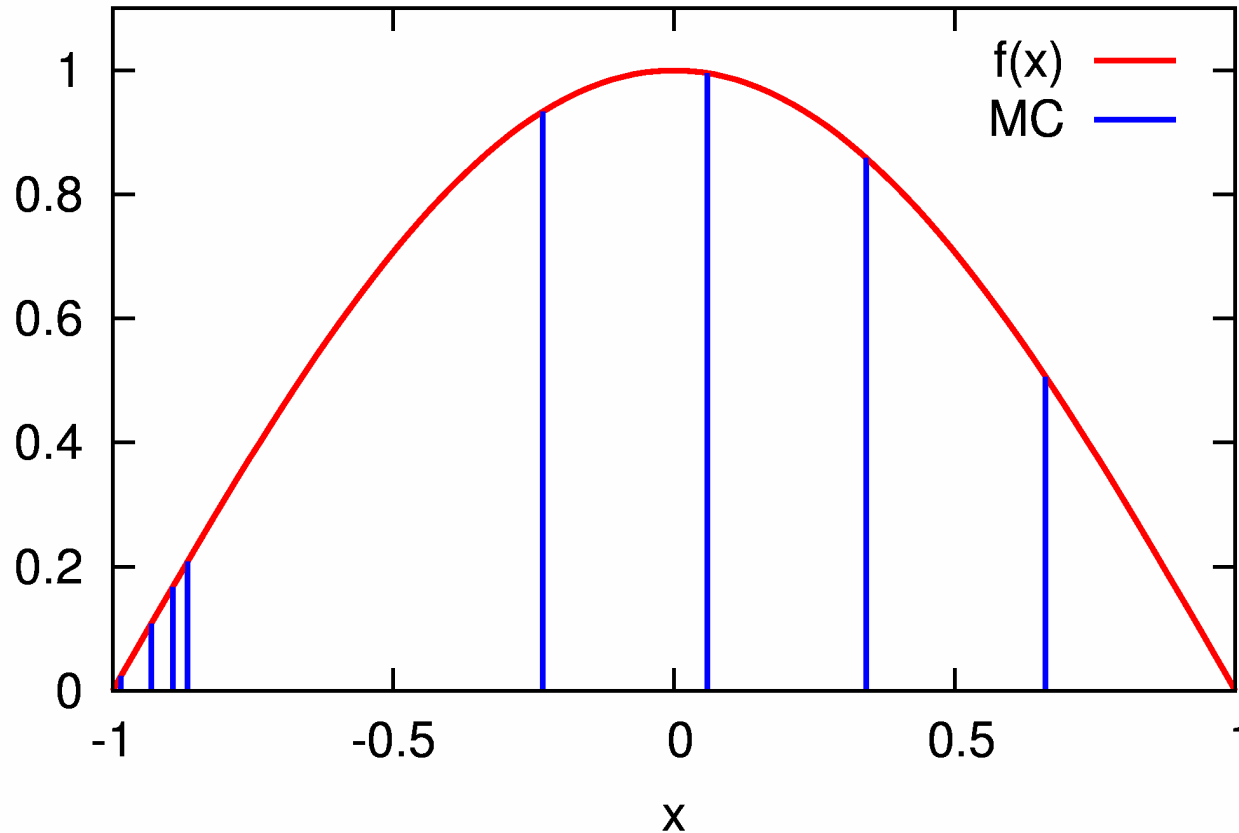


$$I = \int_a^b f(x) dx = ?$$

Numerical methods:

- discretization

## Excursion: numerical quadrature of a convex function (in $d = 1$ )

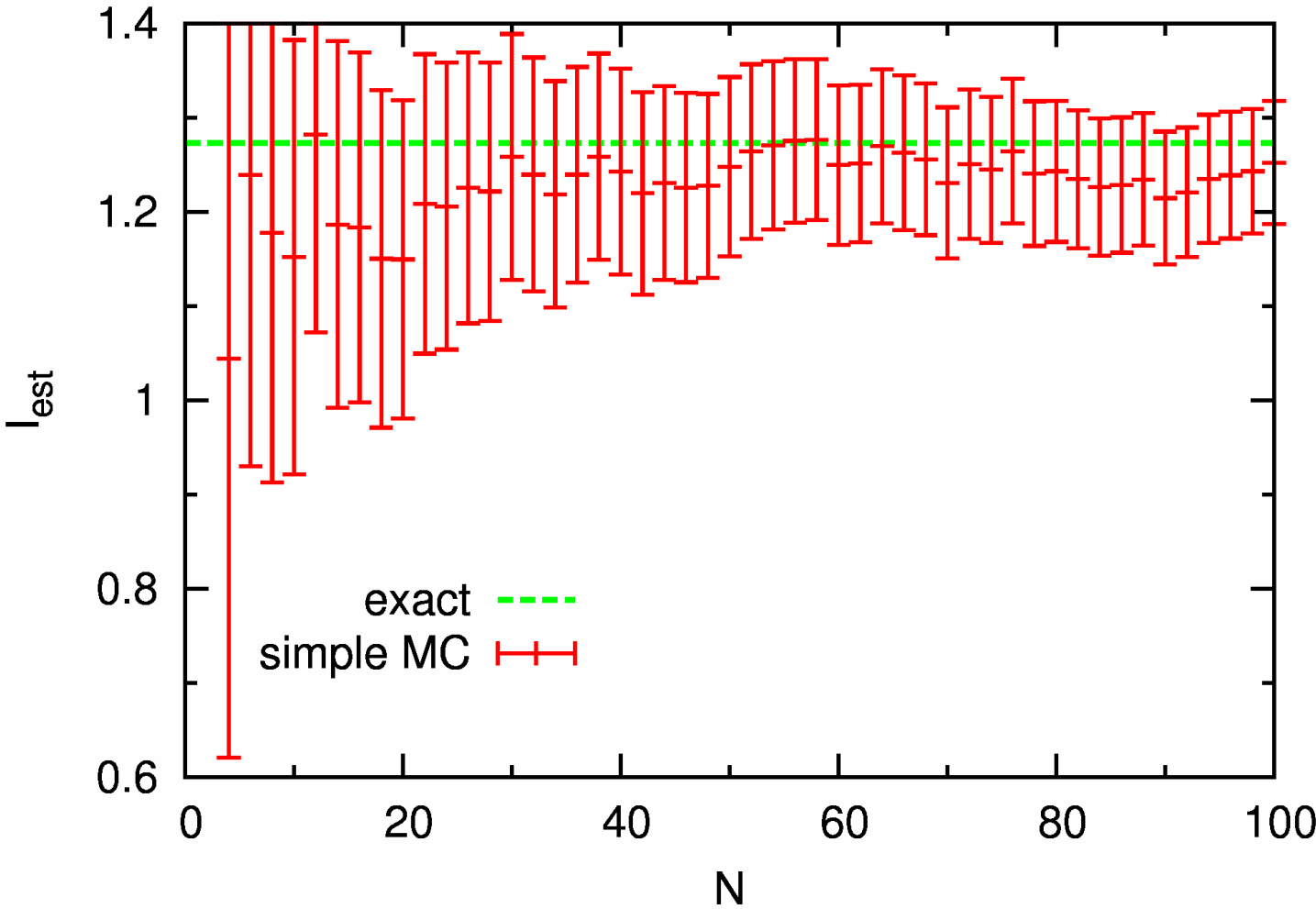


$$I = \int_a^b f(x) dx = ?$$

Numerical methods:

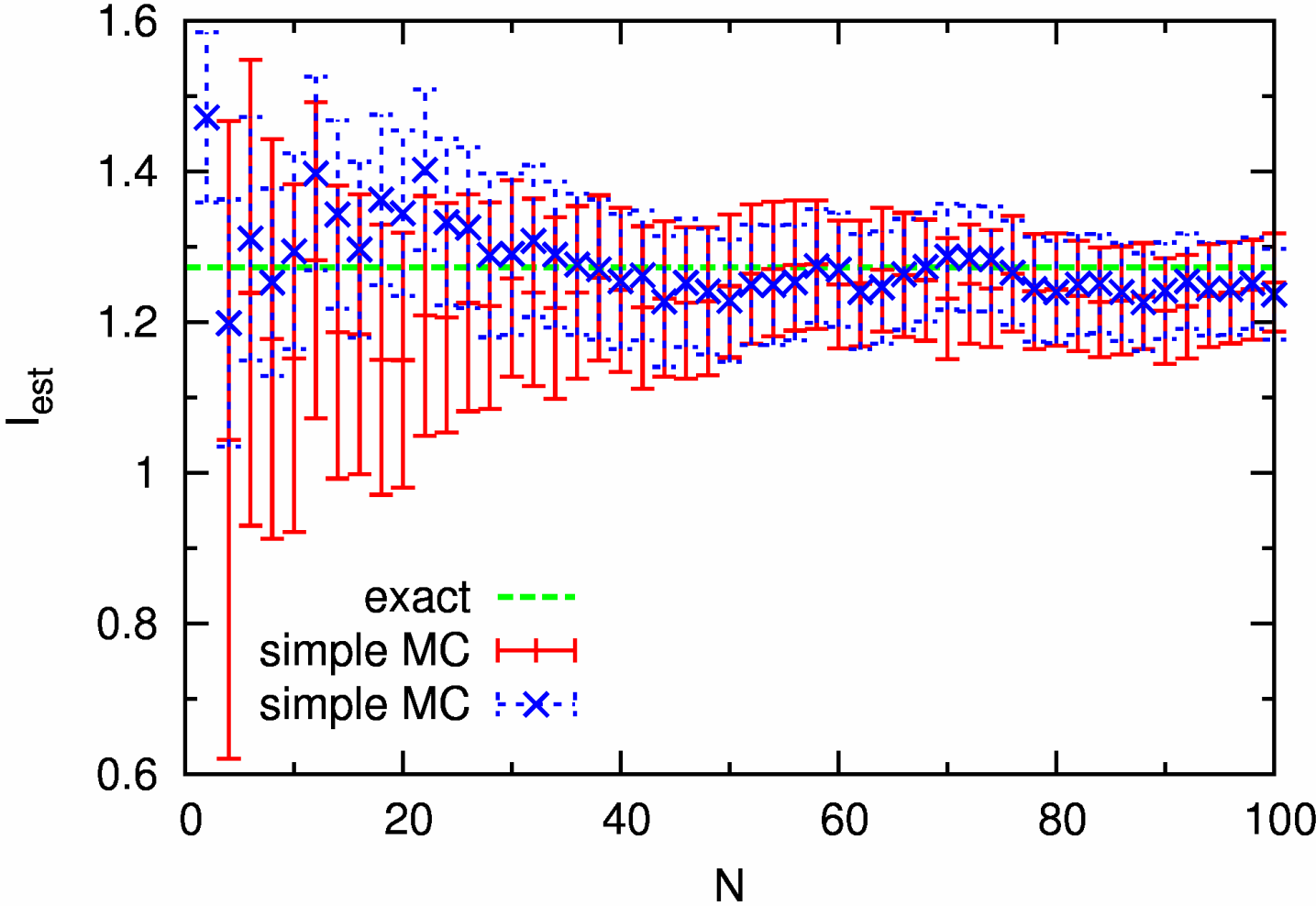
- discretization
- Monte Carlo

# Convergence of results?

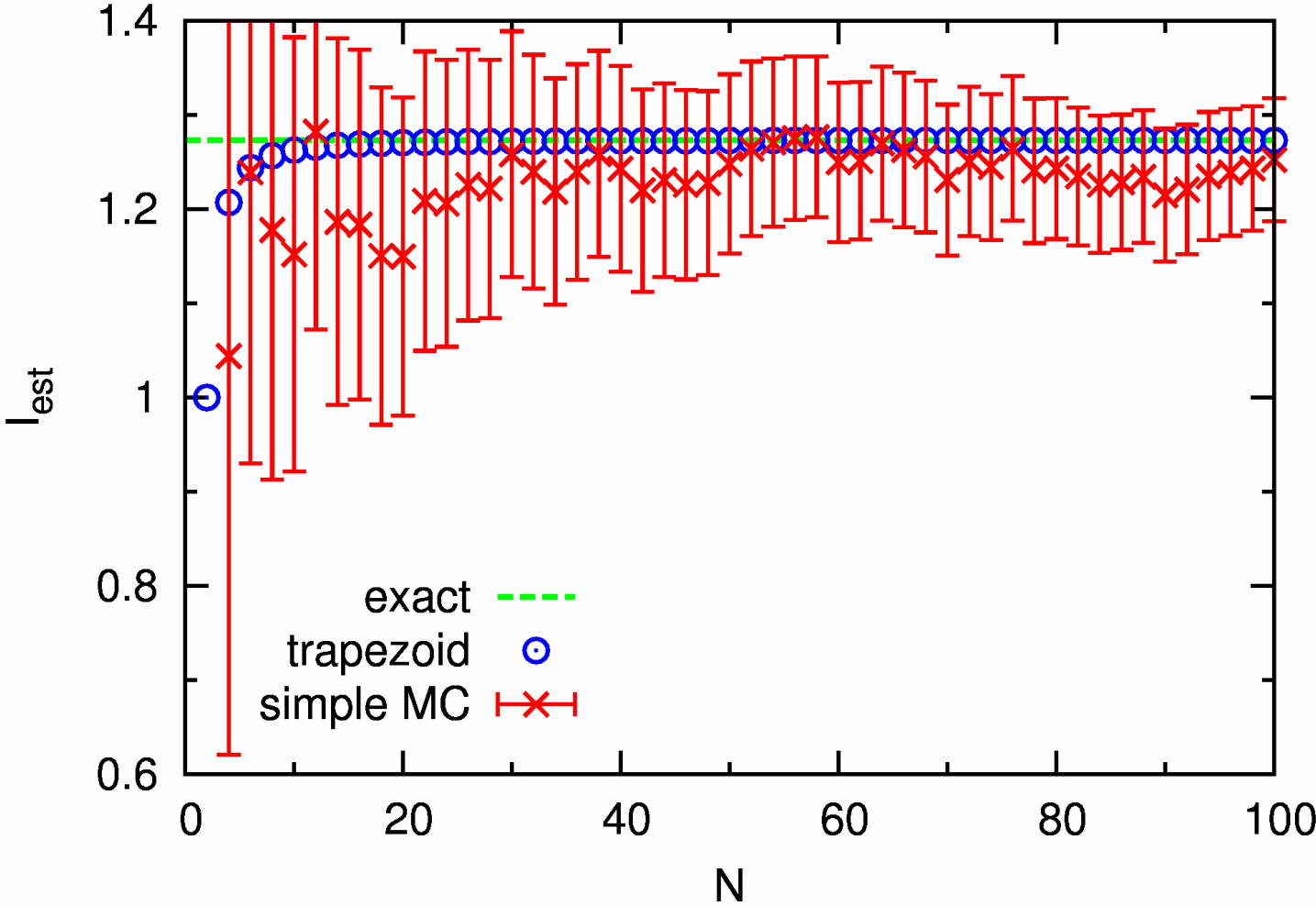




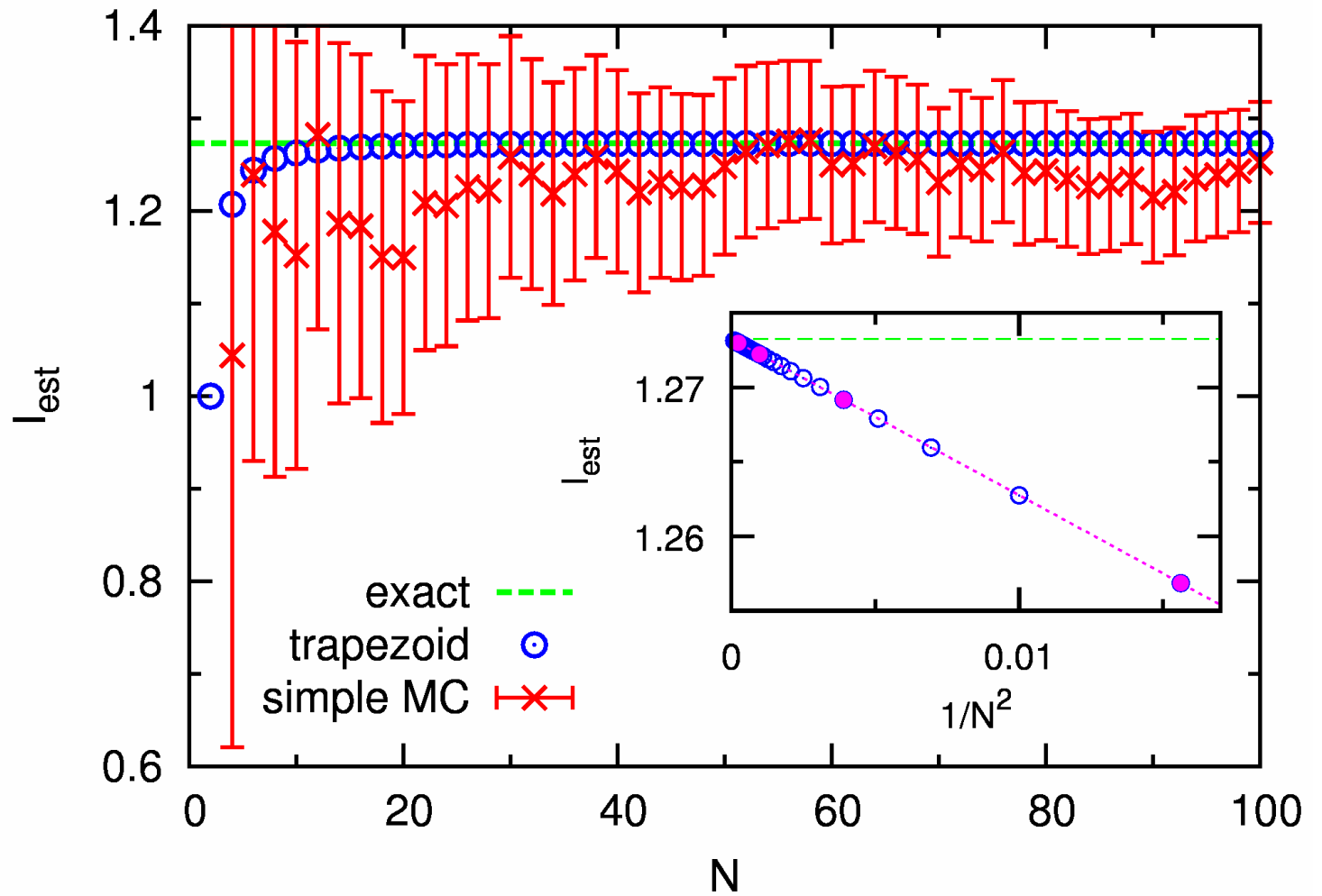
# Convergence of results?



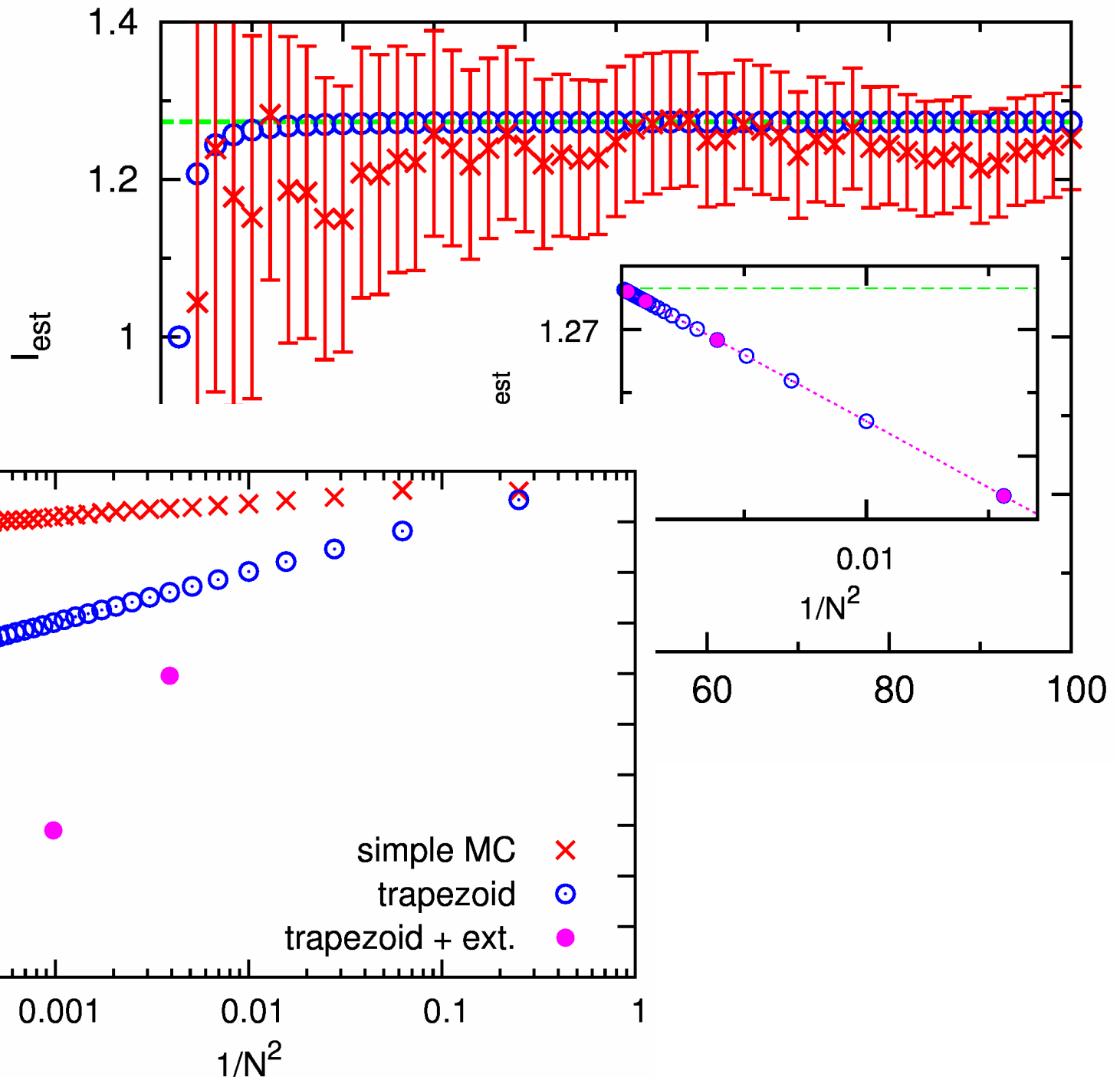
# Convergence of results?



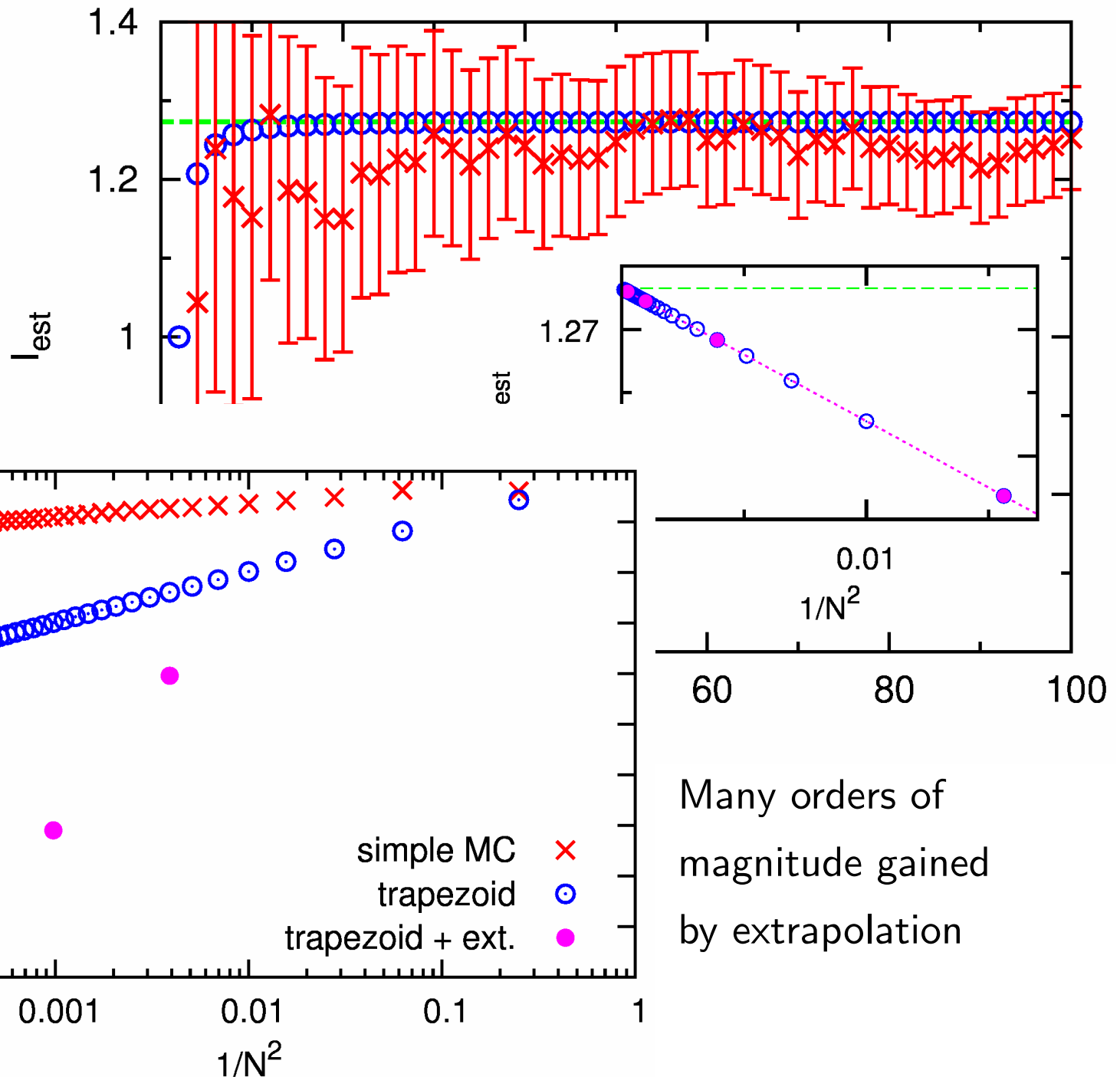
Convergence  
of results?



Convergence  
of results?



Convergence  
of results?



Many orders of  
magnitude gained  
by extrapolation

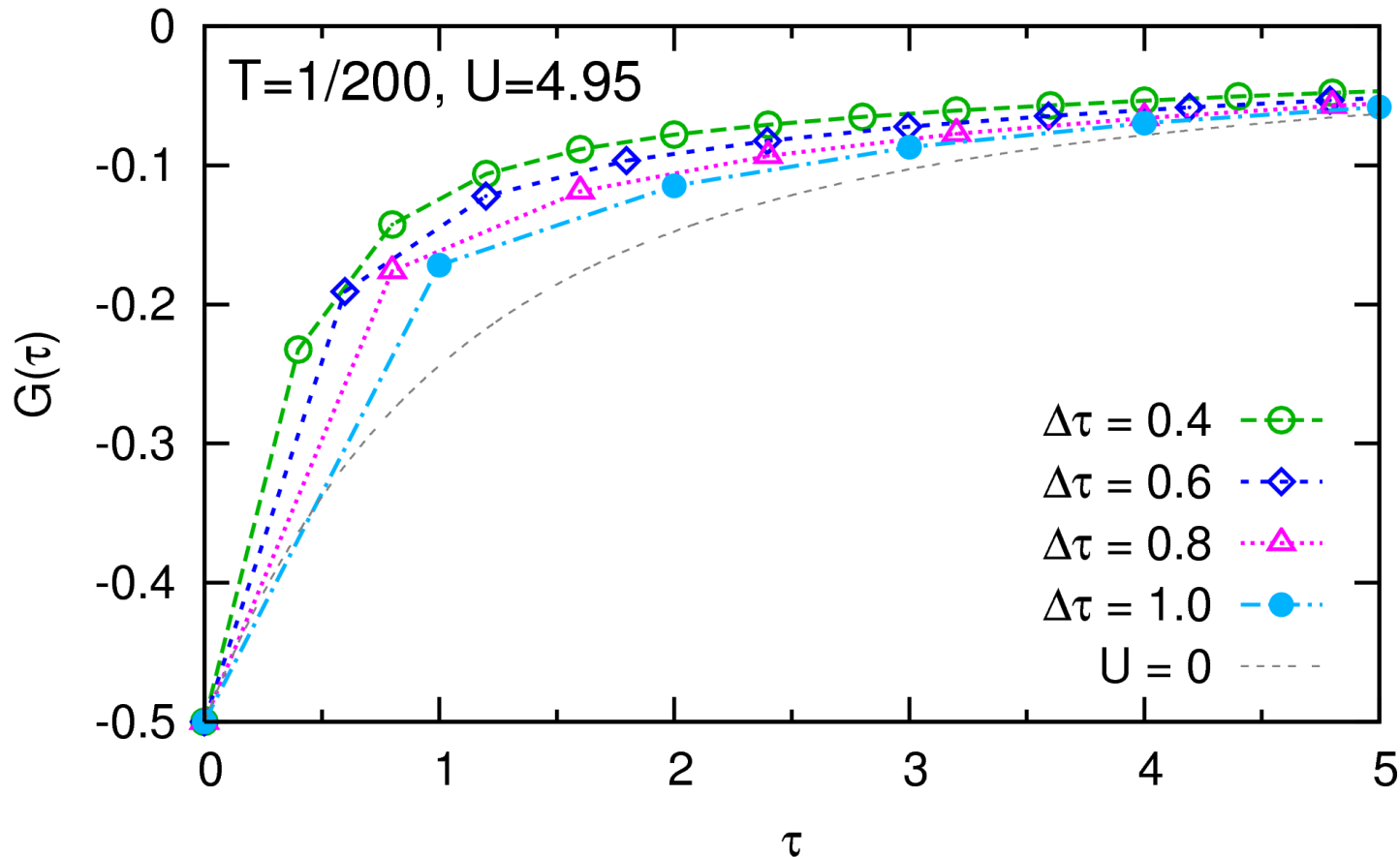
# Unbiased Green functions and spectra from HF-QMC

State of the art: analytic continuation (using MEM) of imaginary-time  
Green function at fixed finite (often large)  $\Delta\tau \rightsquigarrow$  bias

# Unbiased Green functions and spectra from HF-QMC

State of the art: analytic continuation (using MEM) of imaginary-time Green function at fixed finite (often large)  $\Delta\tau \rightsquigarrow$  bias

Reason: no obvious extrapolation scheme for  $G(\tau)$

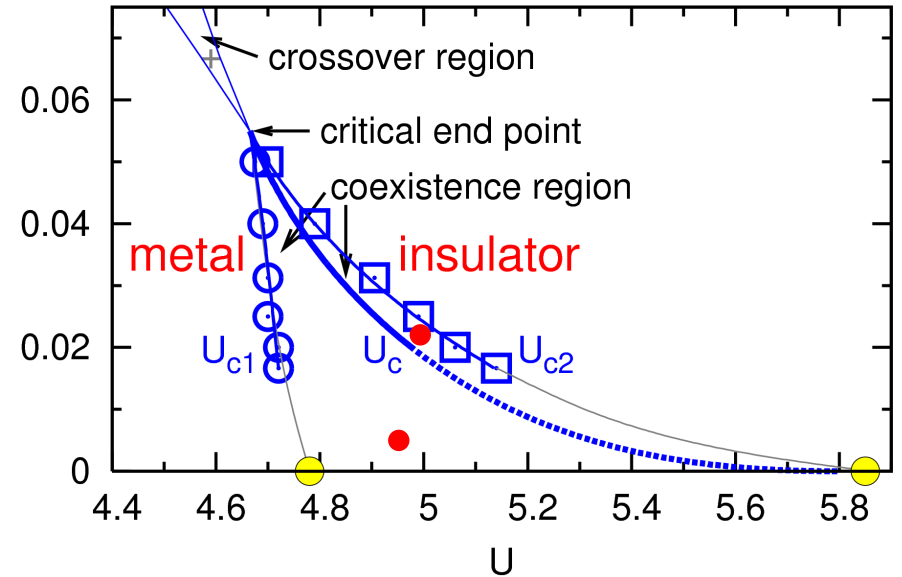
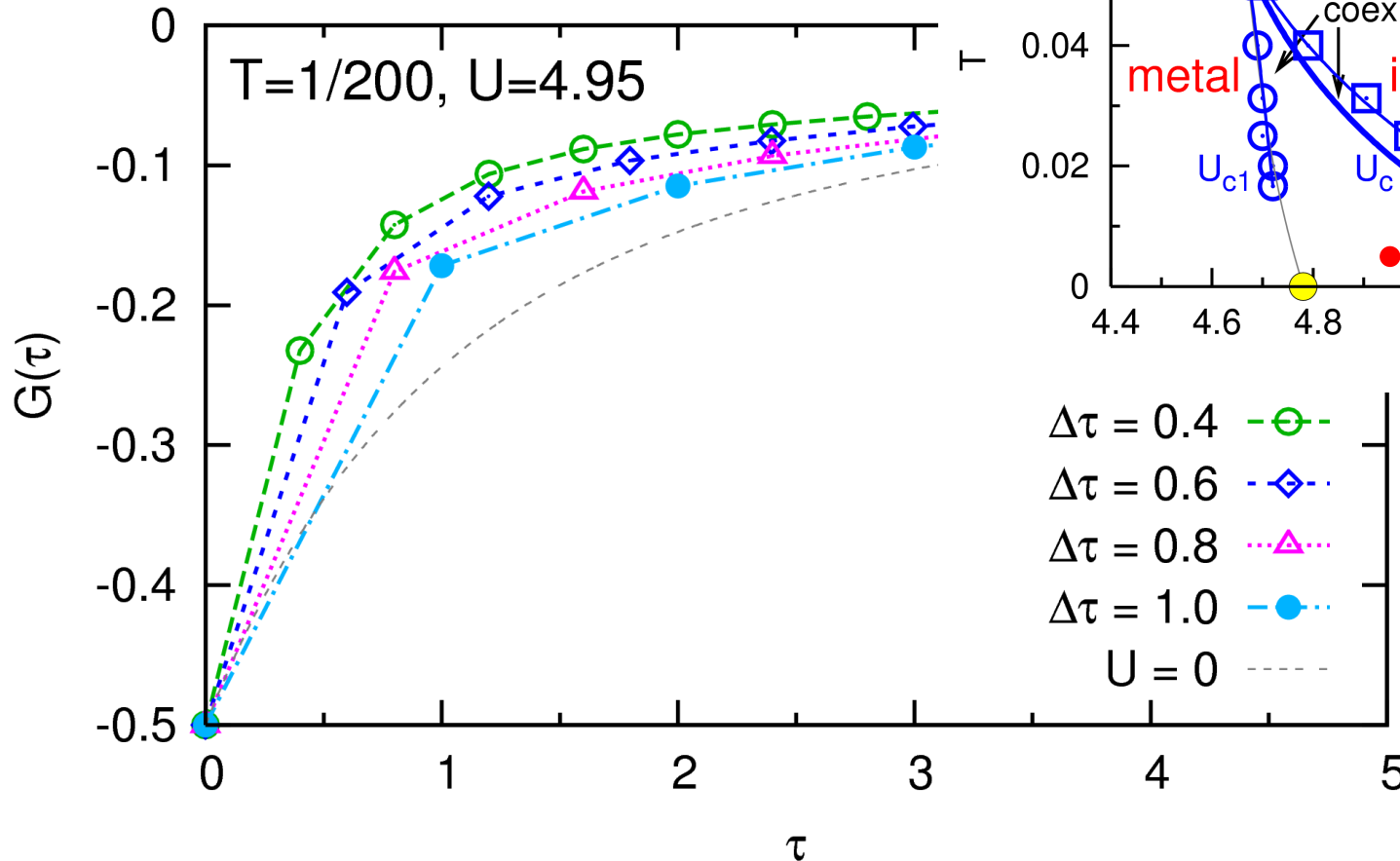


Low temperature (“beyond HF-QMC”): large  $\Delta\tau \rightsquigarrow$  large biases [NB, arXiv:0712.1290]

# Unbiased Green functions and spectra from HF-QMC

State of the art: analytic continuation (using MEM) of imaginary-time Green function at fixed

Reason: no obvious extrapolatic



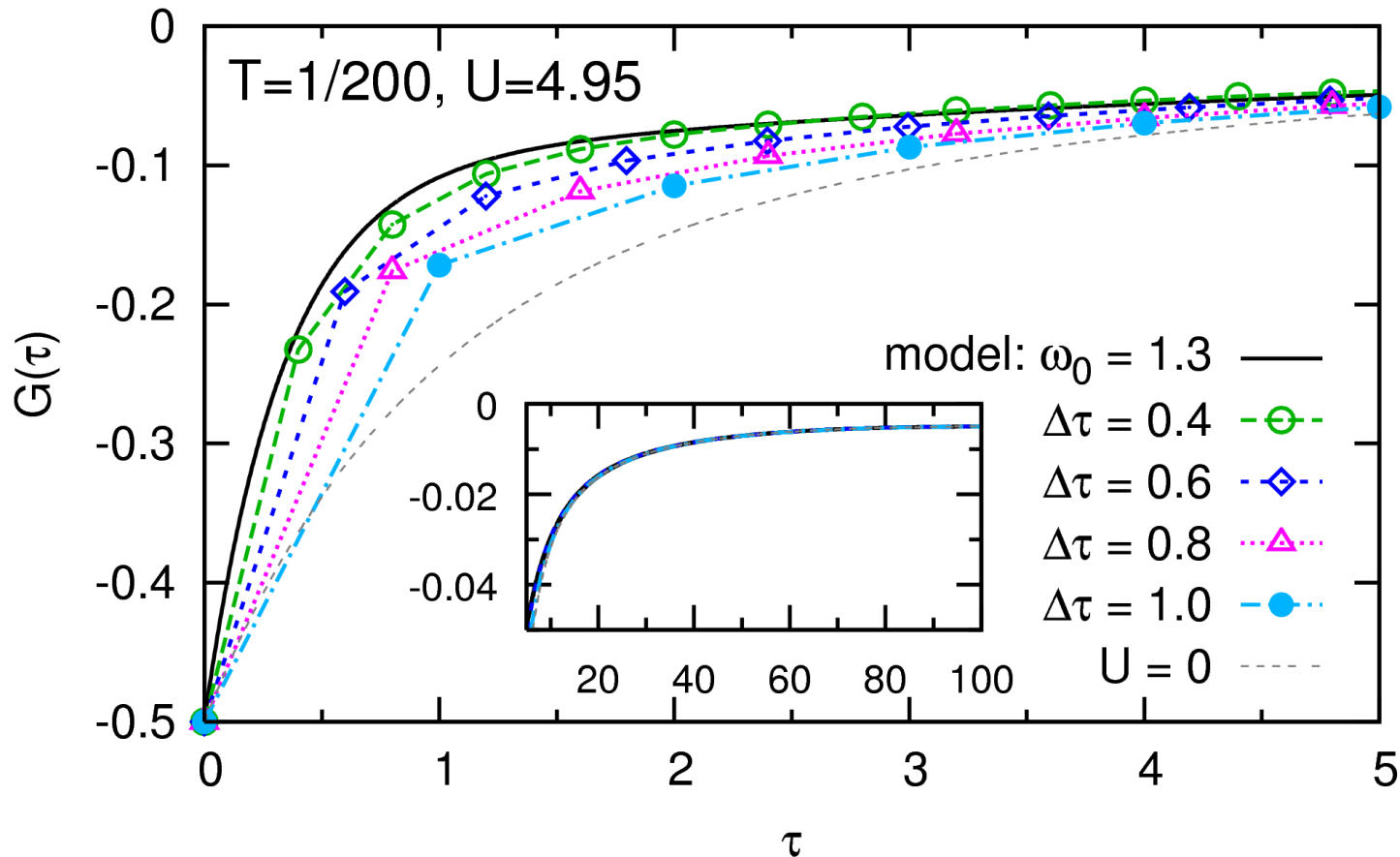
Low temperature (“beyond HF-QMC”): large  $\Delta\tau \rightsquigarrow$  large biases [NB, arXiv:0712.1290]



# Unbiased Green functions and spectra from HF-QMC

State of the art: analytic continuation (using MEM) of imaginary-time Green function at fixed finite (often large)  $\Delta\tau \rightsquigarrow$  bias

Reason: no obvious extrapolation scheme for  $G(\tau)$



Low temperature (“beyond HF-QMC”): large  $\Delta\tau \rightsquigarrow$  large biases [NB, arXiv:0712.1290]

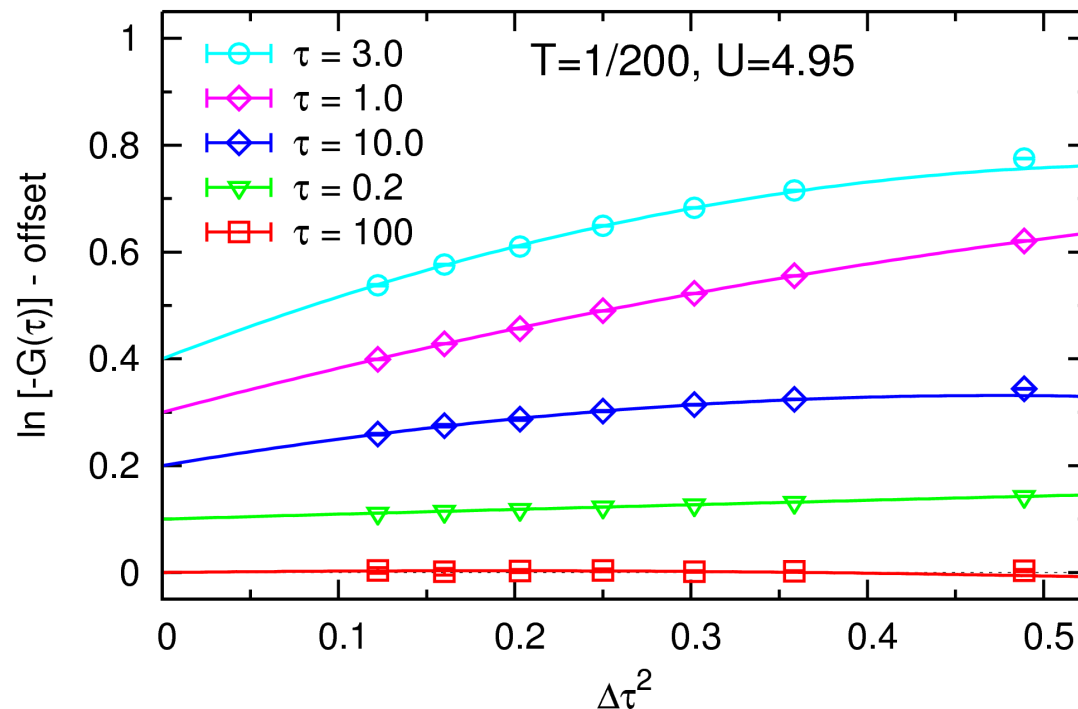
# New Green function extrapolation scheme

- For each  $\Delta\tau$ :
- average  $G_{\Delta\tau}(\tau)$  over parallel runs for same impurity model
  - average  $\log[-G_{\Delta\tau}(\tau)]$  over iterations ( $\sim$  geometric av. for  $G_{\Delta\tau}(\tau)$ )
  - interpolate via difference Green function  $G_{\Delta\tau}(\tau) - G_{\text{model}}(\tau)$

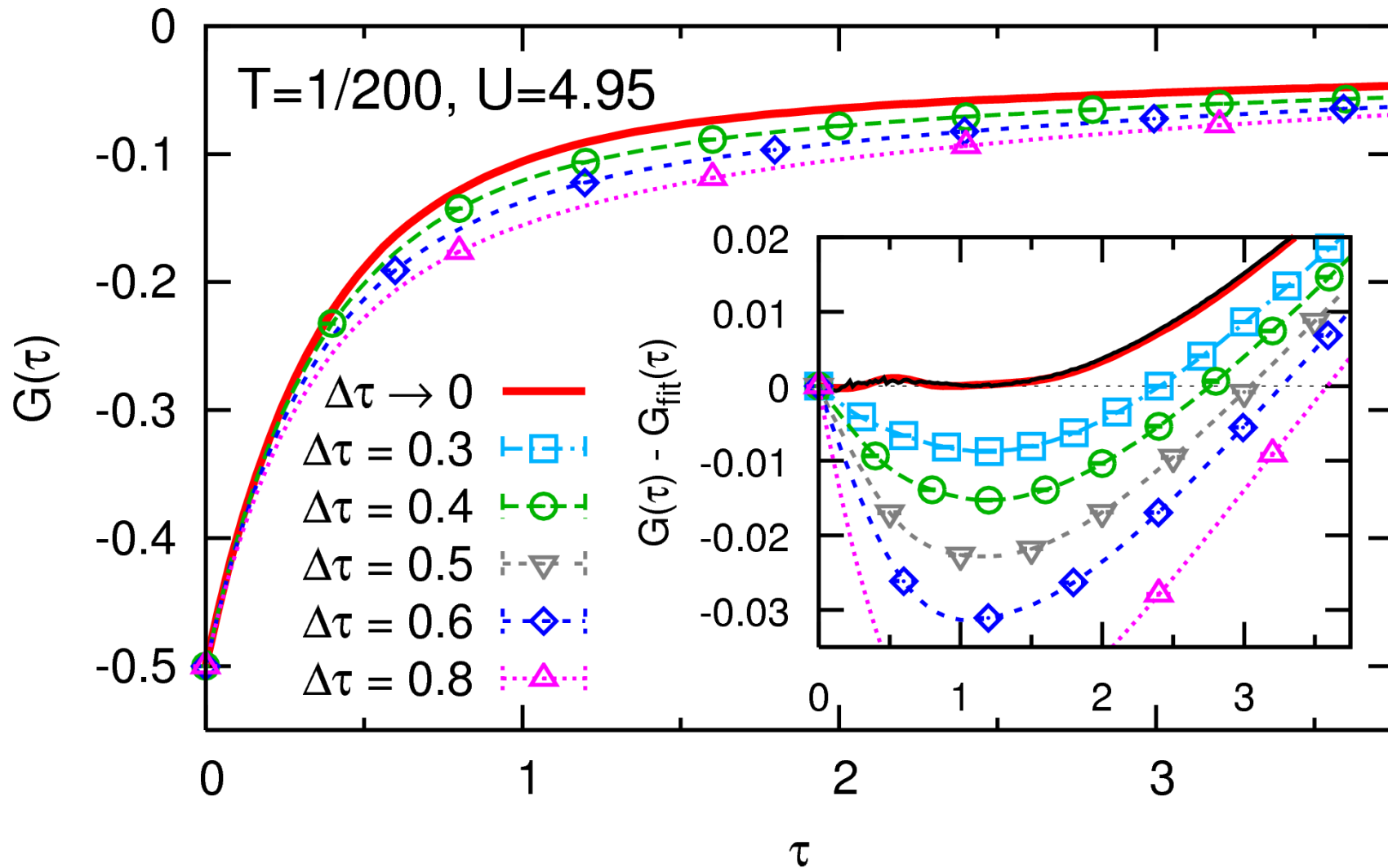
$\rightsquigarrow G_{\Delta\tau_1}, G_{\Delta\tau_2}, \dots, G_{\Delta\tau_n}$  (with error bars) on common fine  $\tau$  grid

# New Green function extrapolation scheme

- For each  $\Delta\tau$ :
- average  $G_{\Delta\tau}(\tau)$  over parallel runs for same impurity model
  - average  $\log[-G_{\Delta\tau}(\tau)]$  over iterations ( $\sim$  geometric av. for  $G_{\Delta\tau}(\tau)$ )
  - interpolate via difference Green function  $G_{\Delta\tau}(\tau) - G_{\text{model}}(\tau)$
- $\rightsquigarrow G_{\Delta\tau_1}, G_{\Delta\tau_2}, \dots, G_{\Delta\tau_n}$  (with error bars) on common fine  $\tau$  grid
- Extrapolate  $\log[-G(\tau)]$  using cubic least-squares fits, overweighting low  $\Delta\tau$



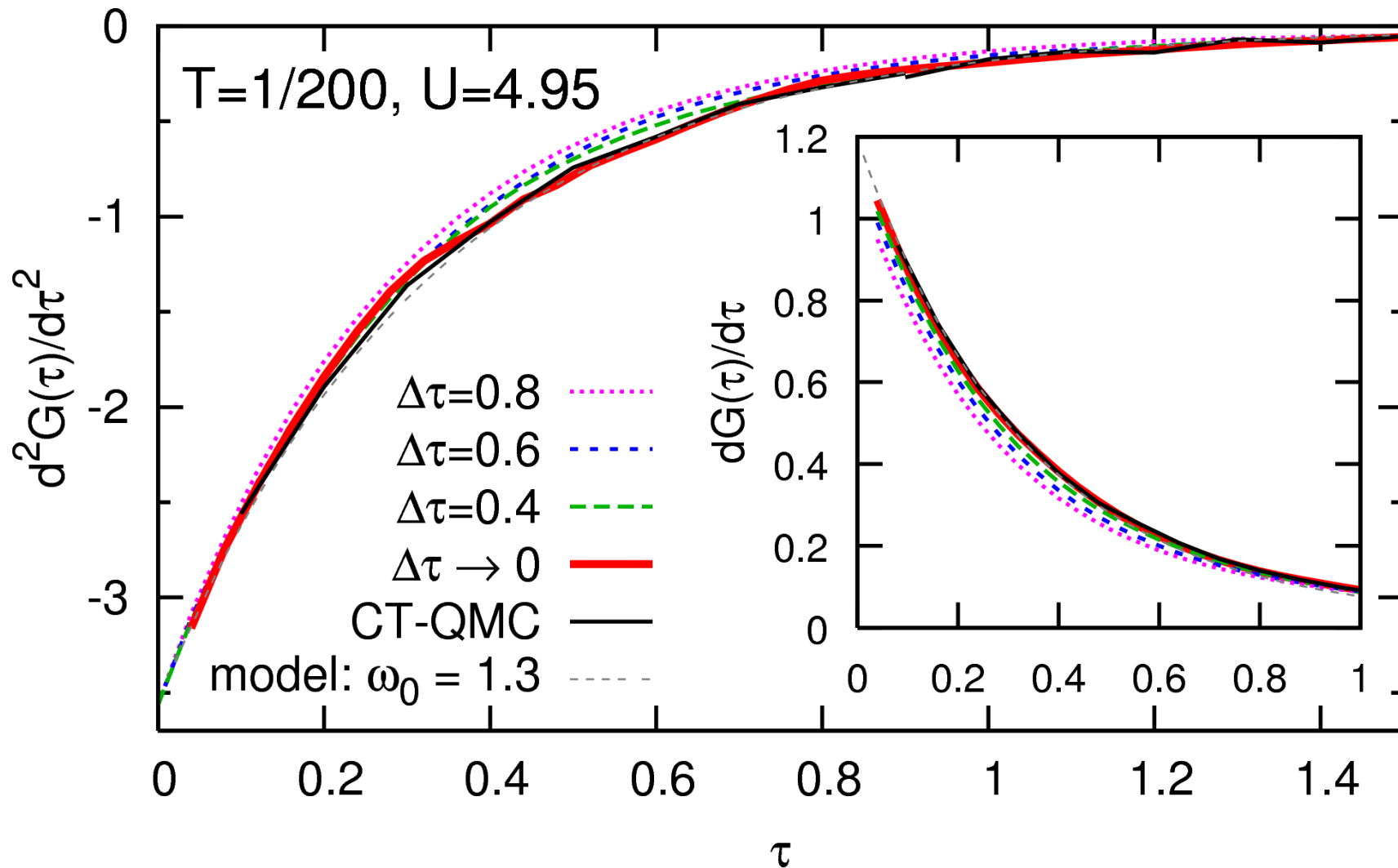
# Result: unbiased, numerically exact Green function



[NB, arXiv:0712.1290]

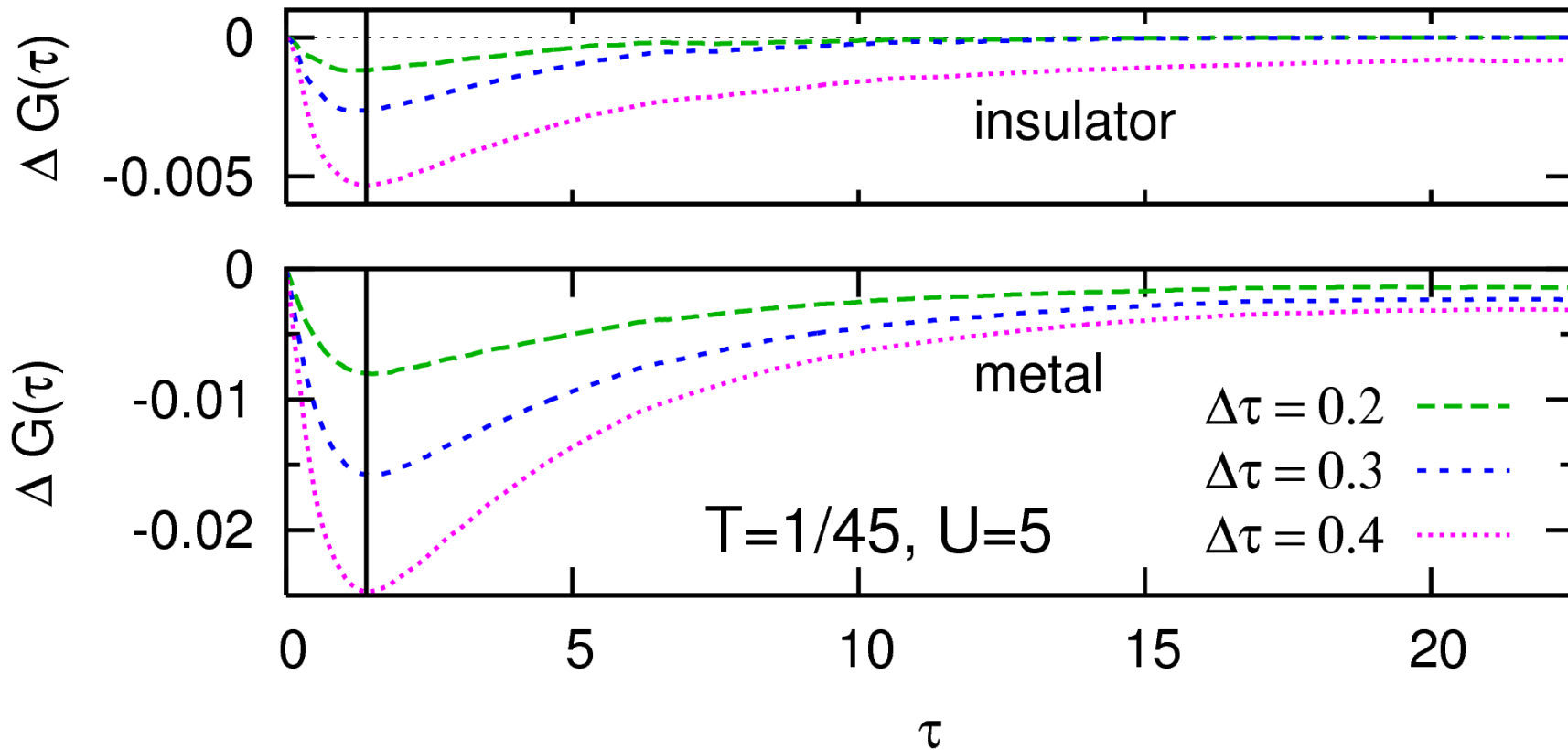
Excellent agreement with hybridization expansion CT-QMC [Werner et al., PRL (2006)]

## 2<sup>nd</sup> and 1<sup>st</sup> order derivatives of Green function



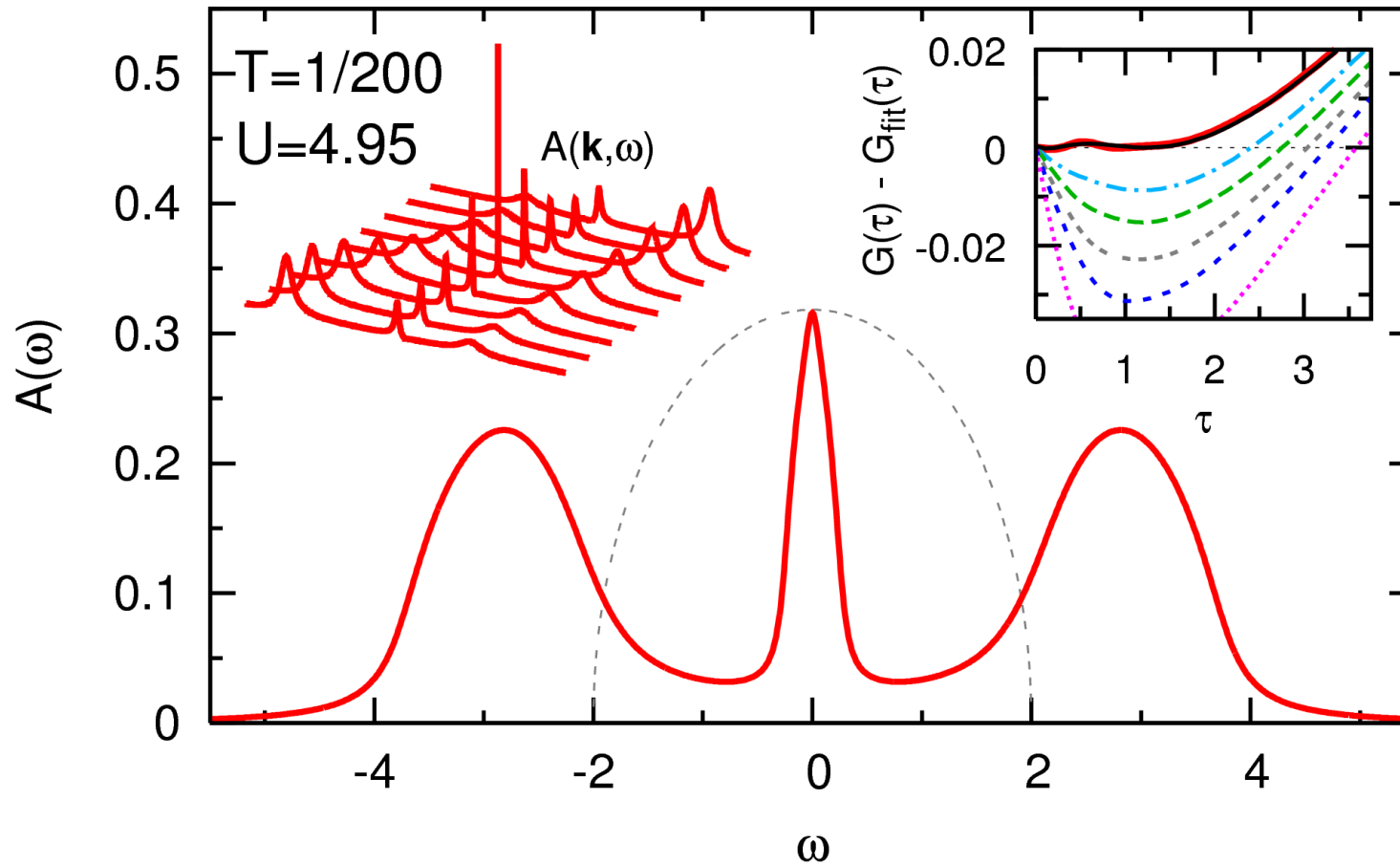
Exact asymptotics  $\left. \frac{d^2 G(\tau)}{d\tau^2} \right|_{\tau=0+} = -\frac{1}{2} \left( 1 + \frac{U^2}{4} \right);$   $\left. \frac{dG(\tau)}{d\tau} \right|_{\tau=0+}$  nonuniversal

Low- $\tau$  resolution limited by  $\Delta\tau$ ? **No!**



Uniform  $\Delta\tau$  dependence, position of max. error independent of  $\Delta\tau$  and phase!

# Analytic continuation using Padé approximant for self-energy



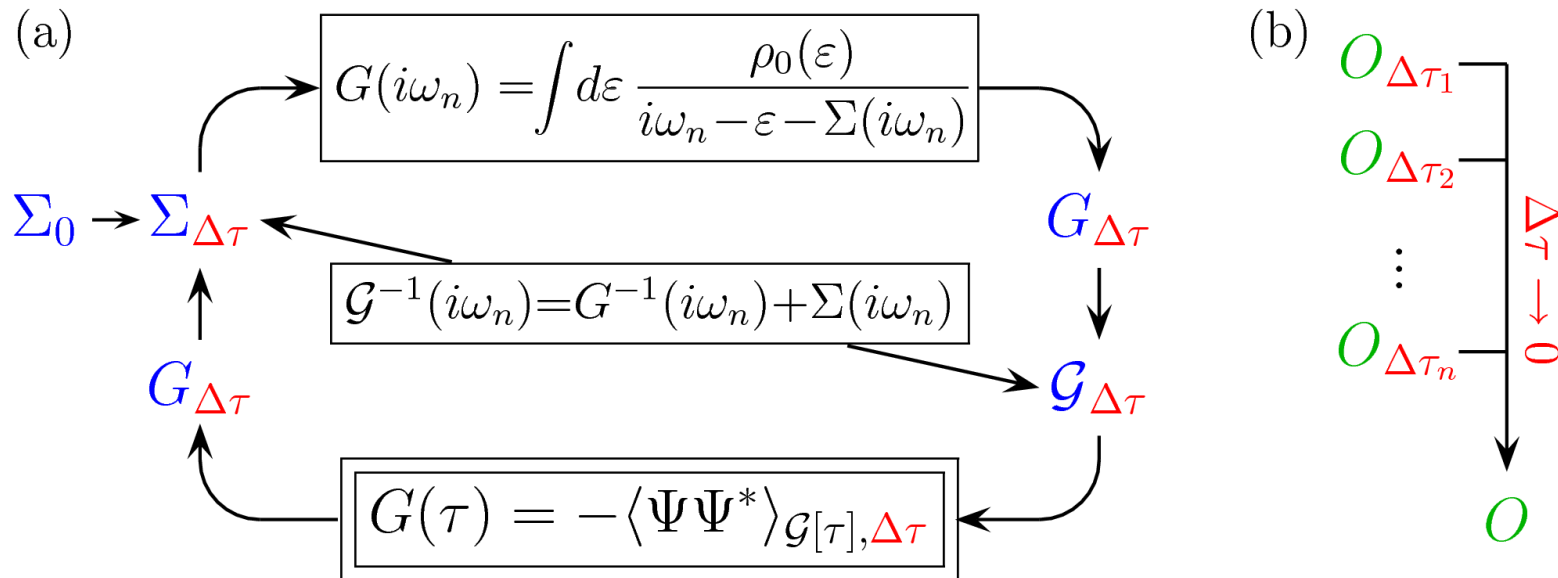
First spectra without discretization error from HF-QMC, at ultra-low  $T$

Method directly applicable, e.g., to LDA+DMFT calculations [NB, [arXiv:0712.1290](https://arxiv.org/abs/0712.1290)]

# Multigrid Hirsch-Fye quantum Monte Carlo algorithm

State of the art: (a) conventional HF-QMC

(b) *a posteriori* extrapolation of selected observables

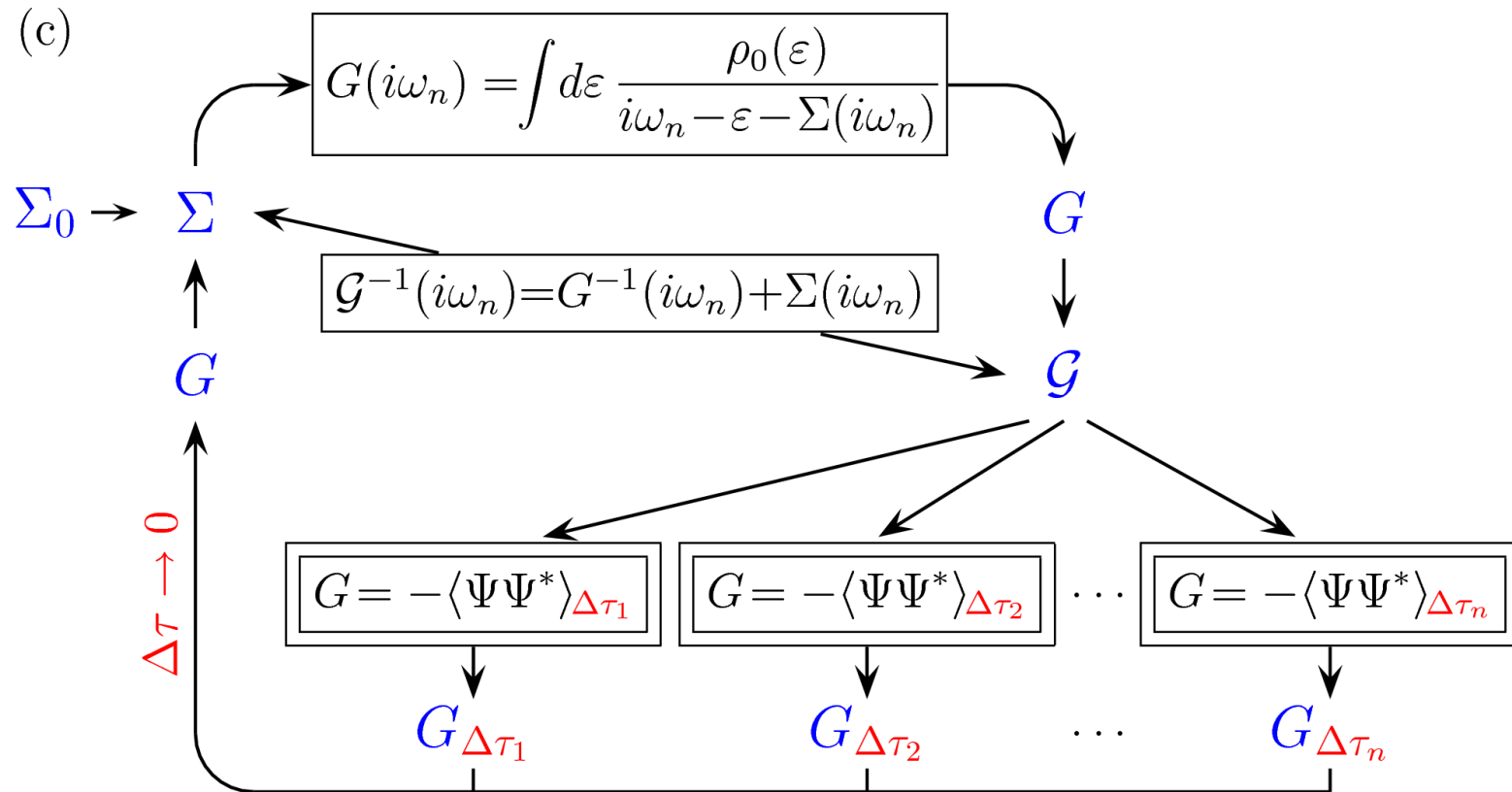




# Multigrid Hirsch-Fye quantum Monte Carlo algorithm

State of the art: (a) conventional HF-QMC

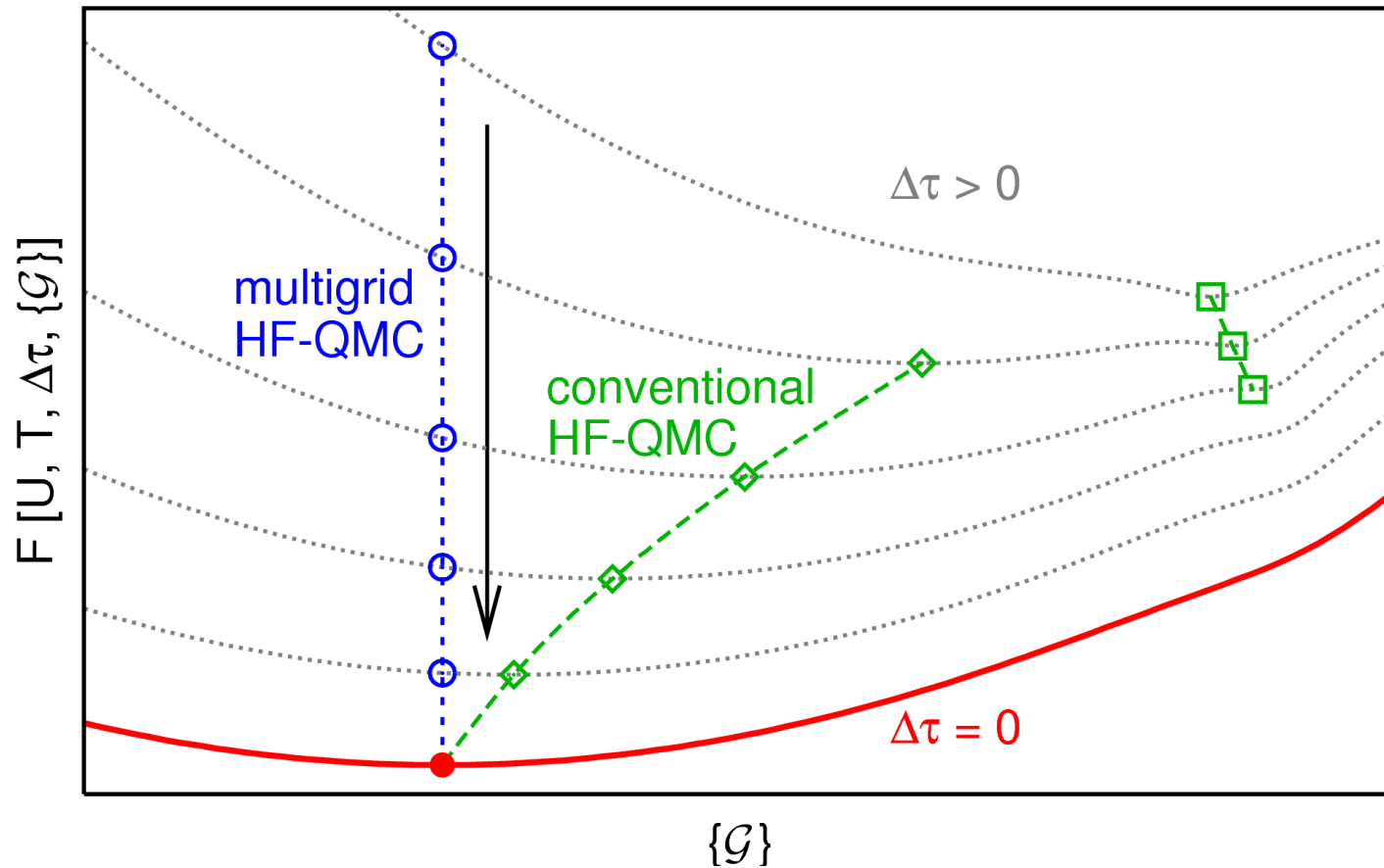
(b) *a posteriori* extrapolation of selected observables



(c) Multigrid HF-QMC: internal elimination of Trotter error

$\rightsquigarrow$  quasi continuous time algorithm [NB, arXiv:0801.1222]

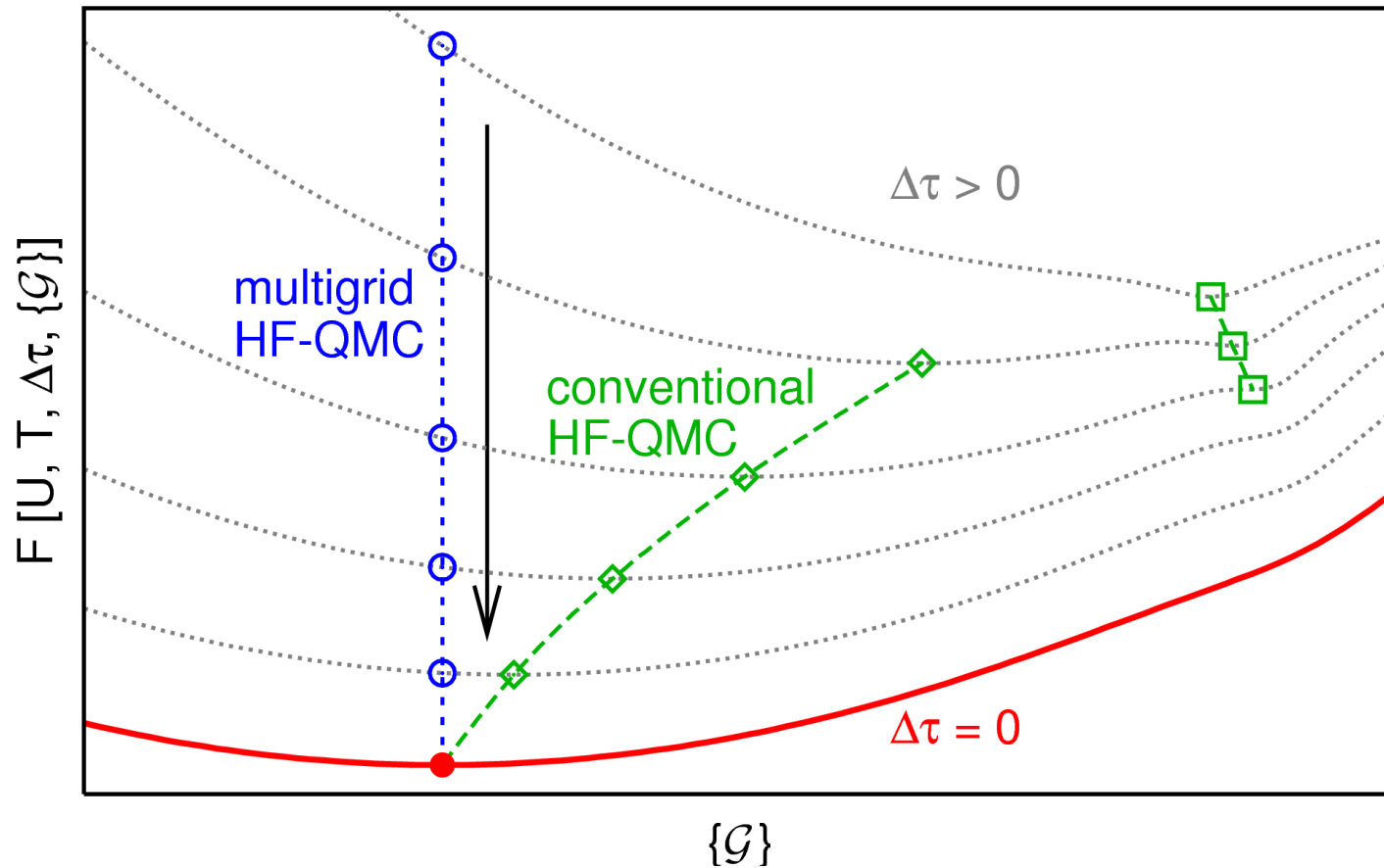
# Schematic comparison via generalized Ginzburg-Landau functionals



Conventional Hirsch-Fye QMC: DMFT fixed point shifts with  $\Delta\tau$

Multigrid Hirsch-Fye QMC: DMFT iteration towards exact fixed point

# Schematic comparison via generalized Ginzburg-Landau functionals

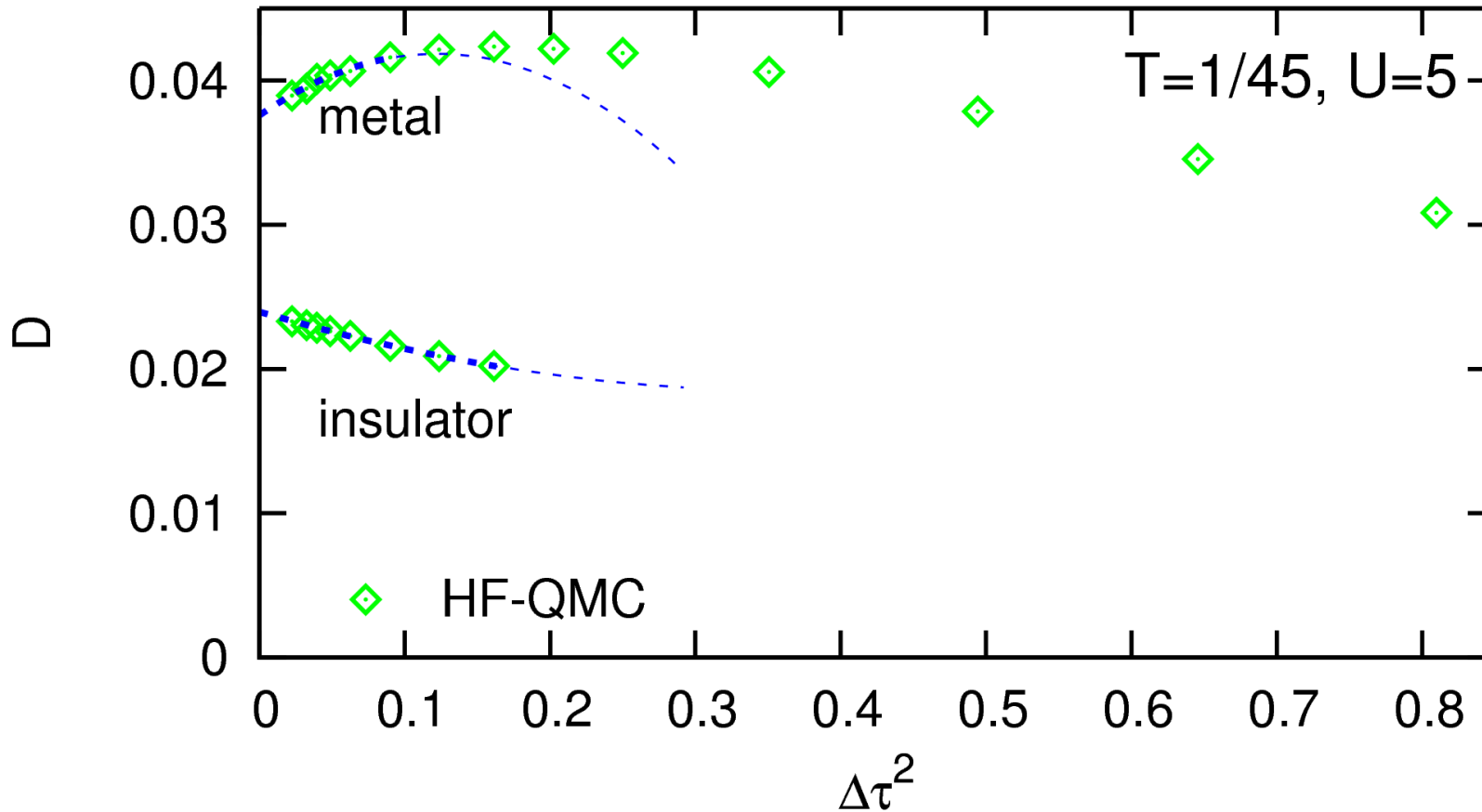


Conventional Hirsch-Fye QMC: DMFT fixed point shifts with  $\Delta\tau$

Multigrid Hirsch-Fye QMC: DMFT iteration towards exact fixed point

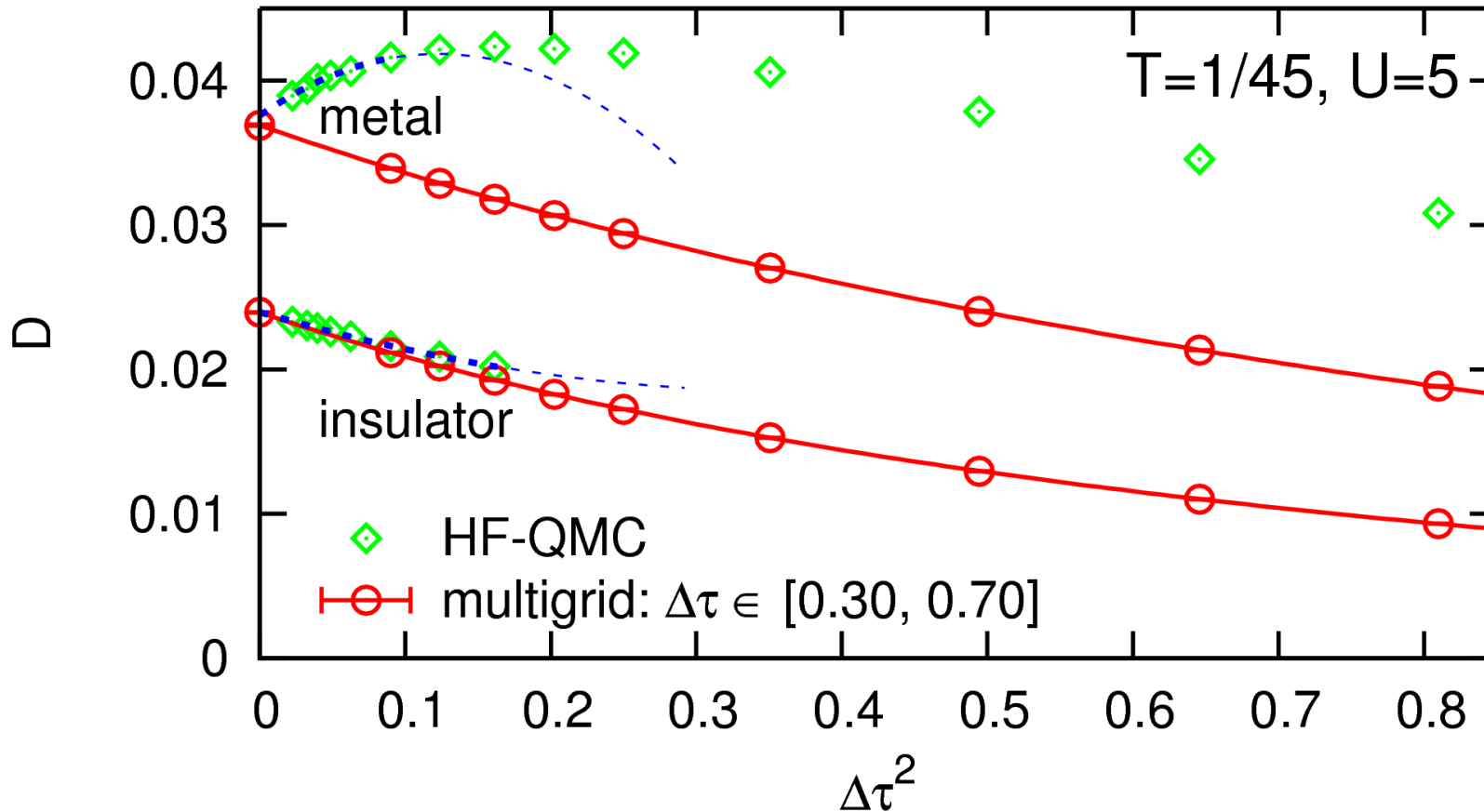
**Implementation:** Green function extrapolation, hierarchy of frequency scales

# Comparison: double occupancy $D = \langle n_{i\uparrow} n_{i\downarrow} \rangle$ near Mott transition



Conventional HF-QMC: no insulating solution for  $\Delta\tau \gtrsim 0.4$   
very irregular  $\Delta\tau$  dependence beyond  $\Delta\tau \approx 0.3$

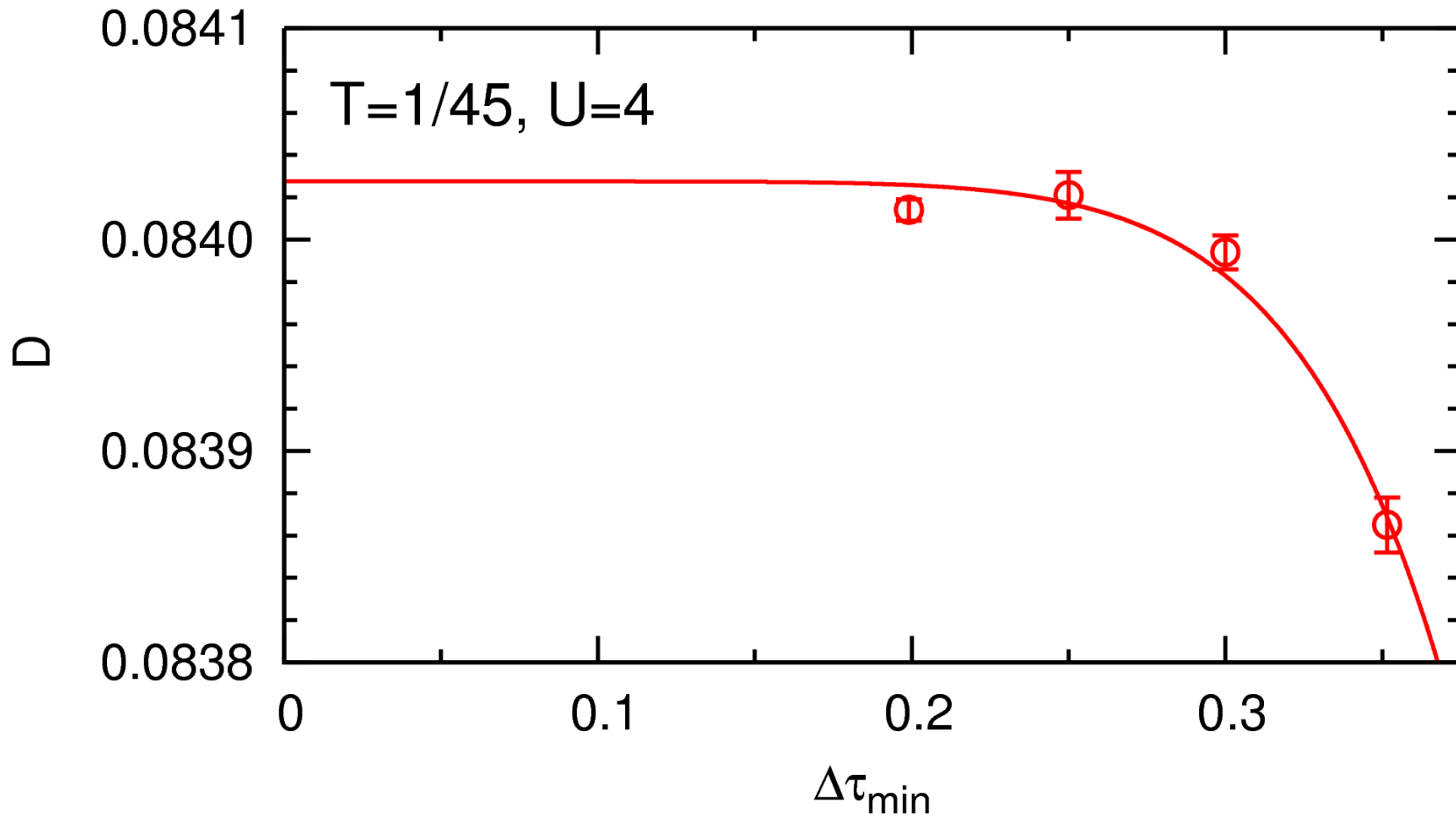
# Comparison: double occupancy $D = \langle n_{i\uparrow} n_{i\downarrow} \rangle$ near Mott transition



Conventional HF-QMC: no insulating solution for  $\Delta\tau \gtrsim 0.4$   
very irregular  $\Delta\tau$  dependence beyond  $\Delta\tau \approx 0.3$

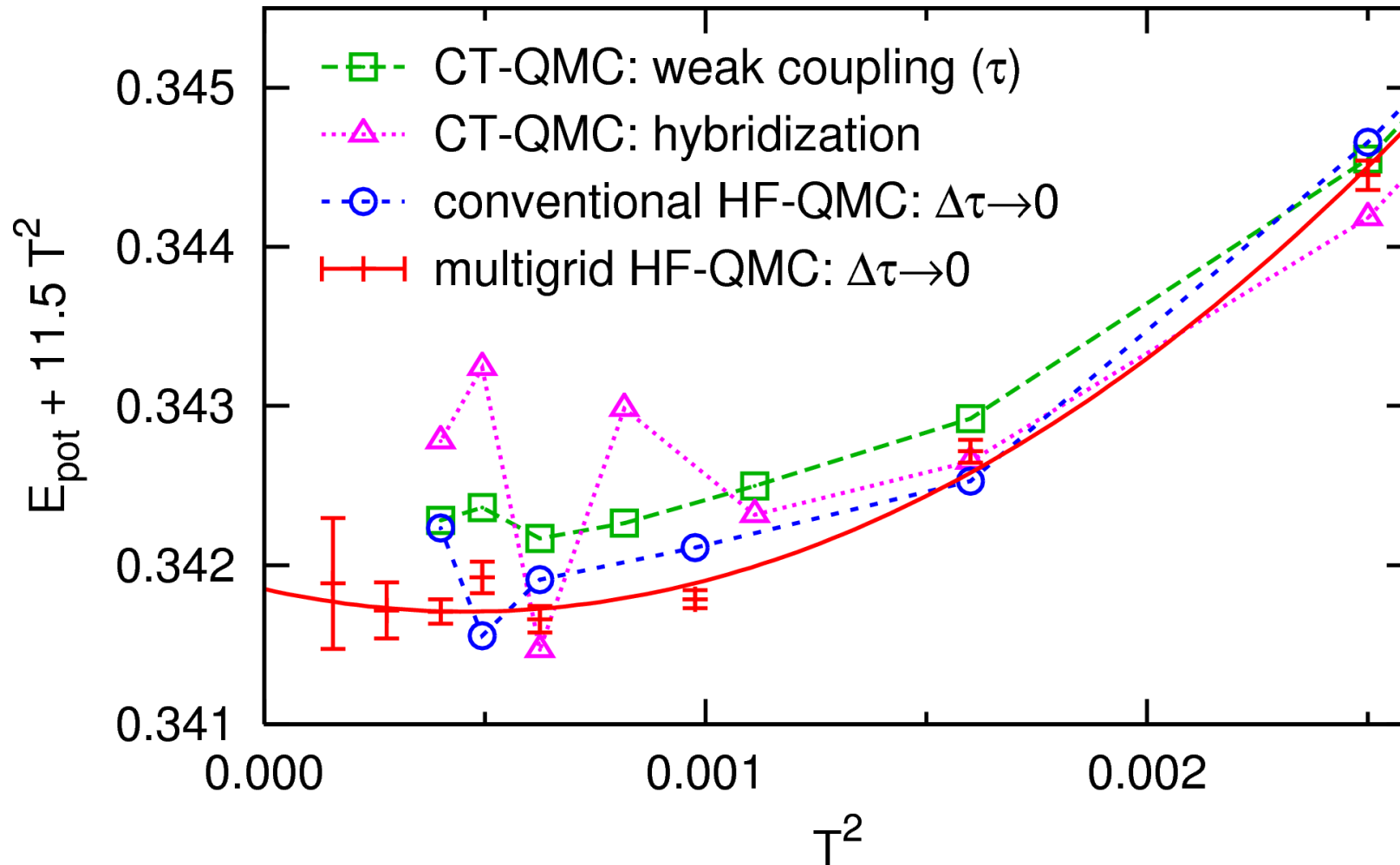
Multigrid HF-QMC: vastly larger useful range of  $\Delta\tau$

# Systematic study: impact of grid range (on double occupancy)



Multigrid HF-QMC usually “numerically exact” for  $\tau_{\min} \lesssim 0.3$

Efficiency: potential energy  $E_{\text{pot}} = UD$  (at  $U = W = 4$ )

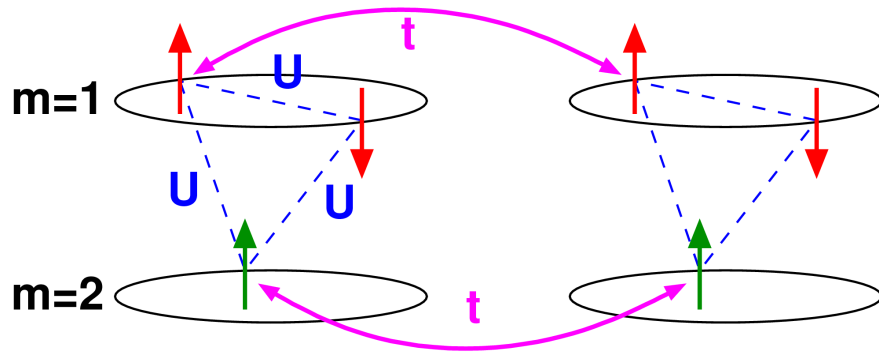


No more “difficult observables” for multigrid HF-QMC  
Higher precision than CT-QMC methods at same effort

# Applications

## Mott transition at variable degeneracy $SU(2M)$ : Motivation

$$H = -t \sum_{\langle ij \rangle} \sum_{\alpha} c_{i\alpha}^{\dagger} c_{j\alpha} + \frac{1}{2} U \sum_i \sum_{\alpha \neq \alpha'} n_{i\alpha} n_{i\alpha'}$$



$$\alpha = (m, \sigma), \quad m = 1, \dots, M, \quad \sigma = \uparrow, \downarrow$$

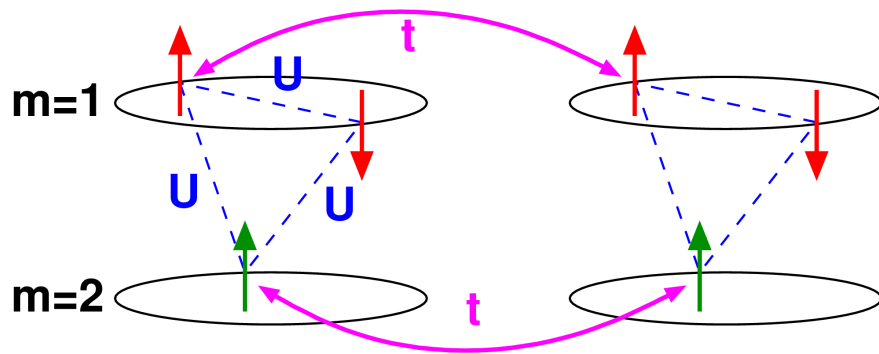
no Hund exchange!



# Applications

## Mott transition at variable degeneracy $SU(2M)$ : Motivation

$$H = -t \sum_{\langle ij \rangle} \sum_{\alpha} c_{i\alpha}^{\dagger} c_{j\alpha} + \frac{1}{2} U \sum_i \sum_{\alpha \neq \alpha'} n_{i\alpha} n_{i\alpha'}$$



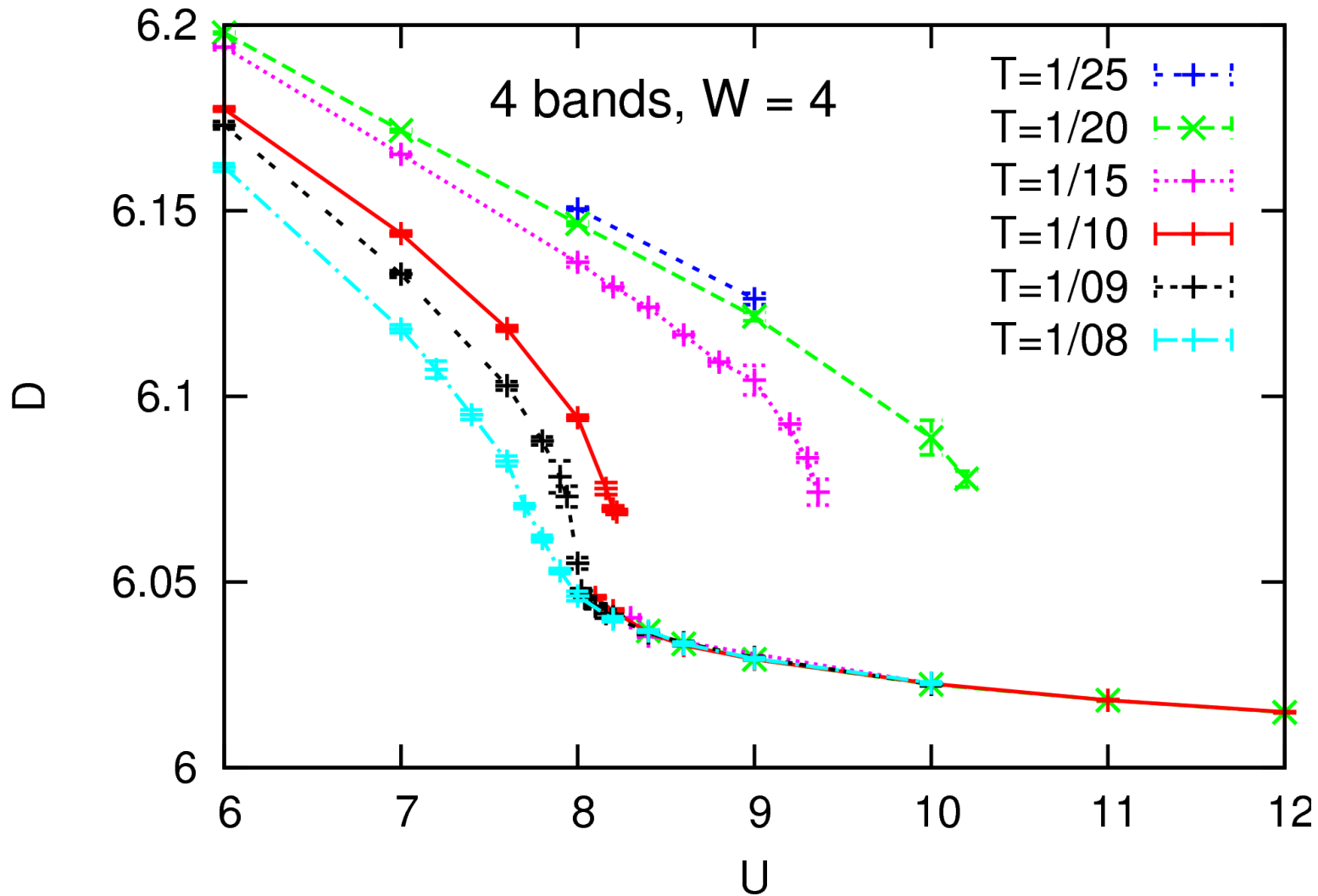
$$\alpha = (m, \sigma), \quad m = 1, \dots, M, \quad \sigma = \uparrow, \downarrow$$

no Hund exchange!

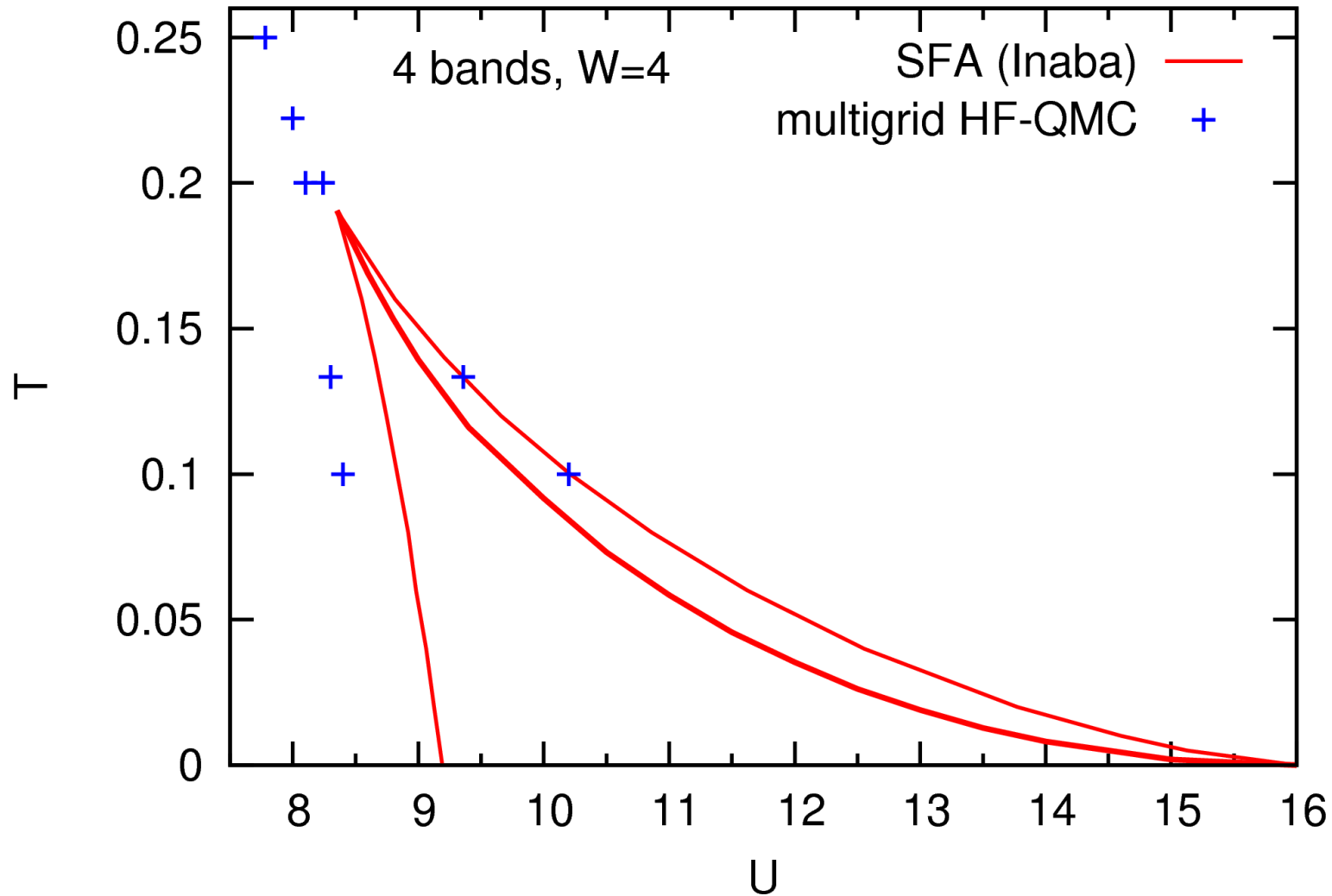
- Mott transition for any  $M = 1, 2, \dots$
- Analytic solutions for  $M \rightarrow \infty$  [Florens et al., PRB (2002)]
- So far: only approximate numerical solution for  $2 \leq M \leq 4$  [Inaba et al., PRB (2005)]

# Mott transition at variable degeneracy $SU(2M)$ : 4-band case

Multigrid HF-QMC: Double occupancy

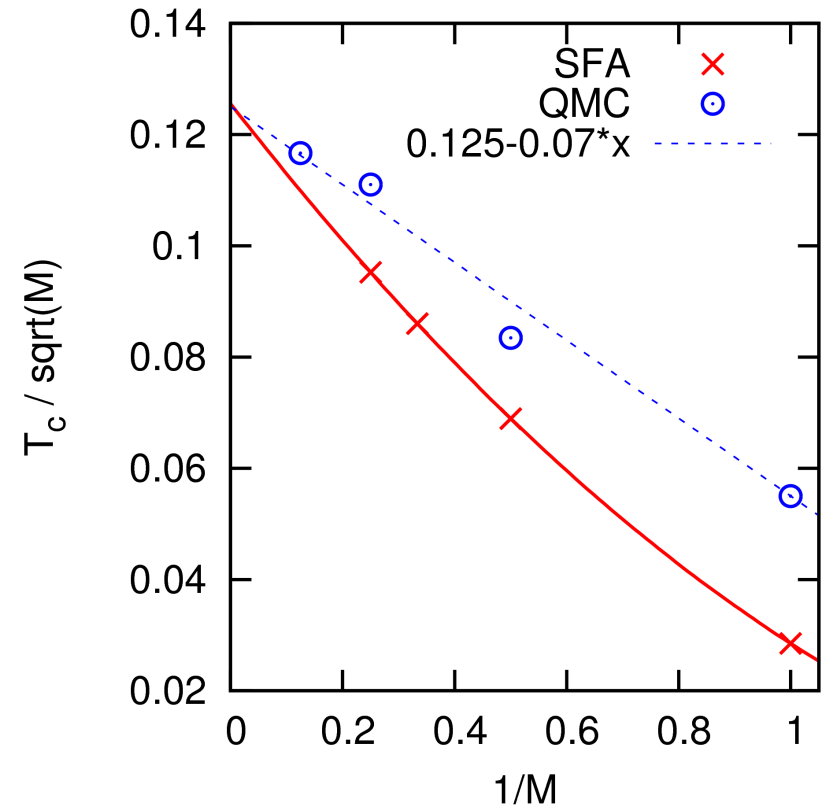
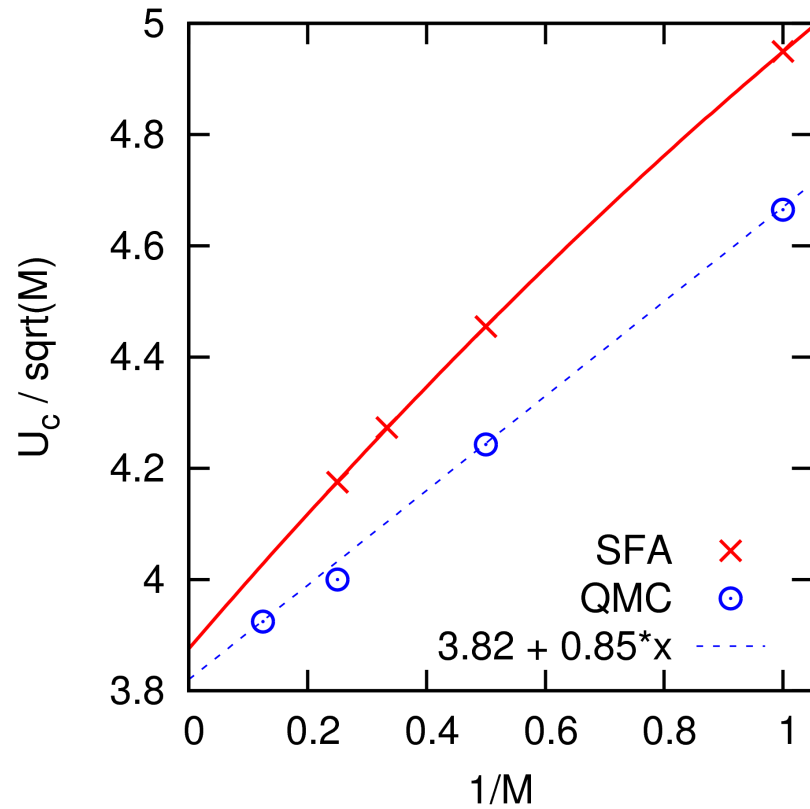


# Mott transition at variable degeneracy $SU(2M)$ : 4-band case



Phase diagram from multigrid HF-QMC: numerically exact results!

# Mott transition at variable degeneracy $SU(2M)$ : scaling of the critical parameters



Multigrid HF-QMC: numerically exact results!

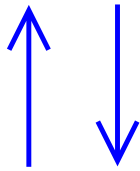
$\Rightarrow$  Phase diagram for arbitrary  $M$

# Beyond electronic systems : Fermions with arbitrary spin multiplicity

## Condensed matter physics

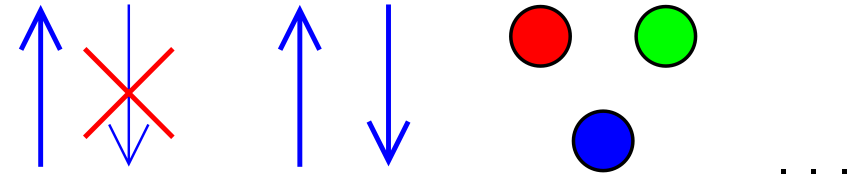
electronic systems

$SU(2)$  spin-rotational symmetry



## Ultracold fermions

combination of  $S$  and  $I$  into hyperfine state with angular momentum  $F \geq 1/2$



Example:  $^{40}\text{K}$

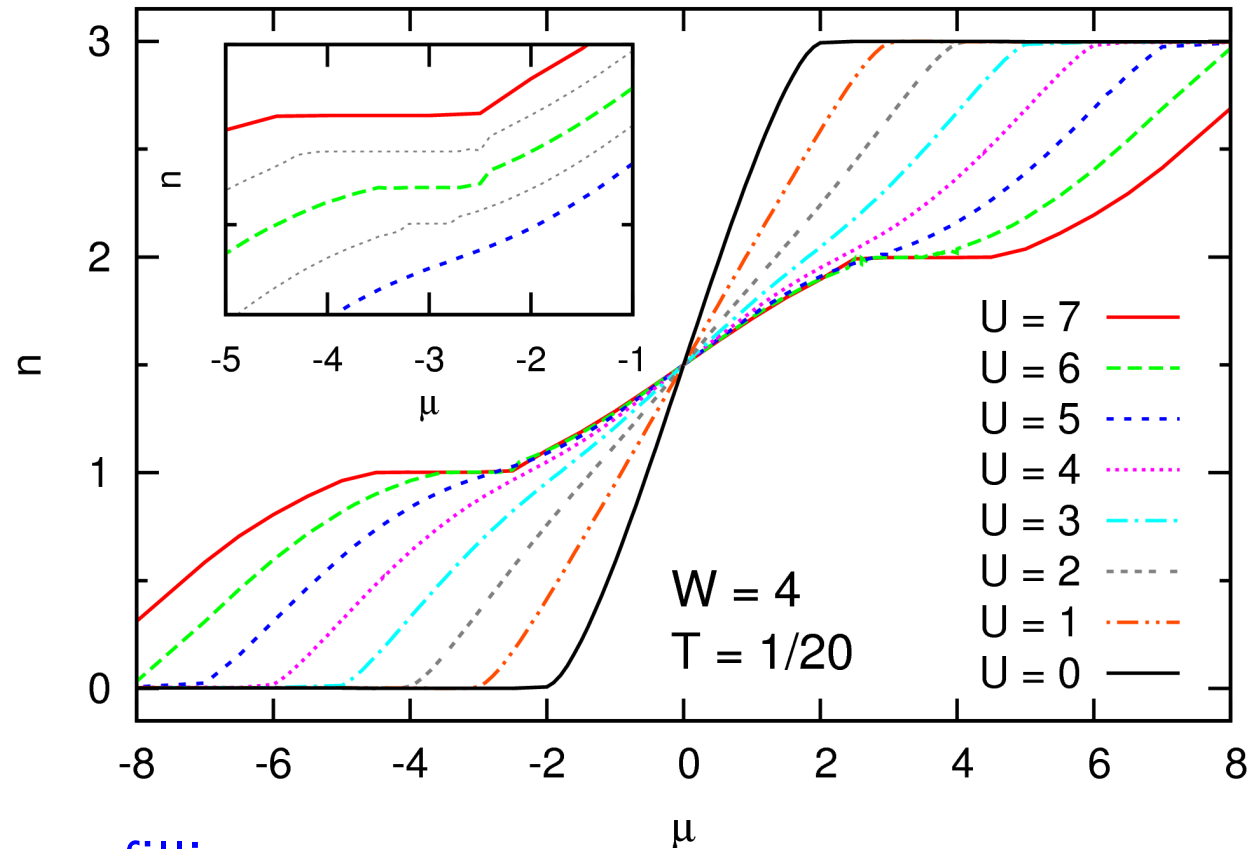
$|F = 9/2, m_F = -5/2, -7/2, -9/2\rangle$

[Regal, Jin, PRL (2003)]

## QMC generalization for arbitrary spin multiplicity

- in principle straightforward, but changes in  $\sim 50\%$  of code
- at this opportunity: cleaner solutions, documentation

# 3-spin/ flavor system in paramagnetic phase

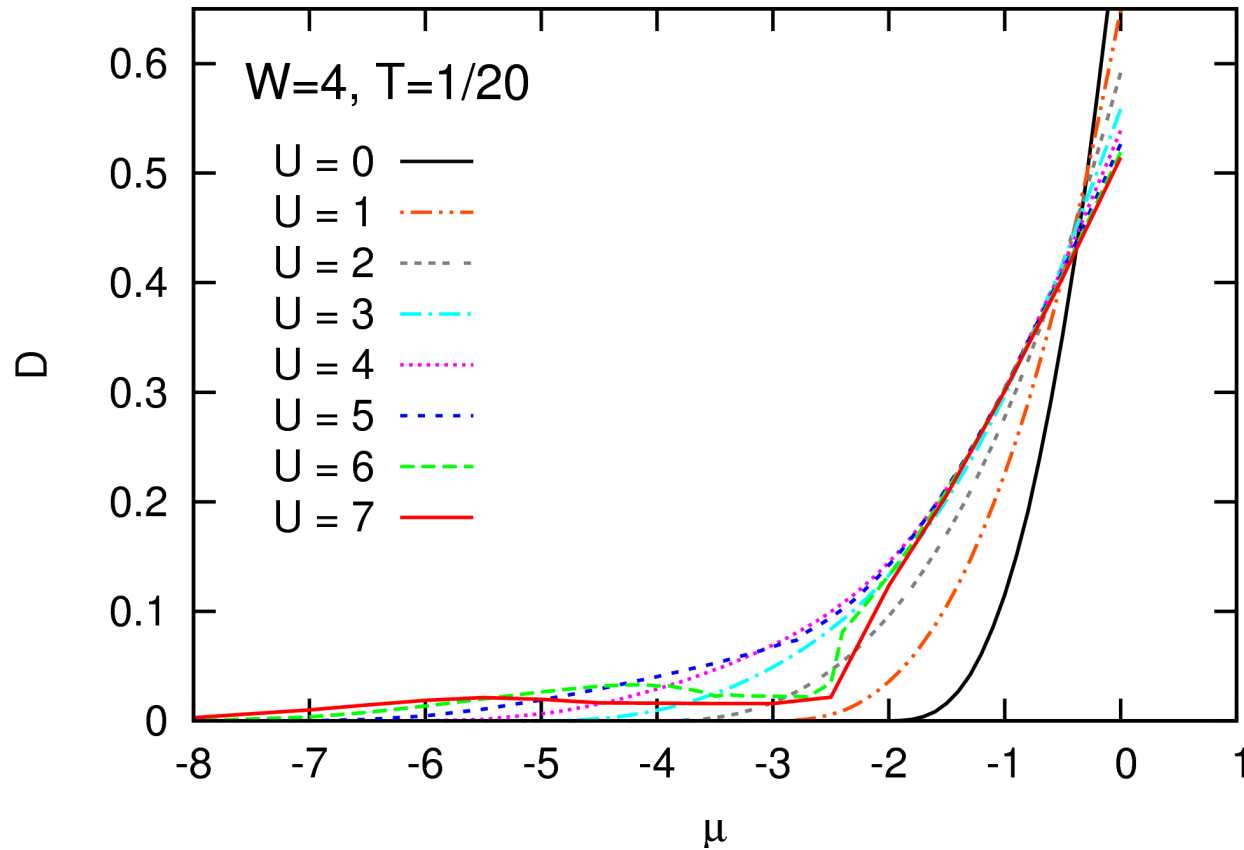


## Density vs. filling

Plateaus: incompressible Mott phase (for  $U \gtrsim 6$ )

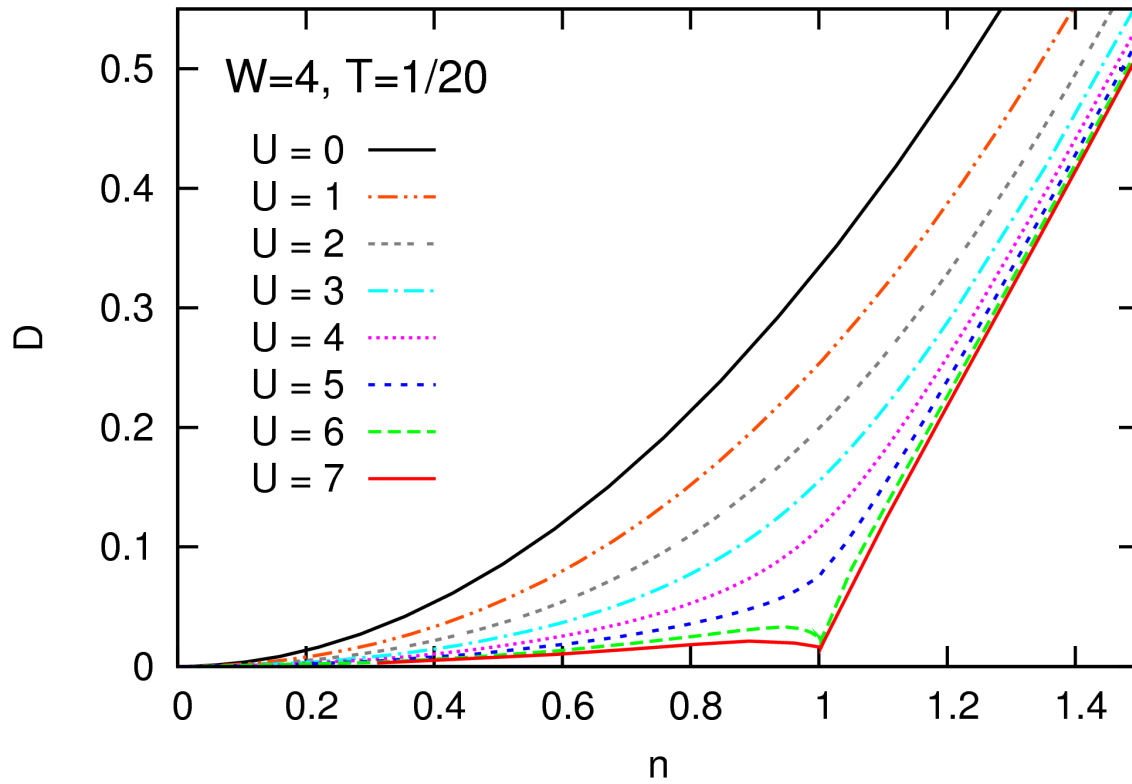
not at half-filling!

# 3-spin/ flavor system in paramagnetic phase



## Double occupancy vs. filling

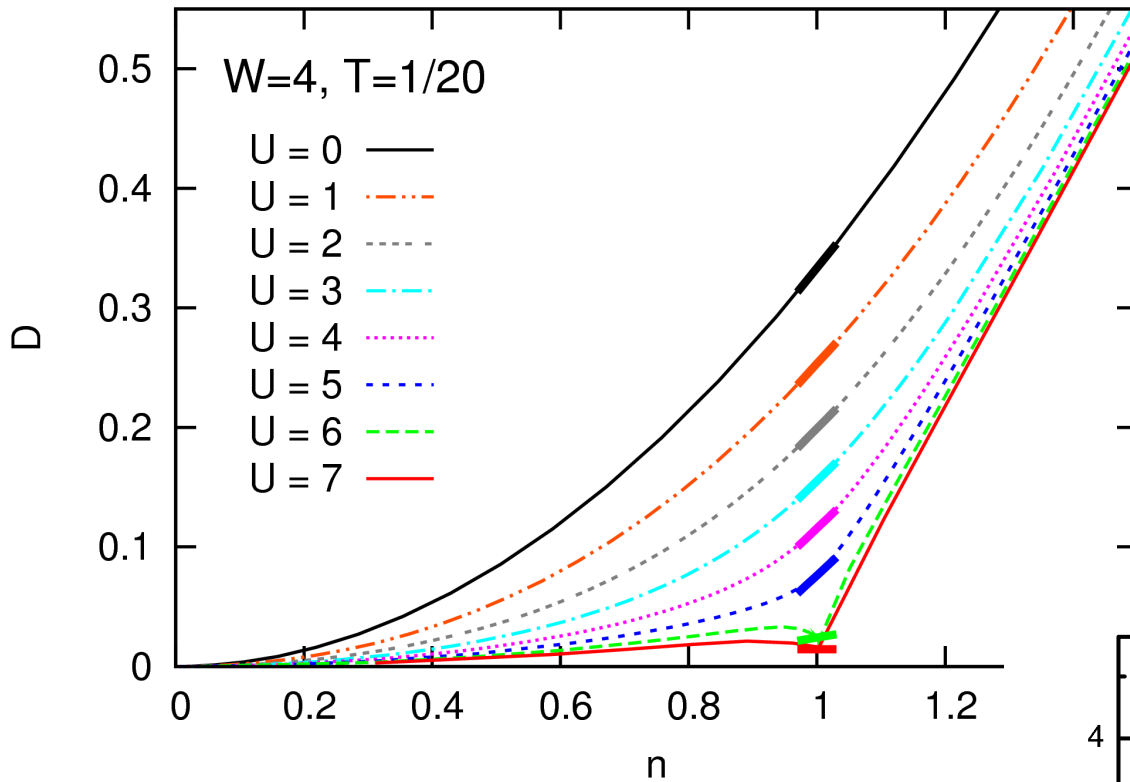
Here mostly density effects



3-spin/ flavor system:

Double occupancy vs. density





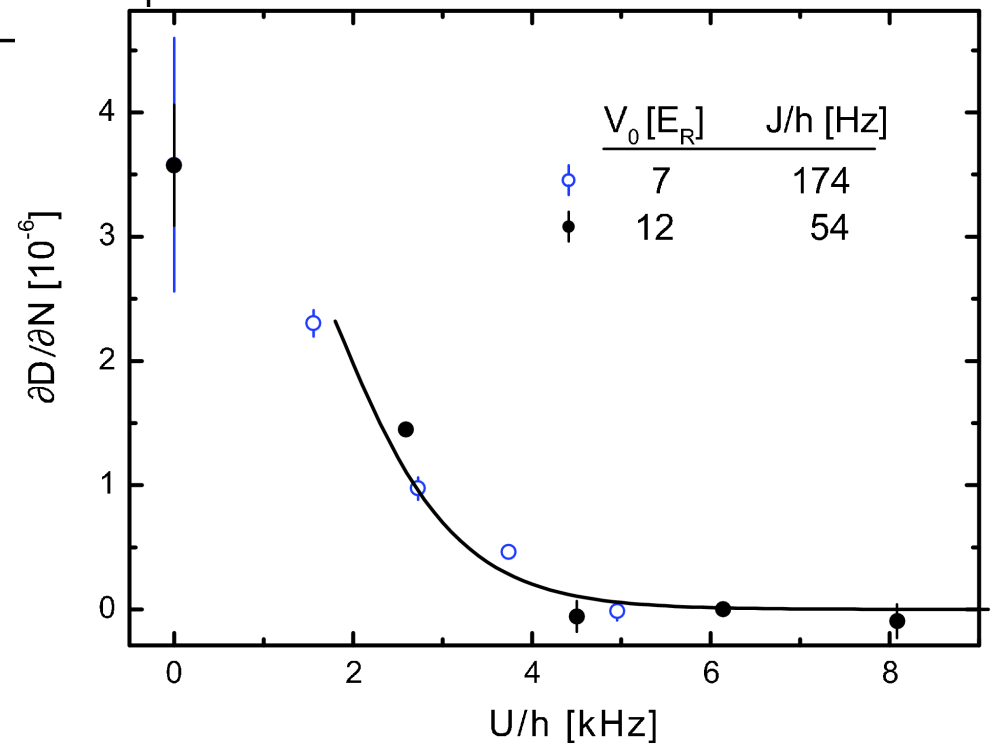
3-spin/3-flavor system:

Double occupancy vs. density

Experiment: 2-spin system

Transition to an incompressible phase

[Jördens et al., Nature (2008)]



# Summary

Auxiliary-field Hirsch-Fye QMC + high-frequency corrections

Efficiency of QMC DMFT solvers: HF-QMC competitive (for not too low  $T$ )

Unbiased Green functions and spectra from HF-QMC

Multigrid Hirsch-Fye quantum Monte Carlo algorithm

Applications: Mott transitions at large degeneracy / in 3-spin system

# Summary

Auxiliary-field Hirsch-Fye QMC + high-frequency corrections

Efficiency of QMC DMFT solvers: HF-QMC competitive (for not too low  $T$ )

Unbiased Green functions and spectra from HF-QMC

Multigrid Hirsch-Fye quantum Monte Carlo algorithm

Applications: Mott transitions at large degeneracy / in 3-spin system

Not shown: Spectral weight transfer at Mott transition, high-precision specific heat, superlinear MPI + OpenMP scaling

New project: real-space DMFT+QMC for ultracold atom clouds on optical lattices

# Summary

Auxiliary-field Hirsch-Fye QMC + high-frequency corrections

Efficiency of QMC DMFT solvers: HF-QMC competitive (for not too low  $T$ )

Unbiased Green functions and spectra from HF-QMC

Multigrid Hirsch-Fye quantum Monte Carlo algorithm

Applications: Mott transitions at large degeneracy / in 3-spin system

Not shown: Spectral weight transfer at Mott transition, high-precision specific heat, superlinear MPI + OpenMP scaling

New project: real-space DMFT+QMC for ultracold atom clouds on optical lattices

## Acknowledgements:

Carsten Knecht, **Elena Gorelik**, Eberhard Jacobi, Peter van Dongen;

Funding by state RLP (Forschungsfonds 2007) and DFG (FG 559, SFB/TR 49)

# Thermal breakdown of a Fermi liquid

Fermi liquid theory: linear specific heat  $c_V = \gamma T$   
linear entropy  $S = \gamma T$   
quadratic resistivity  $\rho \propto T^2$  for “low enough”  $T$

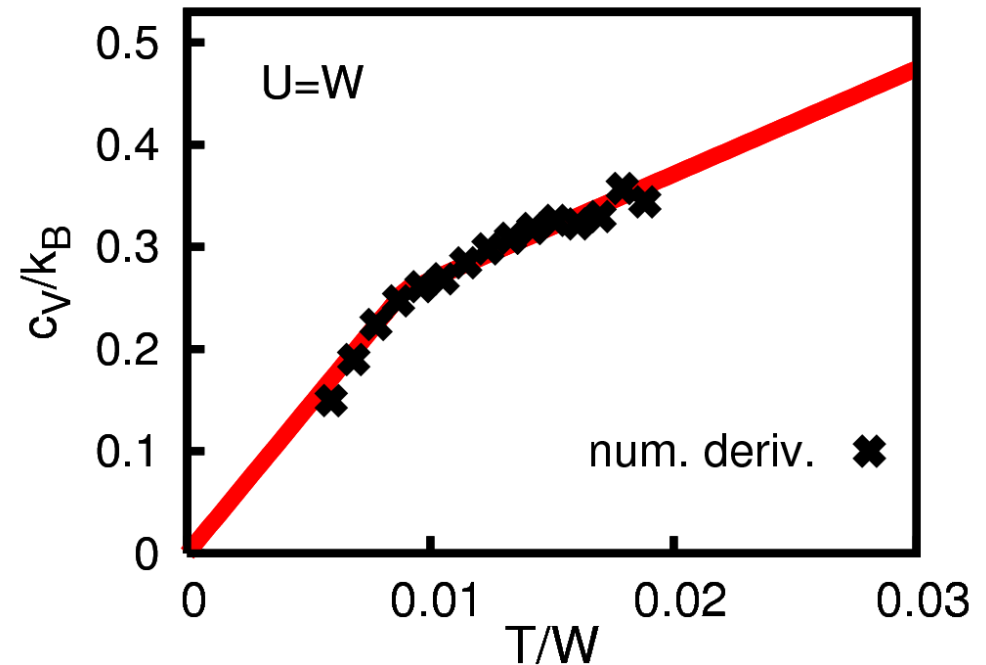
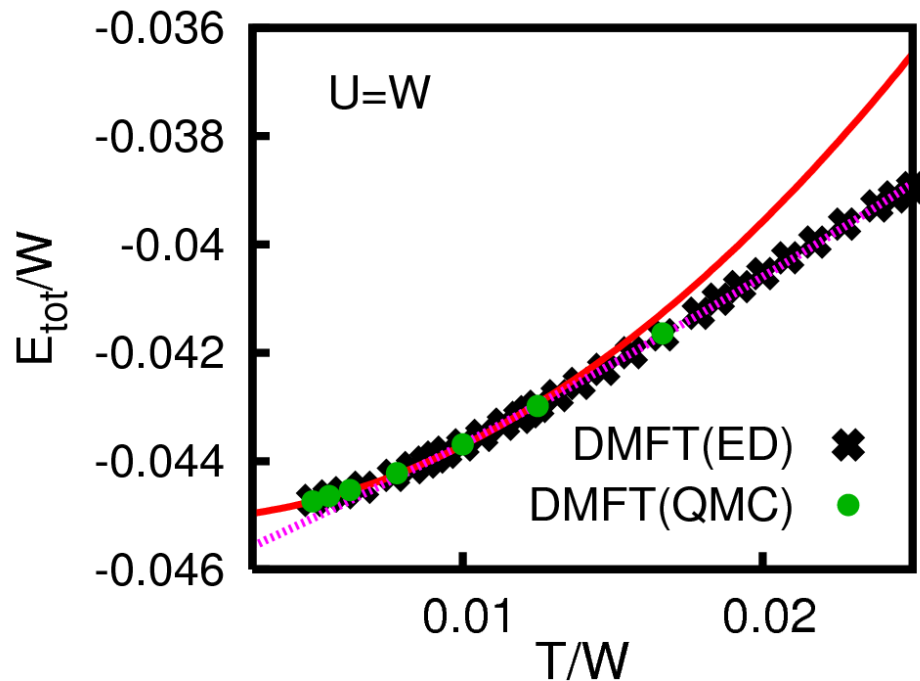
When/how do these laws break down?

# Thermal breakdown of a Fermi liquid

Fermi liquid theory: linear specific heat  $c_V = \gamma T$   
 linear entropy  $S = \gamma T$   
 quadratic resistivity  $\rho \propto T^2$  for “low enough”  $T$

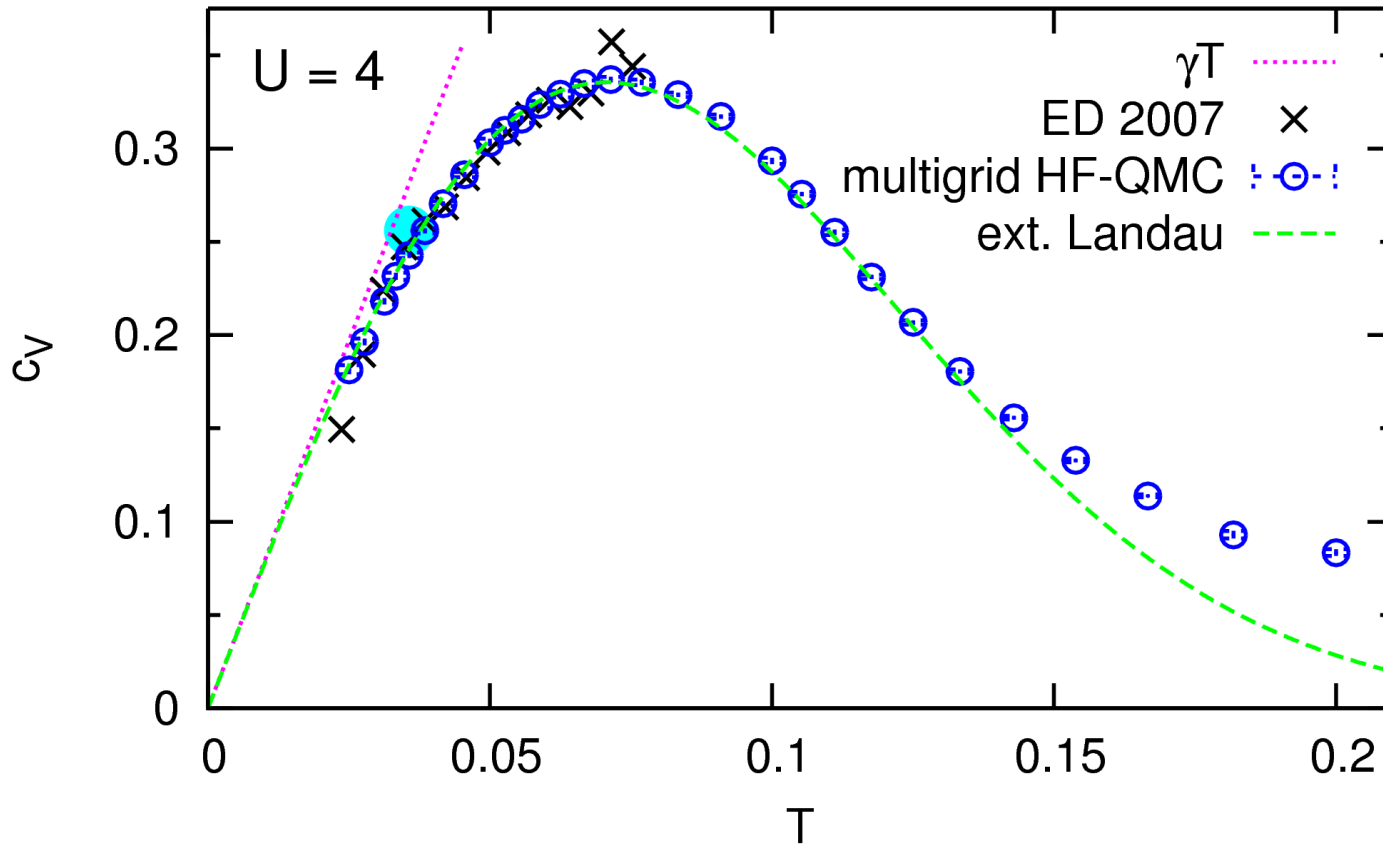
When/how do these laws break down?

Exact diagonalization study (8 sites) for 1-band Hubbard model



Distinct kink in  $c_V$ !

[A. Toschi, M. Capone, C. Castellani, K. Held, [arXiv:0712.3723](https://arxiv.org/abs/0712.3723)]

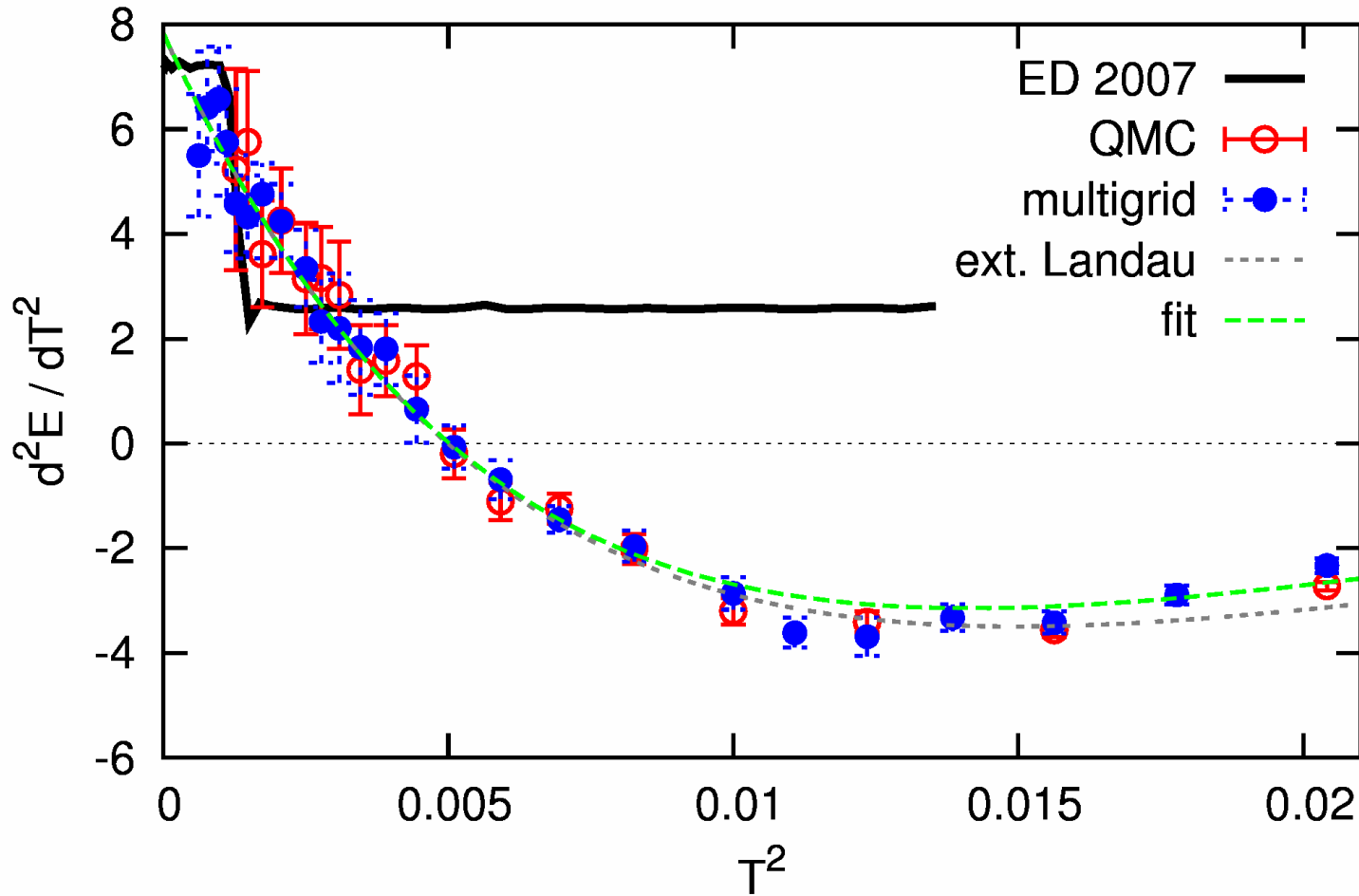


High-precision results  $\rightsquigarrow$  no kink!

Full agreement of (multigrid) HF-QMC with **extended Landau** theory (parameter:  $Z$ )

$$c_V(T) = \frac{2\pi}{3Z} T \exp \left[ - (T/T_0)^2 \right]; \quad T_0 = \frac{3 \log(2)}{\pi^{3/2}} Z \quad (\text{Bethe DOS})$$

# Direct measure of "kinkiness": energy curvature

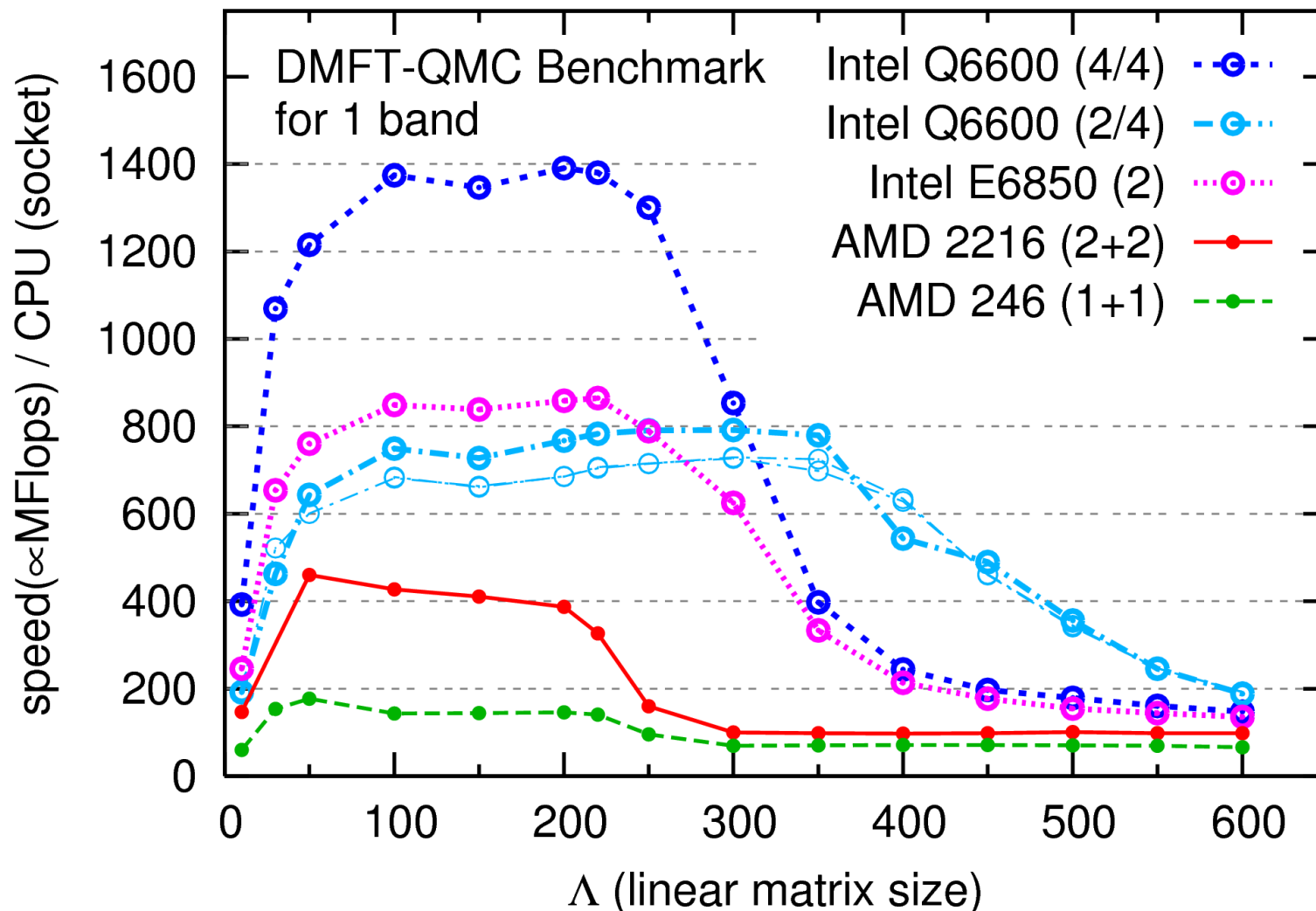


Full agreement of (multigrid) HF-QMC with [extended Landau](#) theory (parameter:  $Z$ )

[Initial slope](#): contributions from Sommerfeld expansion + T-dependence of  $\Sigma(\omega)$



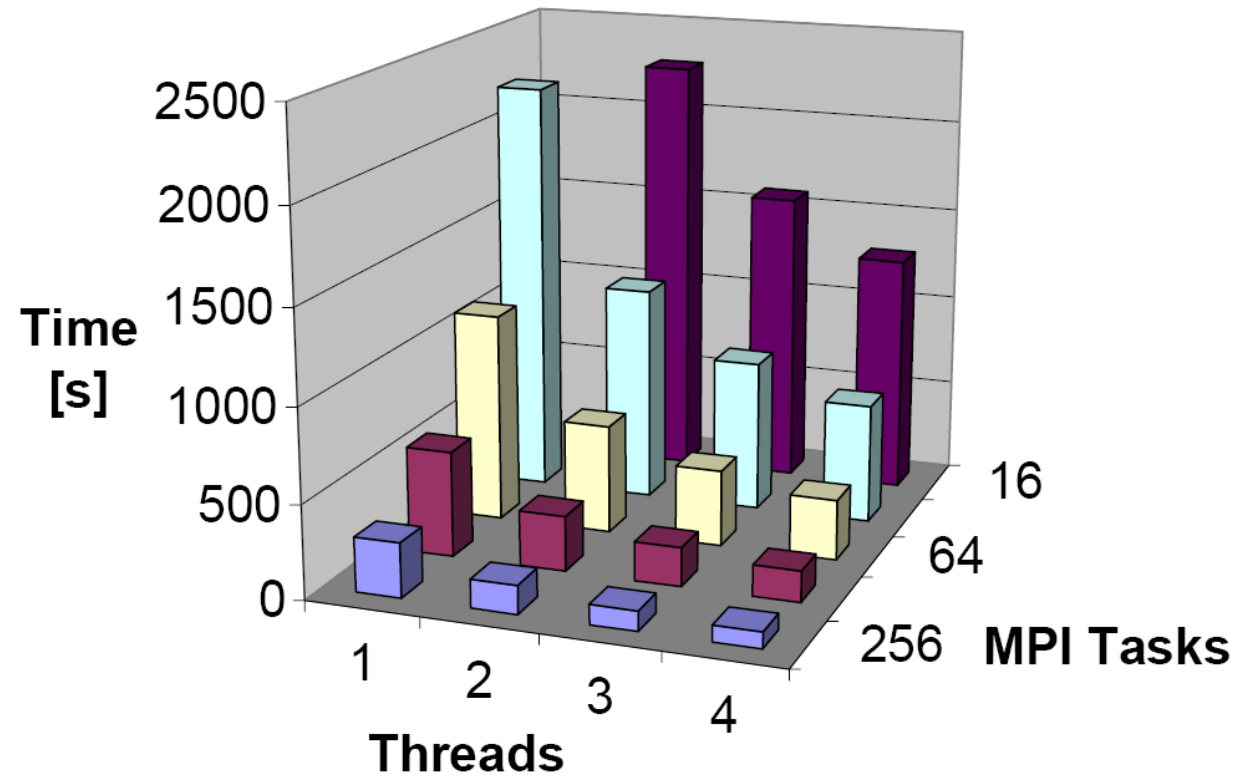
# Benchmarks



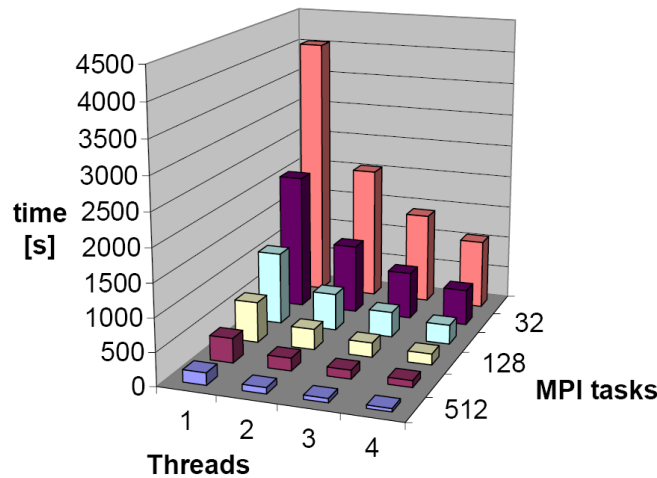
HF-QMC profits strongly from modern large-cache architectures

New (4/2008):  
hybrid parallelization  
(MPI + OpenMP)

## DMFT-QMC L=200 SMP JuGene



DMFT-QMC L=400 JUGENE



Very good scaling: speed roughly linear with number of CPU cores

# Superlinear scaling on JUMP

